

Beam loss monitors at the ESRF

B.Joly, U.Weinrich, G.A.Naylor, ESRF, Grenoble, FRANCE

Abstract

The European Synchrotron radiation facility is a third generation x-ray source providing x-rays on a continuous basis. As a facility available to external users, the monitoring of radiation caused by the loss of high-energy stored beam is of great concern. A network of beam loss monitors has been installed inside the storage ring tunnel so as to detect and localize the slow loss of electrons during a beam decay. This diagnostic tool allows optimization of beam parameters and physical aperture limits as well as giving useful information on the machine to allow the lifetime to be optimized and defects localized.

1 INTRODUCTION

Modern synchrotron light sources are being pushed by users to provide higher photon brilliance. This is achieved both by a reduction of the stored beam emittance and by the increase of magnetic fields with short period undulators. The latter requires the close proximity to the beam of the insertion device magnetic poles. At the European Synchrotron Radiation Facility (ESRF), vacuum chambers of internal dimensions as low as 8mm are used with lengths up to 5m. Large amplitude betatron oscillations excited by Touschek, elastic and inelastic collisions in the vertical plane give rise to a loss of particles on the small aperture insertion device vacuum vessels. The push to low emittance increases significantly the contribution to these losses from Touschek collisions. It is important in order to control these losses that they are continuously monitored. Beam loss detectors have been developed at the ESRF which detect the radiation shower produced by the passage of high energy electrons through the vacuum chamber walls. Two types of detector have been developed:

- i) Short fast losses during injection pulses and sudden beam losses.
- ii) Prolonged beam loss during the decay period of a stored beam.

The former type are required to be very sensitive, whereas the second type should be designed so as to measure linearly very large bursts of radiation.

A good review of the different beam loss detector types is given in [1] and is summarised in table 1.

In all cases care should be taken in the case of a synchrotron light source that the signal detected is not significantly perturbed by the contribution from the background high-energy synchrotron radiation. This may be achieved as in [2] by the coincidence detection on two photodiodes. At the ESRF the higher energy radiation due to the Bremstrahlung of electrons escaping the vacuum chamber is discriminated from the synchrotron radiation by shielding the detector with 10mm thickness of lead and placing the detector on the inside of the storage ring. For the case of the fast detectors, synchrotron radiation is not a problem as they are only sensitive to large bursts from beam losses. A simple detector system is employed using a perspex rod as a scintillator coupled to a high gain photo-multiplier. This method was chosen to allow a large number of detectors to be installed. The average anode current is monitored rather than the count rate of scintillation events. Although in principle scintillation counting should give better linearity over a greater dynamic range, in practice the particle revolution rate and the filling pattern limit the maximum achievable count rate. This maximum rate is different for different filling patterns (eg single bunch and multi-bunch) thus affecting the performance in different filling modes, similarly the maximum count rate during injection is limited to 10Hz by the injection rate. The photo-diode solution although providing a simple solution gave too low a count rate at the locations at which the detectors were to be located. A fast beam loss detector using a 1mm Perspex fibre coupled to a silicon photodiode is also used. Each of the 32 cells of the ESRF storage ring is equipped with one slow beam loss detector and 3 fast beam loss detectors.

Type of Beam loss detector	Advantages	Disadvantages
Long ionisation chamber [7]	Can give position sensitivity	Expensive and complex electronics
Short ionisation chamber [3]	Linear over many decades	Measurement of very low currents is very expensive
Scintillator + Photomultiplier (PM) [6]	Simple and cheap	Long term degradation of scintillator and drift of PM
Pin Photo-diode [5]	Simple and cheap	Limited count rate.

Table 1: Different beam loss detector types.

FAST POSITIONAL GLOBAL FEEDBACK FOR STORAGE RINGS

E. Plouviez. ESRF, Grenoble, France

Abstract

Stability of the closed orbit of a storage ring is limited by the stability of the components defining this orbit: magnets position and field values. Measurements of the variation of the stored beam orbit with respect to a nominal orbit and application of orbit correction derived from these measurements can reduce these distortions. The subject of this talk is the implementation of such correction at high frequencies (up to about 100Hz) using global correction schemes.

The basic theoretical aspects of the problem will be presented:

- Global versus local scheme
- Feedback loop dynamics.

The technical problems associated with the implementation of such systems will also be addressed:

- BPM and correctors design
- Feedback loop electronic design

1 INTRODUCTION

Most modern lepton machines have emittances of the order of 10nmrad and 1% coupling. In order to offer optimum performance to their users, storage rings must achieve excellent orbit stability, especially at the source points on synchrotron radiation sources or interaction points on colliders. The requirements on this orbit stability are usually specified in terms of tolerated orbit centroid motion with respect to the beam size. Depending on the local value betatron function, the beam sizes and divergences are 10 μ m and 1 μ rad or less. So, in order to take advantage of such small beam size, we aim at controlling the orbit with micron accuracy at these specific locations. In the case of light sources the problem is more demanding due to the greater number of source points spread all over the ring compared to the few interaction points of colliders. The reduction of the orbit distortion in the rest of the machine is also mandatory in order to achieve these emittance figures, to obtain a good lifetime and to protect the vacuum chamber against the synchrotron radiation though in the latter case the stability requirements are slightly less stringent [1]. Various sources of perturbation of the closed orbit can be found on most machines [2][3]. Below .1Hz we will find ground motion due to seasonal or tidal causes and thermal effects. They will be dealt with by machine realignments (seasonal effects) and beam position measurements followed by closed orbit corrections using correctors dipoles magnets[4]. Between .1Hz and 100Hz, the perturbation will come from the ground vibration

transmitted by the magnet girders, the water circulation, the AC power distribution. A typical spectrum of these perturbations is shown on figure 4. These additional fast sources of perturbation should be minimised at their source, but the residual orbit perturbation level can still be above 1 μ m, even on well designed machines[2][3]. This level is not high enough to spoil the machine tuning but can increase the apparent emittance for the users. These fast residual perturbations can also be reduced by closed orbit corrections but the repetition rate of these corrections poses specific challenging problems for the orbit control.

2 CLOSED ORBIT DISTORTION AND CORRECTION

2-1 Principle

Variations of the position of quadrupoles or sextupoles, tilts of the dipoles orientation, fields fluctuations, will result in the addition of angular kicks to the nominal dipolar fields of the ring. These kicks are compensated by a change in the closed orbit in order to obtain a new closed orbit, where the perturbation kicks effect is compensated by the kicks produced by the offset of the new perturbed beam closed orbit with respect to the quadrupole center as shown on figure 1. To perform a closed orbit correction an orbit measurement is done, using a set of e⁻ (or photons) BPMs and a set of correction kicks is applied to the beam using correctors dipole magnets in order to cancel the difference between the reading and the desired value.

2-2 Global correction

With this scheme, an adequate number of M BPMs, spread all over the machine are used to measure the orbit distortion. The vector δd of the M beam position offsets is used to calculate a correction vector $\delta \theta$ containing the values of N correction kicks using a M*N correction matrix R^{-1} . R^{-1} is deduced from the N*M response matrix R formed by the response of the M BPMs to individual correctors unit kicks. R can be obtained from a theoretical model or from measurements. The calculation of the correction matrix R^{-1} can be done using various methods; The most common method seems to be the Singular Values Decomposition (SVD)[1]; the SVD method is very flexible and does not require R to be square. The adequate number and location of the BPMs and correctors are function of the lattice design, of the space available on the

THE COMPARISON OF SIGNAL PROCESSING SYSTEMS FOR BEAM POSITION MONITORS

G. Vismara – CERN - Geneva 23- Switzerland

Abstract

At first sight the problem of determining the beam position from the ratio of the induced charges of the opposite electrodes of a beam monitor seems trivial, but up to now no unique solution has been found that fits the various demands of all particle accelerators.

The purpose of this paper is to help instrumentalists in choosing the best processing system for their particular application.

The paper will present the different families in which the processing systems can be grouped.

A general description of the operating principles with relative advantages and disadvantages for the most employed processing systems is also presented.

INTRODUCTION

Beam position monitors (BPM) can be found in every accelerator.

BPM systems have largely evolved since the early days, from the simple scope visualization of coaxial multiplexed P.U. signals into a very complex system. These systems are now capable of digitizing individual bunches separated by a few tenths of ns, with spatial resolution in the micron range, while the resulting orbit or trajectory collected from several hundred planes can be displayed in a fraction of second.

To obtain such a performance the processing electronics have to be optimized to the machine and beam parameters.

A unique solution capable of covering all the possible combinations with satisfactory results seems almost impossible to realize. This is the reason for the wide spectrum of signal processing in use today.

The BPM applications are not only limited to Orbit & Trajectory measurements, but can perform static and dynamic beam parameter measurements by exploiting the large amount of data collected and stored in their memoriesⁱ.

Turn-by-turn measurement can give information on; Betatron oscillation, transfer function, phase advance, optics checks, local chromaticity, etc.

The high resolution allows for energy calibration and machine impedance measurements.

The BPM is also employed in feedback systems to stabilize the beam and even as beam position interlockⁱⁱ.

These applications are much more performance demanding than a simple position measurement.

1. PROCESSING SYSTEM FAMILIES

The various signal processing systems can be grouped into different families according to the employed techniques. At least three different criteria can be used to group them.

1.1 Signal recombination

Four main categories are nowadays mainly employed:

- **Individual signal treatment:** The maximum signal information is still available, therefore a wide-band processing is the most suitable. Due to a very large Gain-Bandwidth, it offers a limited dynamic range.
- **Time MPX:** Electrode signals are sequentially time-multiplexed and processed by a single electronic system. It offers an excellent long-term stability but cannot perform turn-by-turn measurements.
- **Δ/Σ :** The individual signals are immediately converted by the use of hybrids into Δ and Σ . This offers excellent center position stability but requires switchable gain amplifiers.
- **Passive Normalization:** The signal's amplitude ratio is converted into a phase or time difference. It is amplitude independent but loses the intensity information.

1.2 Normalization processes

The Normalization is an analog process that will produce a signal proportional to the position information that is independent of the input signal level. Three conditions apply to all normalization processes: 1) The intensity information is lost. 2) The digitization requires a smaller number of bits. 3) No gain selection is required.

Two active and two passive techniques are actually employed.

- **Constant Sum:** The Normalization is obtained by keeping constant the sum of the two electrode signals using AGC amplifiers. This approach is only valid for the time MPX process where the signals exploit the same amplification chain.
- **Logarithmic conversion:** Since the ratio of the logarithm of two signals is equal to the difference of the logarithm, the signals can be converted by logarithmic amplifiers to give the normalized signal as the difference of the output. It offers a large dynamic range, but limited linearity.
- **Amplitude to time:** This is based on the sum of a direct and a delayed signal coming from the two

BUNCH LENGTH MEASUREMENTS

M. Geitz, Deutsches Elektronen Synchrotron, D-22603 Hamburg, Germany

Abstract

An rf photo-injector in combination with a magnetic bunch compressor is suited to produce high-charged sub-picosecond electron bunches required for electron-drive linacs for VUV and X-ray FELs. This report summarizes time- and frequency domain bunch length measurement techniques with sub-picosecond resolution.

1 INTRODUCTION

Future electron-drive linacs for VUV and X-ray Free Electron Lasers (FEL) require the acceleration of bunches whose length is well in the sub-picosecond regime [1]. A common source for high-charged sub-picosecond electron bunches is an rf gun based on a photo injector using an intense ultraviolet laser beam (typically 20 mJ) to produce up to $5 \cdot 10^{10}$ electrons per bunch from a CsTe₂ photo cathode. The electron bunches are accelerated rapidly by the strong electric fields (about 40 MeV/m) of the gun cavity to avoid an emittance blowup due to space charge. The bunch length obtained from an rf gun depends on both the laser pulse length (typically $\sigma_t = 5$ ps) and the compression occurring from the rf field within the first centimeters of the gun cavity. By a proper choice of the rf phase a velocity modulation can be impressed on the electron bunch leading to a reduction of its length within the gun cavity. Very short bunches can be obtained at the price of sacrificing a large fraction of the bunch charge. In an electron drive linac only a moderate bunch compression is applied, because of the need of intense electron beams. Further compression can be obtained by combining an off-crest rf acceleration with a magnetic chicane. The off-crest acceleration produces a correlated energy spread with higher energy electrons trailing lower energy electrons. The higher energy electrons then travel on a shorter path through the magnetic chicane than the lower energy electrons and a bunch compression is obtained. In the following an overview of established and future time-domain and frequency-domain bunch length measurement techniques with sub-picosecond resolution will be presented.

2 TIME DOMAIN MEASUREMENTS

Streak Camera: The streak camera is a device for a direct (single-shot) determination of the longitudinal

bunch charge distribution. The present resolution limit is 370 fs (FWHM) [2]. The light pulse generated by an

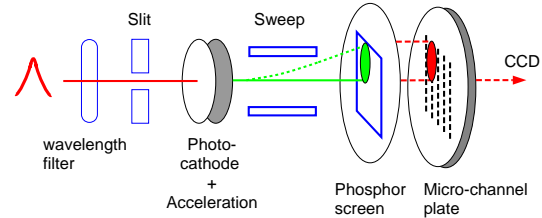


Figure 1: Principle of the streak camera.

electron bunch travels through a dispersion-free optical system, an interference filter and a slit before hitting the photo-cathode of the streak camera. A wavelength filter selects a narrow frequency band and the slit reduces the transverse dimension of the image on the photo cathode. The light pulse is converted to an electron pulse, which is accelerated and swept transversely by a fast rf electric field. The resulting transverse distribution is projected onto a phosphor screen. The image is amplified by a multi-channel plate and then detected by a CCD camera. Space charge effects inside the streak camera tube and the achievable sweeping speed limit the temporal resolution. The energy spread of the electrons generated by the photo-cathode and the dependence of the photo electron energy on the wavelength of the incident light pulse add to the time resolution limit.

A state-of-the-art streak camera measurement performed at the University of Tokyo using a BNL-type rf photo-injector in combination with a magnetic bunch compressor shows a successful compression of a 13 picosecond electron bunch to 440 femtoseconds (FWHM) [3] as shown in Figure 2. The measurement was performed with a bunch charge of 250 pC at an electron energy of 35 MeV.

Rf Kicker Cavity: An interesting proposal to obtain sub-picosecond resolution is the application of the streak camera principle to the electron beam itself [4]. An rf kicker cavity operated in the TM₁₁₀ mode can be used to sweep the electron bunch transversely across a screen located in the vacuum chamber downstream. The transverse

Controls and Beam Diagnostics for Therapy-Accelerators

H. Eickhoff
GSI, Darmstadt

1) Summary

During the last four years GSI has developed a new procedure for cancer treatment by means of the intensity controlled rasterscan-method. This method includes active variations of beam parameters during the treatment session and the integration of 'on-line' PET monitoring. Starting in 1997 several patients have been successfully treated within this GSI experimental cancer treatment program; within this program about 350 patients shall be treated in the next 5 years. The developments and experiences of this program accompanied by intensive discussions with the medical community led to a proposal for a hospital based light ion accelerator facility for the clinic in Heidelberg. [1] An essential part for patients treatments is the measurement of the beam properties within acceptance and constancy tests and especially for the rasterscan method during the treatment sessions. The presented description of the accelerator controls and beam diagnostic devices mainly covers the requests for the active scanning method, which are partly more crucial than for the passive scattering methods.

2) Passive scattering and Rasterscan method

a) Passive scattering

At presently existing therapy-dedicated proton- and light-ion accelerators for cancer treatment the particle beam is delivered to the patient after 'passive' manipulations. A broad and uniform beam profile is generated by wobbling magnets with horizontal and vertical deflection in combination with scatter plates. Whereas the transverse beam profile is matched to the target dimension by means of a collimator, the requested range dose distribution is achieved with range shifters and adequately formed boli. In general for this treatment mode the beam properties requested from the accelerator are constant over the treatment time.

b) The Intensity controlled Rasterscan

An alternative to the passive method is the rasterscan method, which allows an accurate confirmation also of a very irregular tumor volume and avoids mechanical insertion devices for beam shaping and thus minimizes the production of fragment or stray particles, that also contribute to the dose distribution.

One of the key aspects of a future particle therapy accelerator is the use of the intensity controlled rasterscan technique (Fig. 1), which is a novel treatment concept, developed at GSI and successfully applied within patient treatments of the GSI pilot therapy program.

This treatment method demands fast, active energy-variations on a pulse to pulse base to achieve different penetration depths and intensity-variation to minimize the treatment time.

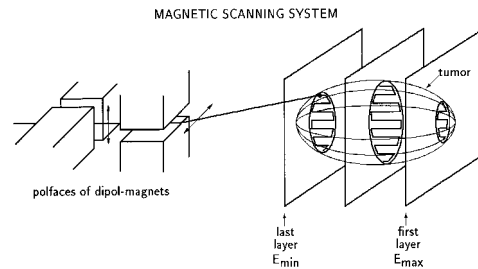


Fig. 1 Rasterscan-Method

The accelerated and slowly extracted beam enters 2 fast scanner magnets, that deflect the beam both in horizontal and vertical direction to cover the lateral dimensions of the tumor. The various ranges in the tumor tissue are realized by different extraction energies of the accelerator.

Fast multiwire proportional counters detect the position and beam width at each scanning point. Ionization chambers in front of the patient measure the number of ions at a specific irradiation point and control the scanner excitation. When a required dose limit has been reached the beam extraction is interrupted very fast (< 0.5 ms).

3) Accelerator requirements

The basis of the accelerator concept has to satisfy the demands of the medical community for the treatment procedures.

Table. 1: Therapy requirements

- 3 treatment areas to treat a large number of patients
- integration of isocentric gantries
- treatment both with low and high LET-ions
- relatively fast change of ion species
- intensity-controlled rasterscan method
- wide range of particle intensities
- ion-species : p, He, C, O
- ion-range (in water) : 20 - 300 mm
- ion-energy : 50 - 430 MeV/u
- extraction-time : 1 - 10 s
- beam-diameter : 4 - 10 mm (hor., vert.)
- intens. (ions/spill) : $1 \cdot 10^6$ to $4 \cdot 10^{10}$
(dependent. upon ion species)

DIAGNOSTICS IN HEAVY ION MACHINES

P. Strehl

Gesellschaft für Schwerionenforschung, Darmstadt, Germany

Abstract

An overview of the measurements of most important beam parameters in heavy ion machines is given. The special characteristics of heavy ions concerning the great variety of parameters with respect to the type of accelerator (linac, circular machine), the species of accelerated ions as well as their energy, beam intensity, beam emittance and time structure are considered. The consequences for the design of beam diagnostic systems are discussed. Typical examples of measuring systems are given. Experimental results taken during the long operating time of the GSI facilities, covering a wide range of parameters, are reported.

1 INTRODUCTION

Due to the large mass, the great variety of isotopes and, especially the large nuclear charge of heavy ions, the lay-out of a beam diagnostic systems may differ considerably from the design for electron or even proton machines. Considering rf-linacs the velocity of accelerated heavy ions will be in general small in comparison to the velocity of light. Therefore, due to the extremely small penetration depth thermal aspects of beam intercepting diagnostic devices become essential. Furthermore, concerning signal calculation for non-destructive pick-ups, the low velocity results in advanced electrical fields, which have to be taken into account designing pick-ups as well as the interpretation of measured signals. In case of circular machines the relativistic mass increase results in an enormous change of revolution frequency and a rather complex relation between rf-frequency and revolution time which may have consequences on the design of diagnostic systems for rings, too. Moreover, depending on the kind of extraction the time structure of the extracted beam can be very different and, considering slow extraction the beam intensity in the external beam lines can be very low. Furthermore, the necessity to separate different charge states and isotopes, generated in the ion sources as well as the need to analyze complex stripper spectra may require special design of diagnostic tools in hard- and software. In the following a short survey on heavy ion beam diagnostics will be presented discussing especially aspects related to the special characteristics of heavy ions. Although contributions are derived mainly from the GSI-facilities, a great variety of heavy ion diagnostics systems has been developed and implemented looking around the laboratories. An review of beam diagnostics in ion linacs is given in [1] and [2].

2 INTENSITY MEASUREMENTS

2.1 Rf-linacs

In most cases heavy ion beams have a time structure with macropulse lengths of some 100 μs up to some ms and a bunch structure, determined by the rather low accelerating rf of some 100 ps up to some ns . Of course, for macropulse currents below some $\mu A's$, Faraday cups are the most frequent used destructive measuring devices. Due to the very small penetration depth of heavy ions in the order of some μm , the heat transfer into cooler regions of the material and, especially to the cooling water may be not fast enough resulting in melting of the cup surface in spite of water-cooling. Some simple formulas for calculation of heat transfer, especially on short time scales are derived in [3].

Above some $\mu A's$ beam transformers offer a non-destructive absolute measurement including monitoring of macropulse shape. The design of beam transformers is discussed in detail for example in [4]. Since sensitivity, resolution, and dynamic range are related to the macropulse length, designing a transformer for heavy ion linacs may require special attention if the macropulse length is in the order of some ms .

2.2 Circular machines

Due to the wide spectrum of ion species and the flexibility of modern machines concerning time structure of the delivered beams, the intensities can be vary from some particles per second (pps) up to about some 10^{12} pps. Figure 1 shows how this wide range of charged particle fluxes can be covered by use of various techniques.

Coming from the very low intensity side, particles can be counted by hitting a scintillation material (plastics, liquids) connected to a photomultiplier. This absolute measurement of particle flux works up to about 10^5 pps using conventional scintillation material in connection with conventional signal processing methods. A very new development is the use of diamond as detector in connection with modern broadband signal processing techniques, extending the range of particle counting more than 2 decades up to some 10^8 pps (see Figure 1). Although the new method of particle counting is described detailed in [5], Figure 2 gives an impression about the capability of the new detector system.

BEAM DIAGNOSTICS, OLD AND NEW*

H. Koziol, CERN, Geneva, Switzerland

Abstract

The performance of accelerators and storage rings depends critically on the completeness and quality of their beam diagnostic systems. It is essential to equip them from inception with all the instruments providing the information on the properties and the behaviour of the beams, needed during running-in, in operation, and for development of performance towards the design goal and often well beyond. Most of the instruments have proven their worth since decades, but their power has been increased through the modern means of data acquisition and treatment. A few new instruments have made their appearance in recent years, some still under development and scrutiny for their operational value and precision. The multi-accelerator chains of today's and tomorrow's big colliders have tight tolerances on beam loss and emittance blow-up. For beam diagnostics this means a great challenge for precision and consistency of measurements all along the chain.

1 INTRODUCTORY REMARKS

Despite an all-encompassing title, evidently not all areas of beam diagnostics can be covered. Specialities like instrumentation for linear colliders, feedback-damping, beam-loss monitoring, collider luminosity measurement and ultra-fast bunch length measurement, must be left aside here. Excellent presentations were given on these subjects at recent conferences. Also, repetition of what was offered in similar review talks will be avoided.

On the other hand, some weight will be given to the diagnostics aspect of CERN's accelerator chain for the future Large Hadron Collider (LHC), and rather than giving detailed descriptions of systems and the results obtained with them, trends of evolution, challenges and open needs will be pointed out.

2 SOME EVERGREENS

It is quite amazing to see many tools of beam diagnostics of a venerable age of many decades, and even up to a century, around accelerators built with the most modern technologies. For example, Röntgen saw the first X-ray images in 1895 on luminescent screens, and still today these are one of the most basic and popular beam diagnostic means, although now more correctly called scintillator screens.

Other examples are: the Faraday-cup, to measure current or charge of beams delivered by low energy accelerators, such as RFQs; the "pepper-pot", which was

the first crude instrument for measuring emittance, also limited to low energy beams; the ionization chamber, still an appreciated means for sensitive detection of beam loss and radiation levels; secondary emission detectors in a great variety of constellations; and so on.

All these venerable detectors have undergone considerable evolution in many aspects, such as resolution, both temporal and spatial, dynamic range and sensitivity. The most remarkable advance came with the advent of digital data acquisition and treatment: with its help one can draw rather precise quantitative data from instruments which previously offered only qualitative information.

We shall mention two examples of aged instruments rejuvenated in this way: the scintillator screen and the pepper-pot.

Scintillator screens are inserted into the path of the beam by a remotely controlled mechanism. The light which is produced when the beam particles strike the screen is observed with a TV camera. The screen may have a graticule, made visible by external illumination (Fig. 1).

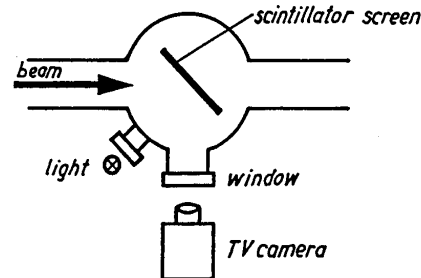


Figure 1: Typical arrangement for observation of beam position and size with a scintillator screen and a TV camera [1].

The light spot observed on a remote monitor permits rather accurate determination of beam position, to 0.5 mm under favourable conditions. One only gets a rough impression of the beam size, because the commonly used systems are driven into saturation, such that on a dark background one only sees a rather uniform white spot, the size of which depends on beam intensity and various equipment settings.

A modern version [2] will use a CCD-camera for good linearity, digital data acquisition (a "frame grabber") and treatment such that a 2-dimensional density distribution can be derived (Fig.2).

* This is essentially a repeat of "Beam Diagnostics Revisited", invited talk given at EPAC, Stockholm, June 1998.

USE OF SUPERIMPOSED ALTERNATING CURRENTS IN QUADRUPOLES TO MEASURE BEAM POSITION WITH RESPECT TO THEIR MAGNETIC CENTRE

S.A.Griffiths, D.J.Holder, N. Marks, CLRC Daresbury Laboratory, Warrington, WA4 4AD, UK.

Abstract

The positional stability of the electron beam in a modern state-of-the-art synchrotron radiation source is critical, as the many experimental users require consistency in the position and dimensions of the incoming photon beams which are incident on their experimental samples. At the Daresbury Synchrotron Radiation Source (SRS), inaccuracies in the measurements of the positions of both beam position monitors and the lattice quadrupoles can be overcome by measuring the position of the electron beam with respect to the magnetic centres of the quadrupoles. This was achieved by superimposing an alternating ('ripple') current on the direct current excitation of a single lattice quadrupole and examining the resulting beam oscillations at remote positions in the storage ring. If the electron beam is then subjected to a local distortion at the position of this quadrupole, the amplitude of the beam oscillation induced by the superimposed current is minimised (nominally zero) when the beam is at the quadrupole's magnetic centre. This paper presents details of the electrical circuit developed to inject an alternating current into the coils of individual quadrupoles and gives details of the results achieved to date.

1 BEAM POSITION IN THE DARESBUURY SRS

The Daresbury Synchrotron Radiation Source (SRS) is an electron storage ring which generates intense beams of electromagnetic radiation to support a wide range of experimental techniques. The facility parameters are given in Table 1.

Table 1: Basic parameters of the Daresbury SRS.

Electron beam energy	2 GeV
Circumference	96 m
Number of experimental stations	~ 40
Magnet lattice	FODO
Number of cells	16
Number of 'F' quadrupoles	16
Number of 'D' quadrupoles	16

The position of the electron beam in the storage ring and the emerging radiation beams are critical because:

- radiation must be supplied simultaneously to the many beam lines and users;
- users require very high beam positional stability throughout the period that they are accumulating experimental data;
- the lifetime of the stored beam should be maximised, which requires the electron beam to be accurately positioned in the centre of the narrow gap and other ring vacuum vessels.

The storage ring therefore contains vertical and horizontal electron beam position monitors (B.P.M.s) in each straight section and the beam lines have tungsten vane monitors (T.V.M.s) at their front ends for measuring the X-ray beam position. However, these all have alignment survey errors and consequentially their true positions are not known, a situation which also applies to the lattice magnets. Furthermore, it is known that all the storage ring elements move with time and hence, some time after a survey has been performed, there are even greater uncertainties concerning the positions of the B.P.M.s and the magnets. It is clear that an electron beam positioned centrally with respect to the B.P.M.s will not be central in the magnets. An off-centre beam in a dipole will not result in any first-order errors in the electron trajectories, but in the quadrupole, if the beam passes through the magnet at a vertical or horizontal position which is not coincident with the quadrupole's magnetic centre, unwanted deflections will occur. Hence the true positions of the electron beam with respect to the magnetic centres of each quadrupole is very relevant to the efficient and stable operation of the storage ring and is required information. In the measurement method described below, a deliberately induced beam deflection is used to locate the centre of the magnet with respect to the beam.

2 EXPERIMENTAL METHOD

A circulating beam in the storage ring is corrected to a central orbit, as indicated by the B.P.M.s. A small, low frequency alternating current is then superimposed on the direct excitation current in the windings of the quadrupole under investigation. If the electron beam is not central in the quadrupole, the non-zero field at the beam position will induce a small closed orbit deflection of the beam around the complete storage ring lattice; this will have a d.c. component and an oscillating component at the frequency of the alternating ripple induced in the

MEASUREMENTS WITH A VERSATILE TEST BENCH FOR THE COMMISSIONING OF THE NEW GSI HIGH CURRENT LINAC

P. Forck, P. Strehl

Gesellschaft für Schwerionenforschung, Darmstadt, Germany

Abstract

For the commissioning of the new GSI pre-stripper a conventional slit-detector system and a single shot pepper-pot system has been installed on a mobile test bench to measure intensity distributions in the two transverse phase spaces. To determine intensity distributions in the longitudinal phase space, including beam energy capacitive pickups and newly developed diamond counters have been installed on the test bench. The set-up of the test bench provides also redundant information for beam current, beam profile and beam position. The most important features of all measuring systems including signal processing and data evaluation are reported. First results from the commissioning of the upgraded pre-stripper of the UNILAC at GSI are reported.

1 INTRODUCTION

The Wideröe pre-stripper part of the UNILAC has been removed at the beginning of 1999. The new pre-stripper [1] consists of an RFQ [2] with a final energy of 120 keV/u followed by two IH structures [3] with the final energies of 743 keV/u (IH1) and 1.4 MeV/u (IH2). The commissioning of the new accelerator structures including the injector has been started in March 1999 and will be performed step by step up to October 1999 using a transportable test bench.

2 GENERAL DESCRIPTION OF THE TEST BENCH

The type of beam diagnostic elements as well as their arrangement on the test bench depends on the expected relevant beam parameters and, therefore on the section under commissioning. The following systems have been provided for installation on the bench:

- An emittance measuring system consisting of a horizontal and a vertical slit - detector, using independently movable harps as detectors. Taking advantage of this feature the resolution in divergence can be improved by intermediate steps of the harp. Additionally, measurable maximum divergences can be extended by so-called off-set positions of the harp with respect to the slit position to cover misaligned beams, too. The system is controlled by a PC including appropriate evaluation of emittance data.

- A newly designed pepper-pot system provided especially for single shot emittance measurements at higher beam energies. The system has been described more detailed in [4] and the mathematical algorithms to extract emittance data are discussed in [5].
- One beam transformer for beam current measurement and monitoring of macro pulse shape.
- One residual gas ionization monitor for nondestructive beam profile measurements.
- One profile grid to compare profiles measured with the residual gas ionization monitor.
- Two segmented capacitive pick ups to determine beam energy and energy jitter by time-of-flight (TOF) measurements as well as nondestructive beam position determination.
- A large vacuum chamber equipped with a thin scattering foil and various detectors to measure parameters in the longitudinal phase space [6].
- To stop the high intense beam, a beam stopper provided for 1.5 MW pulse power can be mounted at the end of the test bench.
- To perform destructive beam profile measurements at full beam power, a movable slit designed also for high pulse power can be mounted in front of the beam stopper.

The test bench has an overall length of nearly 3 meters and is equipped with its own vacuum pump.

3 COMMISSIONING OF THE NEW INJECTOR

Due to the low energy of 2.2 keV/u the maximum pulse power in this section is always below 2.5 kW and therefore all destructive beam diagnostic elements can be used without restrictions. Since there are no prebunchers foreseen monitors provided for measurements in the longitudinal phase space are not needed. The test bench has been equipped as shown schematically in Fig. 1.

Since matching to the RFQ requires a double waist at the RFQ-input, which will be forced by a collimator in front of the RFQ (see Fig. 1) the movable horizontal and vertical slits have been installed just at the position of this waist.

Determination of Radial Ion Beam Profile from the Energy Spectrum of Residual Gas Ions Accelerated in the Beam Potential

R. Dölling, Institut für Angewandte Physik der Universität Frankfurt, D-60054 Frankfurt, Germany
(now at Paul Scherrer Institut, CH-5232 Villigen-PSI, Switzerland)

Abstract

Residual gas ions (RGI) created from collisions of positive beam ions (BI) with residual gas atoms are accelerated out of the ion beam by its space charge potential. It is demonstrated that with one-dimensional radial symmetry the radial distributions of BI density and space charge potential can be determined from the energy distribution of RGI radially leaving the beam tube. RGI energy spectra were taken with an electrostatic analyser of Hughes-Rojansky type on a 10 keV 1.5 mA He⁺ beam. For comparison the radial BI density distribution was determined with a radial wire probe, an electron beam probe and a beam transport calculation based on an emittance measurement located downstream.

1 INFORMATION INCLUDED IN RGI ENERGY SPECTRA

1.1 Dependencies of BI number density, current and space potential

Cylindrical symmetry is assumed throughout. We start from a positive ion beam with radial distribution of number density $n_{BI}(r)$ inside a tube of radius r_{wall} . The space potential is defined to be zero at r_{wall} . The beam current inside radius r is given by

$$I_{BI}(r) = \frac{k q_{BI}}{\epsilon_0} \int_{r'=0}^r n_{BI}(r') r' dr' \quad (1a)$$

with $k \equiv 2\pi\epsilon_0 v_{BI}$ and q_{BI}, v_{BI} charge and velocity of BI. The total beam current is defined as $I_{BI_{tot}} \equiv I_{BI}(r_{wall})$.

The space potential follows from the Maxwell-Eq. as

$$\Phi(r) = \frac{1}{k} \int_{r'=r}^{r_{wall}} \frac{I_{BI}(r')}{r'} dr'. \quad (2a)$$

(It is assumed that the contribution of other particle species to the space potential is negligible. This is true for RGI if the residual gas density is low. For electrons this is valid as long as space-charge compensation does not occur or is suppressed.)

Differentiation of Eq. (2a) and looking at Φ instead of r as the independent variable yields the current from that part of the beam where the potential is higher than Φ :

$$I_{BI}(\Phi) = -k \frac{r(\Phi)}{\frac{dr(\Phi)}{d\Phi}}. \quad (3a)$$

In practice Eqs. (1a), (2a) and correlation of the results are sufficient to calculate $I_{BI}(\Phi)$ from $n_{BI}(r)$.

To perform the calculation in the opposite direction Eqs. (1a), (2a) are rewritten by differentiation as

$$n_{BI}(r) = \frac{\epsilon_0}{q_{BI}} \frac{1}{k r} \frac{dI_{BI}(r)}{dr} \quad (1b)$$

$$I_{BI}(r) = -k r \frac{d\Phi(r)}{dr} \quad (2b)$$

and Eq. (3a) is rewritten by integration

$$-k \int_{\Phi'=0}^{\Phi} \frac{1}{I_{BI}(\Phi')} d\Phi' = \int_{\Phi'=0}^{\Phi} \frac{\frac{dr(\Phi')}{d\Phi'}}{r(\Phi')} d\Phi' = \ln \frac{r(\Phi)}{r_{wall}}$$

and expressing as the exponent

$$r(\Phi) = r_{wall} e^{-k \int_{\Phi'=0}^{\Phi} \frac{1}{I_{BI}(\Phi')} d\Phi'}. \quad (3b)$$

In practice Eq. (3b) and correlation of its results to $I_{BI}(\Phi)$ together with Eq. (1b) are sufficient to calculate $n_{BI}(r)$ from $I_{BI}(\Phi)$.

1.2 Energy spectrum of RGI at the beam tube wall

A residual gas present in the beam tube undergoes ionisation and charge exchange by the BI. RGI are produced at a local source strength

$$\dot{n}_{RGI}(r) = n_{BI}(r) n_{RGA} \sigma_{RGI} v_{BI} \quad (4)$$

with σ_{RGI} production cross section of RGI. (The number density of gas atoms n_{RGA} is assumed to be homogeneous. This holds as long as thinning of the background gas by the ionisation can be neglected. This is the case if

$$\frac{2 I_{BI_{tot}} \sigma_{RGI}}{\pi r_{beam} q_{BI} \langle |v_{RGA}| \rangle} \ll 1 \quad (5)$$

with r_{beam} radius of the ion beam and v_{RGA} thermal velocities of gas atoms.)

From Eqs. (4), (1a) follows the line current (along the beam) of RGI produced inside radius r (or at potentials higher than $\Phi(r)$) as

500 FS STREAK CAMERA FOR UV-HARD X RAYS IN 1KHZ ACCUMULATING MODE WITH OPTICAL -JITTER FREE- SYNCHRONISATION

K.Scheidt and G.Naylor, ESRF, Grenoble France

Abstract

The development at the ESRF of a jitter-free, laser triggered Streak Camera has now yielded time resolution results as short as 460fs while operating in accumulating mode. The so-called jitter-free synchronisation between the laser light and the Streak Camera is performed through a GaAs photo-switch in a simple HV circuit that connects directly to the Streak tube's deflection plates.

The novelty of this technique permits to obtain excellent dynamic range measurements in a shot-to-shot accumulation of ultra fast (laser stimulated) events at up to 1Khz without degrading the time resolution.

Important insight was obtained on the quality of this optical synchronisation and its dependence on the laser characteristics, the switch circuit, and the structure of the GaAs switch itself. This permitted to suppress the jitter causes and today the 500fs limitation is imposed by the streak tube's intrinsic time resolution. This work was done by measuring (with Au or Pd photo-cathodes) the 3rd harmonic (i.e. 267nm) of a 100fs Ti:Saph laser.

Also important progress was made with the reliability of the photo-switch and problems of HV break-down and structural degradation have been completely resolved.

Since the principal use of this system at the ESRF is in ultra-fast X-ray diffraction experiments the exchangeable photo-cathode structure of this tube covers the entire UV-to-X-rays spectrum. The QE of various photo-cathode materials was measured in the 8-30KeV range.

1 MOTIVATION & INTRODUCTION

1.1 Ultra fast Pump-Probe X-ray experiments

A number of ultra-fast time-resolved X-ray scattering experiments can now benefit from both the ESRF unrivalled high brilliance X-ray source and state-of-the-art ultra-fast laser and detector technology. [1] In such an experiment a broad X-ray pulse (typ. 100picosec) probes the structure of the sample under study (e.g. a crystal) while an ultra-short (typ. 100femtosec) laser pulse ($\lambda=200-1000\text{nm}$ by an OPA) triggers an ultra-fast reaction in it (see fig.1). The latter becomes apparent by a modification of the diffracted X-ray beam. An X-ray Streak Camera having this beam centered on its photo-cathode will measure the broad probe pulse while the ultra-fast modulation contained in it will be detectable

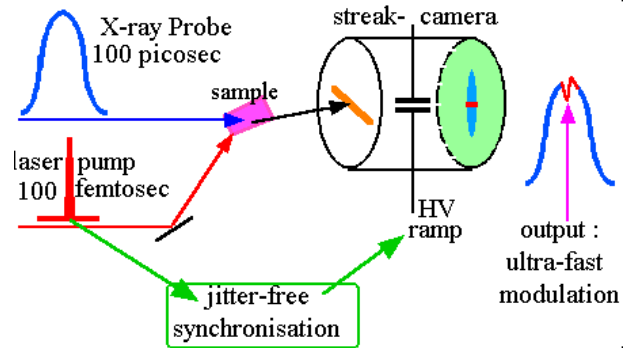


Fig.1 Pump-Probe experiment with Streak Camera optically synchronised

within the time resolution limits of the Streak Camera.

This intrinsic time resolution for X-rays has been measured independantly at the INRS with an ultra-fast 3KeV source and is estimated at below 700femtosec. [2]

1.2 Accumulation for High Dynamic range

However, in single-shot operation the dynamic range of the obtained data will be extremely limited as the intra-tube space charge effects only allow small input photon flux per shot to avoid the loss of the tube's intrinsic time resolution. This is a general problem with all ultra-fast streak cameras.

The requirement for the above experiments of high quality data to discern relatively weak signals within it make operation in repetitive, accumulation mode imperative. However, the effective time resolution of the system in accumulation mode would be impaired unless the un-precision of the trigger synchronisation, or the so-called jitter, would be negligible compared to the tube's time resolution.

2 JITTER-FREE SYNCHRONISATION THROUGH PHOTOSWITCH

The innovation in this system is to obtain this synchronisation optically between the Streak Tube and laser pump pulse by the use of a photo-conductive switch and to attain a truly jitter-free performance.

The generation of the High Voltage Sweep Ramp on the Streak Camera's deflection plates is directly triggered by the laser light on the photo-switch. Its transition to a conductive state is essentially instantaneous and for a perfectly stable ultra short laser

BUNCH LENGTH MEASUREMENTS IN LEP

A. J. Burns, H. Schmickler, CERN, Geneva, Switzerland

Abstract

For many years a streak camera has been used for observing the longitudinal distribution of the particles in any LEP e^+ or e^- bunch (5-50 ps r.m.s. length) on a turn by turn basis, using synchrotron light. In 1996, a comparison made with the longitudinal vertex distributions of 3 LEP experiments allowed the identification and elimination of certain systematic errors in the streak camera measurements. In 1997, a new bunch length measurement technique was commissioned that uses the high frequency slope of the bunch power spectrum from a button pickup. In 1998, this new method was confronted with measurements from the streak camera and the LEP experiments. The measurements made in 1996 and 1998 are presented, with emphasis on the calibration of the two instrumental methods and their respective precision and limitations.

1. STREAK CAMERA SET-UP

Synchrotron light pulses are produced when e^+ and e^- bunches pass through small wiggler magnets on either side of intersection point 1 of LEP [1]. The visible light is extracted by two thin beryllium mirrors and focused on a double sweep streak camera [2] in an underground optical laboratory [3]. The optical set-up allows the simultaneous observation of the *top* and *side* views of any photon bunch from both LEP beams within the same fast sweep [4]. The photon bunch length and longitudinal density distribution corresponds to that of the particle bunch that emitted it. The slow sweep allows up to 100 fast sweeps to be recorded on one image, which can be used to follow successive bunch passages. Although originally requiring local manipulation, the camera can now be fully operated via the control system network [5]. Bunch dimension averages are transferred every 10 s to the LEP measurement database, and a high bandwidth video transmission allows the streak camera images and processed results to be viewed in real time (at 25 Hz) in the LEP control room (Figure 1).

2. STREAK CAMERA BUNCH LENGTH MEASUREMENTS (1995-96)

During an experiment to investigate the LEP machine impedance in August 1995, the lengths of very low current ($3\mu\text{A} \equiv 2 \cdot 10^9 e^+$) bunches were measured. This was the first reliable indication of the existence of a 10 mm^2 offset in the square of the bunch length measured by the streak camera (Figure 2).

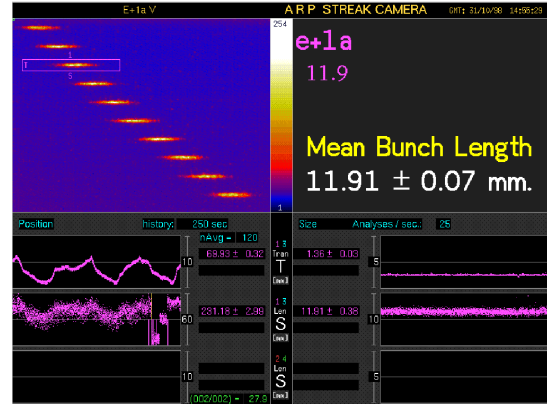


Figure 1: Control room video display updated at 25Hz.

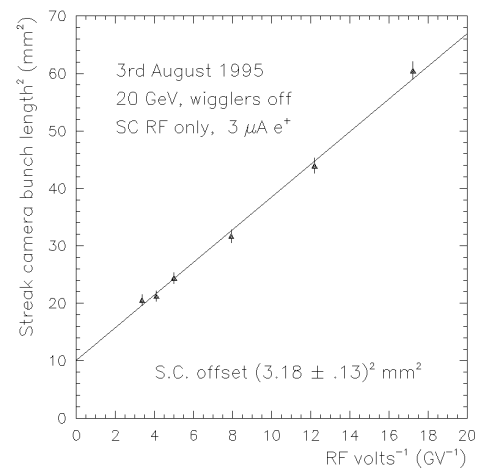


Figure 2: Streak camera bunch length² as a function of inverse RF total voltage at 20 GeV (August 1995), showing clearly the 10 mm^2 offset present at that time.

As the bunch current was well below the turbulent threshold at which bunch length starts to rise with current, the r.m.s. bunch length in metres, σ_s , is given by:

$$\sigma_s = \frac{\alpha_c R \sigma_E}{Q_S E} \quad (1)$$

where α_c is the momentum compaction, R the radius of LEP, Q_S the synchrotron tune, and σ_E/E the relative r.m.s. beam energy spread.

Using the relation $Q_S^2 \propto V_{RF}$ where V_{RF} is the total RF voltage per turn (which has been experimentally verified to apply up to 45 GeV) one obtains:

$$\sigma_s^2 \propto \frac{1}{V_{RF}} \quad (2)$$

DARESBUURY SRS POSITIONAL FEEDBACK SYSTEMS

S. L. Smith and S. F. Hill , CLRC Daresbury Laboratory, Warrington, WA4 4AD UK.

Abstract

The Daresbury SRS is a second generation synchrotron radiation source which ramps from its injection energy of 600 MeV to 2.0 GeV. Beam orbit feedback systems have been in routine operation on the SRS since 1994 and are now an essential element in delivering stable photon beams to experimental stations. The most recent enhancements to these systems have included the introduction of a ramp servo system to provide the orbit control demanded by the installation of two new narrow gap insertion device and development of the vertical orbit feedback system to cope with an increasing number of photon beamlines. This paper summaries the current status of these systems and briefly discusses proposed developments.

1 INTRODUCTION

Orbit position control has been employed at Daresbury to stabilise the photon beam position routinely since 1994. The global horizontal feedback system [1] has been in routine operation for many years and uses a simple inversion of the 16 x 16 response matrix to apply a correction every 30 sec. A global vertical orbit feedback [2] has now replaced the individual local servo systems [3] that pioneered vertical orbit correction for beamlines on the SRS. This global vertical system provides orbit control using tungsten vane monitors (TVMs) at all commissioned ports and will allow expansion of correction to new beamlines including two new multipole wiggler (MPW) sources. A consequence of the introduction of these MPWs and their associated small aperture vessels was an increased requirement for orbit control during the energy ramp. This has been provided by a flexible, automatic orbit control program [4], which runs a dual plane global feedback system using the electron beam position monitors (BPMs).

2 HORIZONTAL GLOBAL FEEDBACK

The global horizontal feedback system reads the horizontal electron orbit at 16 BPMs and applies a global correction at the 16 steering magnets (HSTRs), the strength of the correction is determined by a straight inversion of the steering magnet response matrix. The orbit is read and a correction is applied every 30 sec. This system has been in used on the SRS for many years and considerable experience has been gained. The system has been highly successful in suppressing the orbit shape distortions, although the average radius change is not

corrected. This is because the machine orbit is relatively insensitive to changes in the average position of quadrupole magnets and as a result correction of this orbit component is vulnerable to systematic movements in the BPMs. The global horizontal feedback system corrects all the BPMs to the average of the 16 BPMs, within a precision of the order of the BPM resolution (better than 5 μ m). The latest work on this system has concentrated on dealing with the malfunction of an individual BPM. Clearly with only 15 monitors and 16 correctors a simple matrix inversion is no longer applicable, however it has been shown that an SVD algorithm provides a good solution to the missing BPM problem and work is currently underway to integrate this algorithm and the detection of BPM problems into the global feedback system.

3 VERTICAL GLOBAL FEEDBACK

Currently the global servo system includes TVMs on dipoles 1,2,3,4,6,7,8 and 13, super-conducting wigglers in straights 9 and 16 and an undulator in straight 5. Each port has one TVM except super-conducting wiggler, W16, which has two TVMs at different distances from the source however, the beam is only steered to one of these two monitors. TVMs were fitted as close as possible to the typical experiment distance but this can be anything from 3 - 15 m. So the vertical global feedback in the SRS could potentially use 11 photon monitors and 16 vertical BPMs, with correction supplied by up to 2 x 16 vertical correctors.

An EXCEL program was used as a flexible development environment. This program was designed to provide on-line correction and servo feedback of the orbit together with off-line simulation.. A singular value decomposition, SVD, routine was used to "invert" the appropriate measured orbit response matrix of the corrector magnets at the chosen monitors.

The photon monitors were used for feedback because of problems with the position stability of the vertical BPMs due to thermally induced movements of the vessels. Simulations and beam tests were carried out using 32 and 16 vertical correctors. It was determined that the use of only one family of 16 correctors was adequate to correct the orbit at one TVM on each of the 11 ports.

A simplified version of the correction program has been used for operations. The system has been designed to deal with the slow drift in orbit due to thermal effects in the machine that can be several 100 microns over a stored beam of up to 23 hours duration. Although it would be possible to run at around 2 second update, a

DEVELOPMENTS AND PLANS FOR DIAGNOSTICS ON THE ISIS SYNCHROTRON.

C M Warsop, D J Adams, K Tilley, Rutherford Appleton Laboratory, Oxfordshire, UK.

Abstract

Developments of diagnostics on the 800 MeV High Intensity Proton Synchrotron of ISIS, the Spallation Neutron Source at the Rutherford Appleton Laboratory in the UK, are described. Recent upgrades to instrumentation and control computers have made much more information readily available, which is valuable for control of a loss limited, high intensity machine. Measurements on high intensity beams have fundamental limitations in terms of accuracy, detail and interpretation. However, it is found that use of specially configured low intensity *diagnostic beams* can provide much detailed information not otherwise available, which is extremely valuable after careful interpretation. The methods and systems being developed to help trouble shooting, to find optimal conditions rapidly and systematically, and to improve understanding of high intensity performance are described.

1. INTRODUCTION

Previous papers [1,2,3] have detailed diagnostics developments and progress on the ISIS Synchrotron. Here, overall progress and plans are reviewed. In particular, specialist methods developed in the context of optimising a high intensity machine are highlighted.

The ISIS Synchrotron cycles at 50 Hz, accelerating 2.5×10^{13} protons per pulse from 70 to 800 MeV. Mean beam current and power are 200 μ A and 160 kW respectively. The 22 mA H⁻ injector beam is stripped to H⁺ with an aluminium oxide foil as it enters the ring acceptance; $\sim 2.8 \times 10^{13}$ protons accumulate over the 200 μ s, 120 turn injection process. 2D transverse phase space painting minimises the space charge effects. The initially unbunched beam is trapped and accelerated to 800 MeV in 10 ms by the h=2 RF system. There are six ferrite-tuned RF cavities, which provide up to 140 kV/turn and sweep over 1.3-3.1 MHz. Beam is extracted in a single turn with a fast kicker and transported to the target.

Running intensity is limited by the maximum tolerable losses, which are carefully controlled to keep activation levels low enough for hands on maintenance. Dominant losses of 10 % occur in the first 2 ms of acceleration and are a result of non-adiabatic trapping and space charge. These loss levels depend critically on many parameters, which require careful optimisation. Methods for measuring, optimising and understanding these parameters are the aim of this work.

2. DIAGNOSTICS AT HIGH INTENSITY

2.1 Type and Use of Diagnostics

The ISIS Synchrotron was built with a comprehensive suite of diagnostic devices [4], including 15 capacitive position monitors per plane, residual gas profile monitors, intensity toroids and 40 beam loss monitors spread around the circumference. These give much beam information, including detailed measurement of losses, which ultimately determine running intensity. The beam is set up so that loss levels, times and locations are within strict limits; most is localised on the collector system. Standard use of these devices at high intensity has been very effective over the years, and allowed ISIS to run beyond its design intensity.

Two developments, using the same diagnostic devices, are now making much more information available: improved data acquisition and use of low intensity beams. It is expected that the more detailed knowledge of the machine this gives will allow more consistent running at the highest intensities.

2.2 High and Low Intensity Diagnostics

Though diagnostics on high intensity beams provide much essential information, they do not give all that is available and important. A high intensity beam often fills a large fraction of the available acceptances. This means that any measurement of the, necessarily small amplitude, coherent motion, is of limited accuracy. Generally, much detailed motion is masked from external observation by incoherent motion of particles. Equally importantly, observed motion is also difficult to interpret because of high intensity effects. As a result, the ability to measure many beam parameters in detail, most of which affect high intensity running, is severely limited.

Many of these problems can be overcome with a specially configured, low intensity *diagnostic beam*, which occupies a small fraction of the ring acceptances. Large coherent oscillations can be accurately measured, with negligible high intensity effects, providing detailed information not otherwise available.

Parameters measured at high and low intensity are not generally comparable, but they are complementary; with correct treatment differences illuminate high intensity effects. Comparison of measurements at varying levels of intensity is also valuable. Low intensity diagnostics are valuable probes of 'zero intensity' beam dynamics, and

THE ELETTRA STREAK CAMERA: SYSTEM SET-UP AND FIRST RESULTS

M. Ferianis, Sincrotrone Trieste, Trieste, Italy

Abstract

At ELETTRA, a Streak Camera system has been installed and tested. The bunch length is a significant machine parameter to measure, as it allows a direct derivation of fundamental machine characteristics, like its broadband impedance. At ELETTRA the Light from a Storage Ring Dipole is delivered through an optical system to an Optical Laboratory where it can be observed and analysed.

The Streak Camera is equipped with different time-bases, allowing both single sweep and dual sweep operation modes, including the Synchroscan mode. The Synchroscan frequency equal to 250 MHz, which is half of the ELETTRA RF frequency, allows the acquisition of consecutive bunches, 2ns apart. To fully exploit the performances of the Streak Camera, an optical path has been arranged which includes a fast opto-electronic shutter. By doing so, the optical power deposited on the photo-cathode is reduced in the different ELETTRA fillings.

1 INTRODUCTION

The bunch length measurement on Storage Rings has to be non-destructive; therefore a classical approach to the problem is to measure the length of the Synchrotron Light Pulses generated by the transversely deflected electrons, as it happens in the Bending magnets (Dipoles).

This is correct as the light pulses propagating from the source point to the measurement point preserve, in their longitudinal profile, the electron longitudinal distribution, that is the Bunch Length (σ_b).

In third generation light sources, this measurement is critical due both to the very short duration of the synchrotron light pulses, which lies in the range of Pico-seconds, and to the low energy per pulse available.

Streak Cameras are routinely used as powerful diagnostics tools in both linear (usually observing Transition Radiation rather than Synchrotron Radiation) and circular accelerators.

The main features of a Streak Camera are:

- Pico-second resolution, even in Single Shot
- very high (100s of MHz) repetition rate of the fast sweeps with dual-sweep "Synchroscan" mode
- high sensitivity, thanks to built-in photo multiplier

2 SYSTEM SET-UP

At ELETTRA the Light from a Storage Ring Dipole [1] is delivered through an optical system to an Optical Laboratory: the first vacuum mirror allows only the Visible and near-UV part of the Synchrotron Light

Spectrum to be used. Beside a Transverse Profile Monitor system [1], other instruments [2, 3 and 4] have been installed and tested. Bunch Length measurements have been already performed [5], both with a Streak Camera and an Ultra-Fast Photodiode.

At ELETTRA, a Streak Camera (SC), specifically manufactured by Photonetics [6], has been recently installed and successfully tested [7,8].

The basic operating principle of a SC is a time-to-space conversion of ultra-fast optical events. The incoming photons are converted into electrons by a photo cathode. The emitted electrons are accelerated and deflected by a high-voltage fast ramp applied to deflection electrodes.

As a result, electrons are streaked out on the back-end phosphor screen creating a strip, whose length is proportional to the duration of the photon bunch. The image formed on the phosphor screen is amplified with a Micro Channel Plate (MCP) image intensifier and acquired by a CCD camera.

The ELETTRA SC is equipped with different sweep Units [9], which allow the following operation modes:

- single sweep, providing $<2\text{ps}_{\text{FWHM}}$ resolution
- dual sweep, with Synchroscan Unit at 250MHz

Synchroscan is a deflection technique, widely used in streak cameras, where the high-voltage deflection is driven by a sinusoid rather than a saw-tooth ramp. Thanks to the narrow-band deflection signal, the linearity of the high-voltage deflection amplifier is more easily achieved than in a wide-band amplifier, which is needed for a saw-tooth linear deflection.

The Single sweep unit (FTSU-1) provides the following full-screen deflections: 176ps, 441ps, 882ps, 1.7ns, 4.4ns, 8.8ns and 17.6ns, with $<2\text{ps}_{\text{FWHM}}$ resolution.

The Synchroscan unit (FSSU-1) operates at a frequency of 250MHz (res.= $3.2\text{ps}_{\text{FWHM}}$). The Secondary sweep units (FTSU-2 and STSU-2), used for vertically displacing successive Synchroscan traces, can cover the range from 9.15ns to 69.35ms.

3 THE OPTICAL PATH

The optical path (partial view shown in fig.1) performs the following operations on the synchrotron light:

1. deflection and focusing onto the SC input pin-hole (with 50, 100 or 200 μm diameter)
2. band-pass ($\lambda=500\text{nm}$) filtering and attenuation
3. shutter for interlock purposes
4. optical power reduction

The reduction of the optical power on the time scales typical of a SC is not a straightforward task.

ADAPTIVE OPTICS FOR THE LEP 2 SYNCHROTRON LIGHT MONITORS

G. Burtin, R.J. Colchester, G. Ferioli, J.J. Gras, R. Jung, J.M. Vouillot
 CERN, Geneva, Switzerland

Abstract

The image obtained with the LEP synchrotron radiation telescopes deteriorates, giving multiple and deformed images, when the beam energy goes beyond 80 GeV at beam currents above 2 mA. This problem is due to the deformation of the light extracting beryllium mirror, by as little as 1 μm , and had been predicted at the design stage. To overcome this problem, several changes together with an adaptive optics set-up have been introduced. These essentially consist of a cylindrically deformable mirror to compensate the cylindrical deformation of the beryllium mirror and a movable detector to compensate the spherical deformation. Both components are continuously adjusted as a function of beam current and energy.

1. INTRODUCTION

Four Synchrotron Radiation (SR) telescopes are installed in LEP around IP8 [1]. For each particle type there are two telescopes, one of them looks at the light emitted in the first normal dipole at the exit of the experimental straight section, where the Dispersion is very small, and one is located in the arc where the Dispersion is large: Fig. 1. With the data from the two telescopes it is possible to calculate the emittances and the energy spread of the beam for both horizontal and vertical directions.

The long distance between the telescopes and the accessible area in IP8 means that the telescopes have to be self-contained units incorporating all tuning facilities by remote control.

The optical set-up, the detector and the image signal processing have been optimised during the LEP 1 running period to provide the profile measurements with best precision [2]. The achieved accuracy has been established during cross-calibration runs by comparison with the wire scanners and the luminosity detectors of the experiments. The agreement of the vertical emittances determined by the different instruments has been demonstrated to be within $0 \pm 0.1\text{nm}$ [3].

2. THE LEP 1 SR TELESCOPES

Each telescope is mounted on a standard 3.2 m optical bench housed inside a 3.5 m stainless steel tube for stability and protection. The telescope uses a spherical mirror, with a focal length of 4 m, as imaging device. A Magnification $G = 0.2$ is achieved with the help of folding mirrors. Chromatic filters, polarisation selection filters and linear density filters are incorporated in the set-up to control the wavelength, the polarisation components and to match the light intensity to the detector sensitivity to give the highest dynamic range.

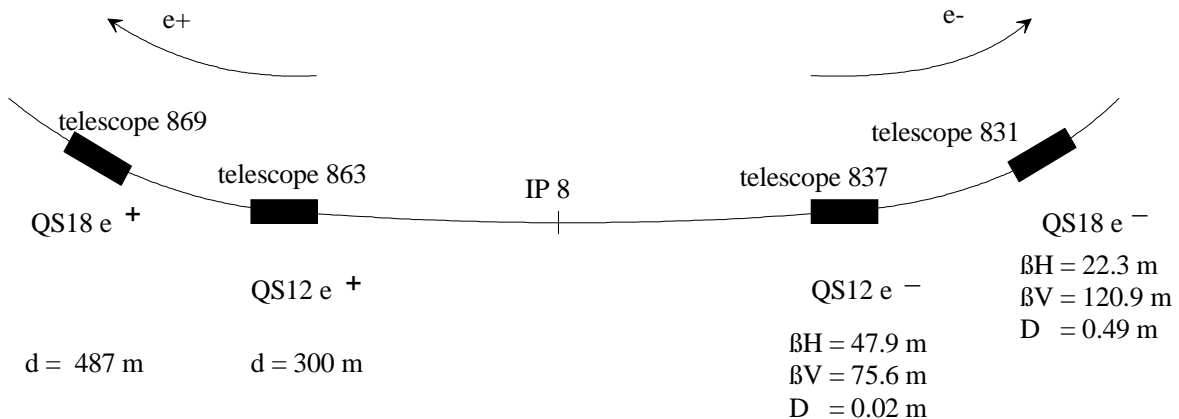


Figure 1: Layout of the Synchrotron Radiation Telescopes in LEP.

LUMINOSITY OPTIMIZATION IN DAΦNE

F. Sannibale for the DAΦNE Commissioning Team¹, INFN LNF, Frascati, Italy

Abstract

DAΦNE the Frascati Φ-factory, started the two beams commissioning on March 1998. Since then a relevant amount of experience concerning the techniques and procedures for optimizing the luminosity has been acquired. All the schemes used are strongly based on the use of various diagnostic systems including a dedicated luminosity monitor, orbit measurement, tune monitor, synchrotron light monitor and others. A summary of the used techniques, with accent on the diagnostic aspects, is presented.

1 INTRODUCTION

DAΦNE is an electron-positron collider with separated vacuum chamber rings and two interaction regions (IR) with horizontal crossing angle [1]. The main design parameters are listed in Tab. 1, while a general lay-out is shown in Fig. 1.

Table 1: DAΦNE Design Parameters

Energy	510 MeV/beam
Single Bunch Luminosity	$4.4 \cdot 10^{30} \text{ cm}^{-2} \text{ s}^{-1}$
Multibunch Lum. (30/120 bunches)	$1.3/5.3 \cdot 10^{32} \text{ cm}^{-2} \text{ s}^{-1}$
Beam-beam Tune Shift (H/V)	0.04/0.04
Ring Length	97.69 m
Dipole Bending Radius	1.4 m
Natural Emittance	10^{-6} m rad
Coupling	0.01
Natural Relative Energy Spread	$4 \cdot 10^{-4}$
r.m.s. Bunch Length	$3 \cdot 10^{-2} \text{ m}$
Damping Times (L/T)	17.8/36.0 ms
Beta Functions @ IP (V/H)	4.5/450 cm
Horizontal Crossing Angle	10-15 mrad
Particles/Bunch	$8.9 \cdot 10^{10}$
Number of Bunches	30÷120
RF Frequency	368.26 MHz

The center of mass energy of the beams is tuned on the mass of the Φ meson in order to study the rare phenomenon of the CP violation that can appear when the Φ's decay in neutral kaons. In order to collect sufficient statistics a very high integrated luminosity is required.

¹ DAΦNE Commissioning Team: M.E. Biagini, C. Biscari, R. Boni, M. Boscolo, V. Chimenti, A. Clozza, G. Delle Monache, S. De Simone, G. Di Pirro, A. Drago, A. Gallo, A. Ghigo, S. Guiducci, F. Marcellini, C. Marchetti, G. Mazzitelli, C. Milardi, L. Pellegrino, M.A. Preger, R. Ricci, C. Sanelli, F. Sannibale, M. Serio, F. Sgamma, A. Stecchi, A. Stella, C. Vaccarezza, M. Vescovi, G. Vignola, M. Zobov.

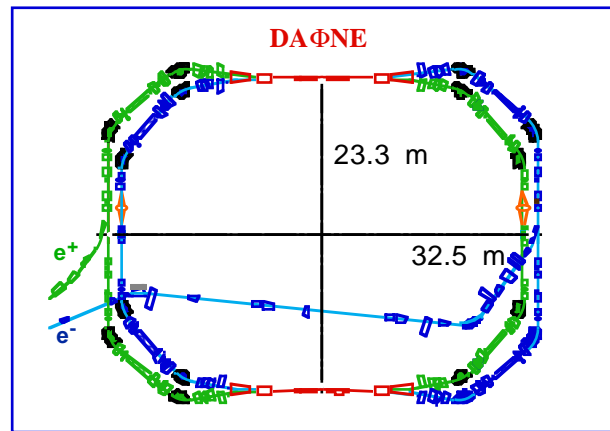


Figure 1: DAΦNE Main Rings Lay-out.

The luminosity commissioning of DAΦNE was organized in two different phases. During the first period, that started on March 1998 and ended on November 1998, the main goal was to obtain a single bunch luminosity of $10^{30} \text{ cm}^{-2} \text{ s}^{-1}$ as a test of the machine capabilities. In order to gain enough comprehension and operational experience, the IR was equipped with a provisional insertion in which all the quadrupoles in the low-beta triplets were normal conducting, instead of permanent magnet type, the vacuum chamber was instrumented with a beam position monitor (BPM) just at the IP and with additional BPM's of electrostatic (button) and directional (strip-line) types. No experiment detector was present at that time. A four months shutdown period followed, during which the CP violation experiment KLOE [2] was installed with its detector totally immersed in the magnetic field of a ~6 m diameter superconducting solenoid. The second phase of the two beams commissioning started few weeks ago, on April 1999, with the solenoidal magnetic field (2.4 Tm) of the detector on. At the low energy of DAΦNE, this field creates a strong perturbation that must be carefully compensated. The compensation operation was successfully performed in few days and since April 14, the KLOE detector is collecting Φ events, making of DAΦNE the first factory running physics. Table 2 shows the main results so far obtained.

Table 2: DAΦNE Achieved Results

Single Bunch Luminosity	$1.4 \cdot 10^{30} \text{ cm}^{-2} \text{ s}^{-1}$
Multibunch Luminosity (13 bunches)	$1.5 \cdot 10^{31} \text{ cm}^{-2} \text{ s}^{-1}$
Particles/Bunch	$2.3 \cdot 10^{11}$
30 bunches Stored Current (e ⁺ /e ⁻) (design: 1.1 A)	0.56/0.54 A
Integrated Luminosity to KLOE Experiment (May 12, 1999)	30 nb^{-1}

REAL TIME DISPLAY OF THE VERTICAL BEAM SIZES IN LEP USING THE BEXE X-RAY DETECTOR AND FAST VME BASED COMPUTERS

Jones, R.; Manarin, A.; Pignard, G.; Rossa, E.; Schmickler, H.; Sillanoli, M.; Surback, C.
SL Division- European Laboratory for Particle Physics (CERN) - Geneva - Switzerland

Abstract

Fast X-ray detectors based on CdTe photoconductors have been installed in LEP since the beginning of its operation in 1989. The angular divergence of the high energy photons from the synchrotron radiation (x-rays) and the narrow spacing of the 64 photoconductors of the detector allow a good measurement of vertical beam profiles down to an rms beam size of 300 μm .

This paper presents some specific parameters and experimental results of an upgrade program in which the local processing power of the front-end electronics has been increased by a factor 50. Such a powerful tool has allowed a real time display of the time evolution of the vertical beam sizes. An online correlation plot between the electron and positron beam sizes (turn by turn) is also displayed.

These online video images are available in the LEP control room and are used in daily operation for luminosity optimisation.

1. PRINCIPLE OF THE DETECTOR

The vertical beam sizes in LEP are measured, in single shot, by a photoconductive device known as the BEXE detector. A detailed description of this detector can be found in references [1] to [6]. Figure 1 gives an overview of the whole system. The synchrotron X-rays emitted by the bunches give an image of the vertical beam profile via the 64 channels of the detector [3]. All these signals are digitised by 8 bits Flash ADCs. The digitised raw data are used in two ways. One set is sent to the old master crate working with a 68k-CPU. This produces a PAL video image, which was used by the main control-room for daily operation during the commissioning of the slave crate. A copy of the data is also sent to the new slave crate, which uses a Power-PC running under LYNX-OS for the data analysis. This increases the processing power by a factor 50. The raw-data are analysed very quickly and sent through a dedicated video channel to the main-control room, thus providing a real time display of the results.

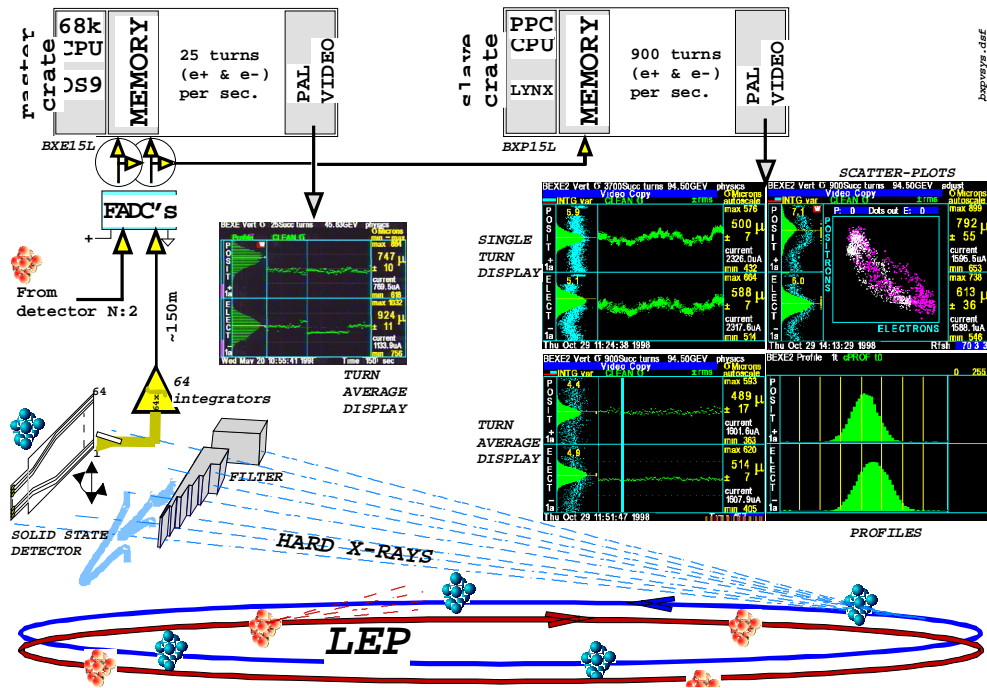


Figure 1: Synoptic of the whole.

THE OTR SCREEN BETATRON MATCHING MONITOR OF THE CERN SPS

C. Bovet, R.J. Colchester, G. Ferioli, J.J. Gras, R. Jung, J.M. Vouillot
CERN, Geneva, Switzerland

Abstract

In order to satisfy the stringent emittance requirements of LHC, betatron matching monitors, based on multiturn beam profile measurements, have been proposed for the SPS and LHC. A test monitor has been installed for evaluation in the CERN SPS first in 1996 and improved in 1997. It is based on an OTR screen and a fast beam profile acquisition system. It has been used with proton beams to assess the quality of the betatron matching from the PS to the SPS in 1998. Experience and results are presented.

1. INTRODUCTION

During the many transfers needed in the injector chain for the LHC it is vital to preserve the highest possible phase space density by avoiding emittance blow-up due to mismatch of beam optics. With bunch to bucket transfer from one circular machine to the next, the loss of phase space density results from filamentation of bunches which are not well placed and shaped in the 6-dimensional phase space.

Filamentation which is responsible for the emittance blow-up, does not occur in transfer lines where the chromaticity is too small to give significant phase shifts in a single passage. If the transfer line aperture is large enough, no blow-up or beam loss should happen and therefore matching becomes a real issue only when the beam reaches the next circular machine.

Twelve parameters are needed to adjust the centre and the shape of beam ellipses in the three phase planes. Adjusting to theoretical values is a good first approximation and is, of course, implemented at the beginning to get a circulating beam. But a final transfer optimisation can best be achieved by the fine tuning of some elements in the transfer line, as a function of observations made on the beam circulating after injection:

- i) the injection trajectory in 6-dimensions ($x, x', y, y', z, Dp/p$) is optimised by minimisation of coherent oscillations measured with beam position monitors;
- ii) in longitudinal phase plane, ellipse matching is obtained by minimising quadrupolar oscillations that can be observed with a wide-band pick-up;
- iii) transverse phase plane matching is traditionally done by observing the beam size with three detectors in

the transfer line, separated by known optical conditions and relying on the optical matching of the transfer line to the downstream circular machine. But values obtained from MAD for the Courant & Snyder invariants cannot be trusted, since those invariants are, in reality, sensitive to all magnet imperfections which are not known to the optics modelling program. LEP has shown beta beating of up to 40% !

The diagnostic method proposed for performing the third step mentioned above, does not rely on a precise knowledge of machine optics. The idea is to observe the beam for many turns, after its injection in the considered circular machine, with the help of a single detector.

A detailed simulation of the process is described in Ref. [1] where the cases of SPS and LHC are exemplified with realistic machine optics, beam properties and existing detector characteristics, and the effect of multiple scattering in the detector is rigorously taken into account. Thin screens observed with a CCD camera working in a fast acquisition mode, are proposed as a practical solution for the detector. It is an inexpensive and extremely powerful solution. After the number of turns necessary for data taking, the beam is dumped to protect the detector from overheating and to reduce the flux of secondaries produced in nuclear interactions. The beam energy loss due to dE/dx is less than one per mil even after 80 turns and can be taken into account in the data analysis.

2. DIAGNOSTIC PRINCIPLE

Betatron matching at injection is traditionally done using the knowledge of the beam emittance measured either in the previous machine or in the transfer line and the knowledge of the optics of the machine where the injection takes place. Regardless of the care put into the process, this methodology has a weak point with large accelerators where beta-beating can alter completely the invariants of motion obtained from a computation of the machine optics with ideal quadrupoles. The resulting emittance blow-up cannot be avoided and will, in most cases, be measured only after filamentation, with beam profile monitors like wire scanners or synchrotron radiation telescopes.

PRELIMINARY TEST OF A LUMINESCENCE PROFILE MONITOR IN THE CERN SPS

J. Camas, R. J. Colchester, G. Ferioli, R. Jung, J. Koopman
CERN, Geneva, Switzerland

Abstract

In order to satisfy the tight emittance requirements of LHC, a non-intercepting beam profile monitor is needed in the SPS to follow the beam emittance evolution during the acceleration cycle from 26 to 450 GeV. Beyond 300 GeV, the synchrotron light monitor can be used. To cover the energy range from injection at 26 GeV to 300 GeV, a monitor based on the luminescence of gas injected in the vacuum chamber has been tested and has given interesting results. This monitor could also be used in LHC, where the same problem arises. Design and results are presented for the SPS monitor.

1. INTRODUCTION

For the LHC project, there is a severe constraint on the transverse emittance preservation from PS ejection to LHC. The allowable beam blow-up will be from $3\mu\text{m}$ to $3.4\mu\text{m}$ for the normalised one sigma emittances in both transverse directions. As presented in other papers [1,2], the emittances will be measured in the transfer channel TT10 and the matching from PS to SPS checked on dedicated injections by means of an OTR screen in the SPS ring where the injected beam will be dumped after 100 revolutions. A specific beam monitor is then needed to check the emittance preservation in the SPS up to the extraction towards the LHC.

Wire Scanners are available for precision reference measurements, but they are beam perturbing and of low repetition rate, allowing a maximum rate of only two measurements per SPS cycle.

A non-intercepting beam profile monitor with a high sampling rate of at least 25 Hz is essential to identify beam blow-ups and their causes.

From 300 GeV to the extraction at 450 GeV, a Synchrotron Radiation (SR) monitor is available, but from injection at 26 GeV up to 300 GeV, no monitor is yet available. If this monitor is fast and sensitive enough, it could also be used to check on-line the matching preservation which has been established with the OTR screen monitor.

Two types of monitors are being considered for this task: the Ionisation Profile Monitor (IPM) of which a monitor from DESY has been installed in the SPS and is being tested [3] and a Luminescence monitor which will be discussed in this paper. In the Luminescence monitor, the information is transported by photons and will not be influenced by the beam space charge as is the case for the IPM. This is very interesting and makes the effort to test

the usefulness of such a device as a beam profile monitor worthwhile.

2. THE LUMINESCENCE MONITOR

This type of monitor has been used at Los Alamos in the late seventies where it gave interesting results with low energy and high intensity proton beams passing in Nitrogen [4]. It seems that this type of monitor has never been used in high energy accelerators. This is probably because it was felt that the light production is too low at higher energies, above several tens of MeV [5], despite a study made for HERA [6].

The luminescence monitor makes use of the excitation of gas molecules by the particle beam to generate light. This light production is proportional to the particle density and to the gas pressure [7]. Several types of gas can be considered. Nitrogen has been studied for many years in the context of the aurora borealis. It is a good candidate, because it emits light close to the lower limit of the visible spectrum, within the sensitivity region of normal intensifiers. The light production cross section of nitrogen is high and is well known at low energies [7]. An additional advantage of Nitrogen is that it is easily pumped by the vacuum system.

As the available data is given for energies below 1 MeV, the light production at SPS energies was estimated by using the Bethe-Bloch equation: Fig. 1.

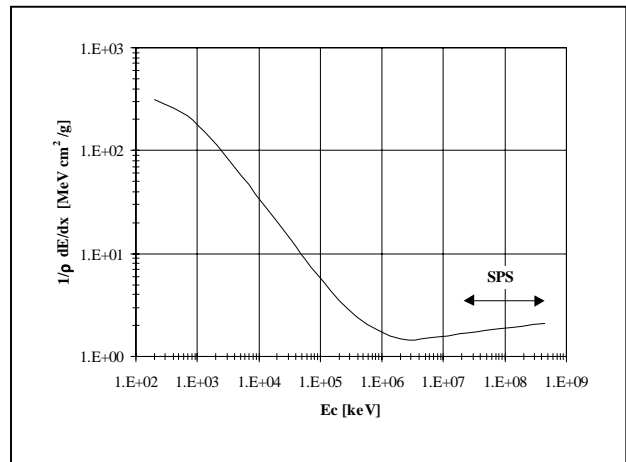


Figure 1: Energy dependence of the normalised proton energy loss to Nitrogen molecules as a function of proton energy as given by the Bethe-Bloch equation.

If the light production is only proportional to the energy loss of the charged particle, then there is a reduction

CHROMATICITY MEASUREMENTS AT HERA-P USING THE HEAD-TAIL TECHNIQUE WITH CHIRP EXCITATION

A. Boudsko, TRIUMF, Vancouver, Canada
O. R. Jones, H. Schmickler, CERN, Geneva, Switzerland
M. Wendt, F. Willeke, DESY, Hamburg, Germany

Abstract

Experiments have been performed in the HERA proton ring (HERA-p) to test a quasi non-destructive method of chromaticity measurements for protons. The method is based on the detection of the head-tail phase shift of coherent betatron oscillations using a broadband beam position pickup and a commercial “fast-frame” oscilloscope. Previous experiments have relied on a single kick for transverse excitation, whereas the results presented here were carried out using swept frequency “chirp” excitation. The tests proved to be successful, and the method seems to be a good candidate for chromaticity measurement in new large hadron accelerators, such as LHC.

1 INTRODUCTION

In any superconducting accelerator the control of *chromaticity* during machine transitions like energy ramping or beta squeezing is of paramount importance. The classical method of chromaticity determination, i.e. measurements of the betatron tunes for different settings of the beam momentum, is in this case only of limited use. In this paper we describe the results of applying the so-called *head-tail* chromaticity measurement [1] to the beams in HERA-p. This method relies on the fact that for non-zero chromaticity a dephasing/rephasing of the betatron oscillations occurs between the head and the tail of a bunch during synchrotron oscillations. After transverse excitation, the measurement of the turn-by-turn position of two longitudinal positions in a bunch allows the relative phases to be extracted and the chromaticity to be calculated.

In contrast to the results reported in previous publications [1, 2] which used a single kick for beam excitation, the data in this report is obtained by *resonant chirp beam excitation*. Although the primary motivation for using this technique in HERA-p is the lack of a sufficiently strong deflection kicker in the vertical plane, the results are of general interest.

2 THE HEAD-TAIL PRINCIPLE

Assuming longitudinal stability, a single particle will rotate in longitudinal phase-space at a frequency equal to the synchrotron frequency. During this longitudinal motion the particle also undergoes transverse motion, which can be described by the change in the betatron phase, $\Theta(t)$, along the synchrotron orbit. If the whole bunch is kicked transversely, then the resulting transverse oscillations for a given

longitudinal position within the bunch can be shown [1] to be given by

$$y(n) = A \cos [2\pi n Q_0 + \omega_\xi \hat{\tau} (\cos (2\pi n Q_s) - 1)] \quad (1)$$

where n is the number of turns since the kick, Q_0 is the betatron tune, Q_s is the synchrotron tune, $\hat{\tau}$ is the longitudinal position with respect to the centre of the bunch, and ω_ξ is the chromatic frequency and is given by

$$\omega_\xi = Q' \omega_0 \frac{1}{\eta} \quad (2)$$

Here Q' is the chromaticity, ω_0 is the revolution frequency and $\eta = 1/\gamma^2 - 1/\gamma_{tr}^2$. If we now consider the evolution of two longitudinal positions within a single bunch separated in time by $\Delta\tau$, then from (1) it follows that the phase difference in the transverse oscillation of these two positions is given by

$$\Delta\Psi(n) = -\omega_\xi \Delta\tau (\cos (2\pi n Q_s) - 1) \quad (3)$$

This phase difference is a maximum when $nQ_s \approx 1/2$, i.e. after half a synchrotron period, giving

$$\Delta\Psi_{\max} = -2\omega_\xi \Delta\tau \quad (4)$$

The chromaticity can therefore be written as

$$Q' = \frac{-\eta \Delta\Psi(n)}{\omega_0 \Delta\tau (\cos (2\pi n Q_s) - 1)} \quad (5)$$

$$Q' = \frac{\eta \Delta\Psi_{\max}}{2\omega_0 \Delta\tau}$$

3 EXPERIMENTAL PROCEDURE

3.1 Hardware Setup

Fig. 1 shows the hardware setup. The transverse displacement signal of the proton beam was detected with the two horizontal 40 cm long stripline-like electrodes of a broadband beam position pickup ($\beta \approx 33$ m)¹. Their signals were adjusted in time with a variable delay-line and combined in a Δ/Σ -hybrid (*M/A COM*, model H-9). Additional fixed and variable attenuators were used to minimize the common mode signal due to the static beam displacement, i.e. the transverse beam orbit. Both output signals of the hybrid, Δ (displacement) and Σ (intensity), were acquired using a *Tektronix 784C* digital oscilloscope (1 GHz analogue

¹slotted coaxial electrodes, usable bandwidth ≈ 4 GHz

INFLUENCE OF TRANSVERSE BEAM DIMENSIONS ON BEAM POSITION MONITOR SIGNALS

A. Jankowiak, T. Weis, DELTA, Institute for Accelerator Physics and Synchrotron Radiation, University of Dortmund, Germany

Abstract

In this paper we will evaluate the influence of transverse beam dimensions on the signal functions of a beam position monitor (BPM) with capacitive pick-up electrodes. The error which occurs in the determination of the beam position when disregarding these effects is calculated as an example for the DELTA¹ BPM.

The possibility to use this effect for the measurement of the beam size / emittance is discussed.

1 CALCULATION OF THE SIGNAL FUNCTIONS

Fig.1 shows a typical BPM with 4 capacitive pick-up electrodes. When the beam passes through the BPM, the electric field, accompanying the beam, induces a charge pulse on the pick-up electrode, which depends on the beam charge and the position of the beam in the cross section of the BPM. To determine the beam position it is necessary to know the signal function S_i for each pick-up i . These $S_i(x,y)$ represents the response of the pick-ups for a normalised point charge ($q=1$) at the position (x,y) .

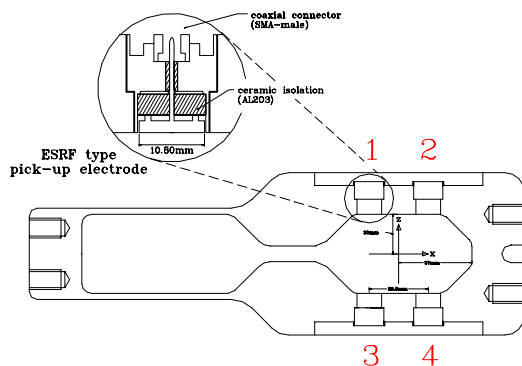


Fig.1 Sketch of the DELTA BPM.

In the case of relativistic beams ($\gamma \gg 1$) the electric and magnetic fields are nearly transversal and therefore the determination of the signal functions can be treated as a 2-d problem.

1.1 Signal Function of a Point Charge

The obvious solution to calculate the S_i is to solve for the electric field E of a point charge (pencil beam) at position (x,y) and to integrate E over the surface of pick-up i to get the induced charge which is proportional to the signal function. Because these calculations must be repeated for each position (x,y) a more clever way is to make use of the reciprocity theorem [1].

The potential $\phi_{\text{pick-up}}$ is allocated to pick-up i and the Laplace equation $\Delta\phi_i(x,y)=0$ with the vacuum chamber on zero potential is solved. The solution ϕ_i is proportional to the signal function. These calculation can easily done by using programs like MAFIA or Poisson (see. Fig. 3).

1.2 Signal Function of a Gaussian Charge Distribution

In most cases a good representation for the transverse charge distribution $\rho(x',y')$ of a particle beam at position (x,y) is a 2-d Gaussian distribution.

$$\rho(x', y') = \frac{1}{2\pi \cdot \sigma_x \cdot \sigma_y} \cdot \exp \left[-\frac{1}{2} \left(\left(\frac{x-x'}{\sigma_x} \right)^2 + \left(\frac{y-y'}{\sigma_y} \right)^2 \right) \right]$$

The signal function $\tilde{S}_i(x,y)$ of a beam with beam size σ_x and σ_y can be described in the following way:

$$\tilde{S}(x, y) = \iint \rho(x', y') \cdot S(x', y') \cdot dx dy \quad (1)$$

To study the effect on the determination of the beam position usually the calculation will be done numerically. To get a better understanding of the influence of the beam size we will give a analytical solution.

In the following we expand, at a fixed position, the signal function S_i in a Taylor series and use a Cartesian co-ordinate system with the origin at the centre of the beam. This gives (after evaluating the double integral and using identities concerning integration of Gaussian distributions [2]) for a fixed beam centre

$$\tilde{S} = \sum_{i=0}^{\infty} \sum_{j=0}^{\infty} a_{2i,2j} \cdot m_{2i,2j} \cdot \sigma_x^{2i} \cdot \sigma_y^{2j} \quad (2)$$

¹ Dortmund ELection Test Accelerator (1.5 GeV Synchrotron Radiation Source)

RECENT IMPROVEMENTS OF A CRYOGENIC CURRENT COMPARATOR FOR nA ION BEAMS WITH HIGH INTENSITY DYNAMICS

A. Peters, H. Reeg, P. Forck, GSI, Darmstadt, Germany
 W. Vodel, R. Neubert, Institut für Festkörperphysik,
 Friedrich Schiller Universität, Jena, Germany
 e-mail: A.Peters@gsi.de

Abstract

Former measurements of extracted ion beams from the GSI heavy ion synchrotron SIS showed large current fluctuations in the microsecond region with a high peak-to-average ratio. To adapt our Cryogenic Current Comparator (CCC) to this time structure the detector's electronics have been carefully modified.

The most important improvement of the new DC SQUID system affects the enlargement of the bandwidth and the slew rate of the measuring system. In addition the existing data acquisition system for e.g. SEMs (Secondary Emission Monitors) was extended to digitize the CCC signals simultaneously. Measurements of Argon beams will be shown to demonstrate the improved capabilities of the upgraded Cryogenic Current Comparator.

1 MODIFICATION OF THE SQUID ELECTRONICS

The CCC has demonstrated its excellent capabilities to measure nA beams with absolute calibration [1]. The most important component of the CCC is the new DC SQUID system developed and manufactured at the Friedrich Schiller University Jena, Germany. This device is able to detect extremely low magnetic fields, for instance, caused by the extracted ion beam of the SIS. For this reason the SQUID input coil is connected with the pick-up coil for the ion beam. This pick-up coil consists of a superconducting niobium toroid containing a special VITROVAC 6025-F core (VAC GmbH, Hanau, Germany) providing a high permeability, even at the low working temperature of 4.2 K. The large diameter of the pick-up coil of 200 mm provides a "warm" hole for the ion beam passing the dewar (see Fig. 1). Both the SQUID input coil and the pick-up coil form a closed superconducting loop so that the CCC is also able to detect DC currents.

As already known from earlier measurements the spill structure of the extracted ion beam pulses shows a strong modulation with current peaks up to 130 nA while the average current is only about 15 nA [2]. The beam consists of individual bursts with a steep rise and a slower fall. As a consequence, the current rise time of this spill structure sometimes exceeds the slew rate limit of the SQUID system, if the value goes beyond $5000 \Phi_0/s$ or about $1 \text{ nA}/\mu\text{s}$. In those cases the feedback loop of the CCC electronics be-

comes unstable and negative spikes or other unpredictable effects could be observed [3]. For this reason a further development of the CCC was necessary and, above all, a new DC-SQUID system with a higher slew rate was designed and realized within the last year. The simplified block diagram of the DC SQUID Control is shown in Fig. 1.

The main improvement affects the enlargement of the bandwidth. For this reason a wide band transformer at room temperature is used instead of a cooled high quality factor resonant circuit for the readout electronics of the SQUID signal. The corresponding increase of the intrinsic noise of the SQUID system is much lower than the noise level of the CCC. It is caused, mainly, by the VITROVAC core of the antenna and can be neglected. Furthermore, the modulation frequency of the PLL-loop was essentially increased from 125 kHz in the former SQUID system up to 500 kHz using faster operational amplifiers in the SQUID controller. As a result of these design features the system bandwidth of the SQUID system was increased up to 50 kHz per 1 flux quantum (full range signal). This corresponds to an increase of the slew rate of the CCC up to $1.6 \times 10^5 \Phi_0/s$ or $28 \times 10^6 \text{ nA/s}$. But with the detector system connected and a calibration signal as the input a reduced value of $6 \times 10^4 \Phi_0/s$ was measured. For this phenomena we have no electronic model up to now and further investigations are necessary to understand this.

Another important feature is the realization of a distance of 25 m between the preamplifier on top of the cryostat and the SQUID controller in order to allow the operation of the SQUID system also when the beam line is activated. To meet this requirement without decreasing the current resolution of the CCC several special buffers for most of the leads and a special double-screened cable between preamplifier and SQUID controller were used to avoid rf interferences.

A point of special interest is the coupling of the SQUID output with an A/D converter and the data acquisition unit (see Fig. 2). According to our experience this is only possible by using an optical coupler between the analog and digital circuits. Otherwise the whole SQUID system is not working at all because of the disturbances generated by the digital circuits. In addition, the analog output of the SQUID electronics is equipped with an isolating amplifier.

As the result of all improvements the CCC is now working at a sufficiently high slew rate so that we can mea-

TURN-BY-TURN PHASE SPACE DIAGRAM CONSTRUCTION FOR NON-LINEAR BETATRON OSCILLATION

A. Kalinin, V.Smaluk, Budker Institute of Nuclear Physics, Novosibirsk, Russia

Abstract

The problem of phase space diagram construction for non-linear betatron oscillation measured by pickup, is considered. The conventional two-pickup method [1] of phase trajectory construction was improved. Discrete Fourier filter applied to data measured yields a large dividend in accuracy. The result of our investigations is the method of turn-by-turn phase trajectory construction using data measured by single pickup. The single-pickup method developed was tested by computer simulation of non-linear betatron oscillation in several models of magnet lattice. Practicality of the method and its accuracy limitation were studied. The method applying for experimental study of beam dynamic is discussed.

1 INTRODUCTION

Phase space diagram of non-linear betatron oscillation gives a lot of information about the non-linearity type, non-linear resonances, dynamic aperture, etc. It is useful to compare phase trajectories of the beam motion measured with results of analytical estimations and numerical simulations.

A problem of phase trajectory construction is obtaining $x'(x)$ dependence, where $x(t)$ is transverse coordinate, and $x'(t)$ is transverse momentum of a beam centre of charge, t is a time variable. The problem is troublesome because of impossibility to measure directly the momentum $x'(t)$.

Diagnostic systems give an information about beam motion as series of turn-by-turn samples x_k of the coordinate measured by pickup. Due to the discreteness, calculation of the momentum samples x'_k , by numerical differentiation of the x_k , is impossible in general.

Let's consider a problem of construction of turn-by-turn phase trajectory $x'_k(x_k)$ of non-linear betatron oscillation using the coordinate samples x_k .

It is convenient to analyse phase trajectories in the (x, \bar{x}') coordinates defined by the variables conversion:

$$\bar{x}' = \alpha x + \beta x'. \quad (1)$$

A shape of phase trajectory in these coordinates is independent of the value of alpha-function $\alpha = -\beta/2$, but this shape is determined by pure non-linear effect.

2 TWO-PICKUP METHOD

There are conventional two-pickup method [1] of turn-by-turn phase trajectory construction. Let's consider particle motion in a linear section of magnet lattice with two pickups, first of them placed at the input of the section and second at the output of it.

If a particle passes through the section, its coordinate x_2 measured by the second pickup is:

$$x_2 = (\beta_2/\beta_1)^{1/2} \cdot (x_1 \cos \Delta\psi_{21} + x'_1 \cdot \sin \Delta\psi_{21}), \quad (2)$$

here x_1 is the coordinate and x'_1 is the normalized momentum at the first pickup, $\beta_{1,2}$ are the values of beta-function at the pickups, $\Delta\psi_{21}$ is the betatron phase advance between the pickups. From this expression an equation of turn-by-turn phase trajectory is derived:

$$\bar{x}'_{1k} = [(\beta_2/\beta_1)^{1/2} \cdot x_{2k} - x_{1k} \cos \Delta\psi_{21}] / \sin \Delta\psi_{21}. \quad (3)$$

If $\beta_1 = \beta_2$ and $\Delta\psi_{21} = \pi/2 + \pi n$, then $\bar{x}'_{1k} = x_{2k}$.

An accuracy of the method is determined by pickup resolution in the frequency band with upper bound equal to the revolution frequency. The noise error leads to poor quality of phase trajectories constructed by this method.

For decrease the noise error, a method of discrete Fourier filtering was developed. Let's expand the arrays x_{1k} and x_{2k} of N turn-by-turn coordinate samples in terms of harmonics $\Phi_{1,2,j} = A_{1,2,j} + iB_{1,2,j}$ of betatron frequency Q :

$$A_{1,2,j} = 2/N \cdot \sum_{k=0}^{N-1} x_{1,2,k} \cdot \cos(2\pi k \cdot jQ) \quad (4)$$

$$B_{1,2,j} = 2/N \cdot \sum_{k=0}^{N-1} x_{1,2,k} \cdot \sin(2\pi k \cdot jQ)$$

Amplitude of harmonics $|\Phi_{1,2,j}| = (A_{1,2,j}^2 + B_{1,2,j}^2)^{1/2}$ in (4) decreases rapidly with the harmonic number j .

Procedure of turn-by-turn phase trajectory construction is just the synthesis of the arrays X_{1k}, X_{2k} :

$$X_{1,2,k} = \sum_{j=1}^n (A_{1,2,j} \cdot \cos 2\pi k j Q + B_{1,2,j} \cdot \sin 2\pi k j Q) \quad (5)$$

The $X_{2k}(X_{1k})$ dependence describes the phase trajectory.

Noise component of the j -th harmonic in (5) is $N^{1/2}$ times lower than broad-band noise component of the x_{1k}, x_{2k} arrays. If the number of harmonics in (5) $n \ll N$, then noise reduction is $(N/n)^{1/2}$. So, combination of the expansion (4) with the synthesis (5) is a discrete filter. Usually $N = 1024, n = 4 \div 8$, so typical noise reduction by the filter is 10÷15 times.

An example of the filter applying to the two-pickup method is given in Fig. 1. There are phase trajectories of radial betatron oscillation in the VEPP-4M near the sextupole resonance $3Q_x = 26$. The trajectory $x_{2k}(x_{1k})$, constructed by the two-pickup method without filtering, is plotted by circles, the trajectory $X_{2k}(X_{1k})$ constructed using the filter is plotted by triangles.

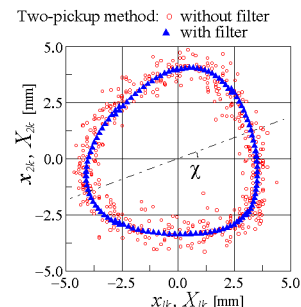


Figure 1: Applying of the discrete Fourier filter.

TRAJECTORY MEASUREMENTS IN THE DAΦNE TRANSFER LINES

A. Stella, C. Milardi, M. Serio, INFN-LNF, Frascati (Rome), Italy

Abstract

An improved beam position monitor system has been installed in the Transfer Lines (TL) connecting the DAΦNE Linac to the collider Main Rings through the Damping Ring, to monitor the beam trajectory and optimize the transmission efficiency.

Signals from stripline type beam position monitors are stretched, sampled through Track & Hold circuits and digitized to 12 bits. The sampling stage is triggered, according to the timing of the desired beam, to measure the amplitude of the signals induced on a BPM.

Hardware control, data collection and reconstruction of the beam position along the Transfer Lines are performed by the DAΦNE Control System on a VME standard local processor.

Design issues, implementation and performance of the system are presented.

1 INTRODUCTION

The injector chain of DAΦNE consists of a e⁺/e⁻ Linac injecting into an intermediate storage ring (Accumulator), employed to accumulate the required single bunch current and to damp the longitudinal and transverse emittances before the injection in the DAΦNE main rings.

Linac, Accumulator and Main Rings are interconnected by ~140 m of Transfer Lines altogether.

Due to the requirement of using the pre-existing buildings, the TL are designed in such a way that different beams (electrons or positrons from the Linac into the Damping Ring and from the Damping Ring into either one of the Main Rings) traverse the same portion of the TL in opposite directions with different timing.

2 SYSTEM OVERVIEW

2.1 Pick-up Electrodes and Signal Processing

The low repetition rate (50 Hz from the Linac to the Damping Ring and 1 Hz for the injection in the Main Rings) requires a single shot detection system to measure the beam position.

To acquire the whole trajectory of the beam, 23 beam position monitors (BPMs) are installed along the lines.

The BPMs consist of 50Ω strip-line electrodes, with 0.15 m length and 30 degrees angular width, short circuited at one end inside the vacuum chamber of 37 mm radius.

The signal induced by the beam consists of two pulses of opposite polarities, according to the shape of the bunch. The different characteristics of the beam injected and extracted from the Damping Ring (Tab. 1) give a wide range of amplitudes and widths of the pulses (Fig. 1).

Table 1: DAΦNE Injector Beam Parameters

Parameter	Typical
LINAC bunch charge	1 nC
LINAC bunch length	10 ns FWHM
LINAC repetition rate	25-50 Hz
ACC bunch charge	3÷12 nC
ACC bunch length	300 ps FWHM
ACC repetition rate	1-2 Hz

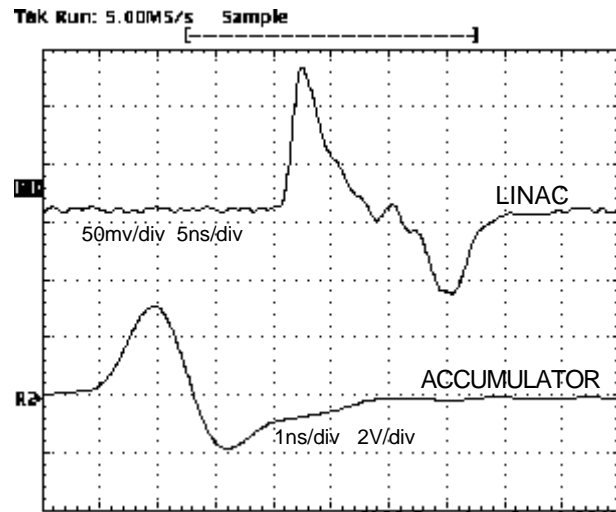


Figure 1: Typical pickup signals at the input of the BPM detection electronics, induced by the Linac beam and the Accumulator, measured at the end of ~50 m long coaxial cables.

In our case the Linac delivers bunches with a 10 ns FWHM length, while the damped beam extracted from the Accumulator has a 300 ps FWHM bunch length.

Each pickup signal is sent (through coaxial cables of typical length between 40m and 100m) to a wide band multiplexer system equipped with HP-E1366A boards and then to the detection electronics.

The beam position is determined by measuring the peak amplitude of the signals induced on each electrode, then calculated from a linear combination of the measured voltages through a non linear fitting function, in order to correct the non linear response of the BPMs.

BEAM STEERING WITH IMAGE PROCESSING IN THE CRYRING INJECTION BEAMLIN

A. Källberg, A. Simonsson, Manne Siegbahn Laboratory,
Frescativägen 24, SE-104 05 Stockholm, Sweden

Abstract

By varying six quadrupoles and observing how the beam spot moves on three fluorescent screens the beam is aligned in the injection beamline. The method is now automated and upgraded by using image processing of the picture to get the position of the beam.

1 CRYRING

CRYRING is a 52-m circumference storage ring for atomic and molecular ions [1]. In the injection line an RFQ pre-accelerates ions with $q/m > 0.22$. Thus, in the injection line right before injection, where the system below is used, the beam can be of two types: "Fast", 290 keV/u and $q/m > 0.22$, or "slow" with 40q keV total energy. Examples of ions are Pb^{54+} , HCN^+ , and Sr^+ . The beam current varies from 20 μA down to below 50 nA. For the fast beam the pulse length is 0.1 ms and the repetition rate is 3 Hz.

2 THE OLD SYSTEM

For several years a Pascal program running on the PDP-11 computer has been used which aligns the beam horizontally in three focusing quadrupoles and vertically in three defocusing quadrupoles. The magnets are varied approximately 15% up and down while the operator looks at a monitor showing the beam spot on a fluorescent screen.

Changing the focusing naturally changes the shape of the beam, but when the centre of the beam moves the



Figure 1. Grey-scale picture of the beam spot.

beam doesn't go through the centre of the quadrupole and the preceding steering element should be adjusted.

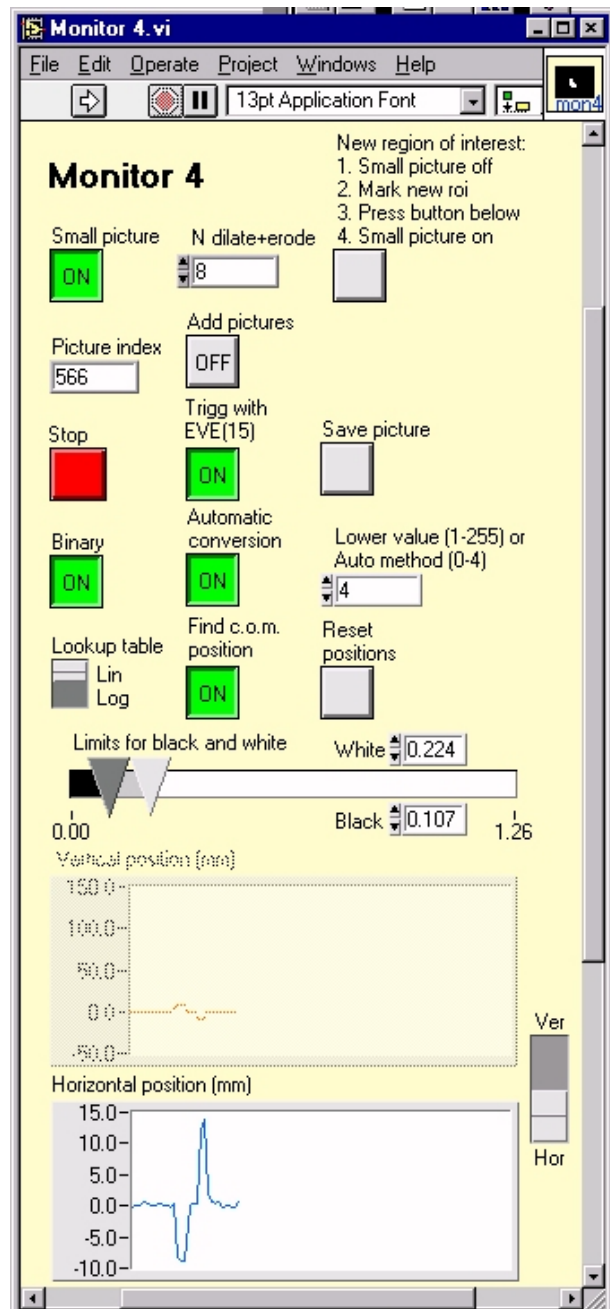


Figure 2. The front panel of the LabVIEW program shows the image processing options. The diagram at the bottom shows large movements of the horizontal beam position when a focusing quadrupole is varied.

IONISATION LOSSES AND WIRE SCANNER HEATING: EVALUATION, POSSIBLE SOLUTIONS, APPLICATION TO THE LHC.

C. Fischer

CERN - CH-1211 Geneva 23, Switzerland

Abstract

Harmful heating mechanisms, resulting in wire breakage, limit the utilisation of wire scanner monitors to below a given beam intensity. This threshold depends on the accelerator design parameters. In lepton colliders, the short beam bunches generate strong wake-fields inside the vacuum pipe which are sensed by the wire and are the predominant current limit. These effects can be minimised by a smooth design of the monitor cross section and by choosing a wire made of an insulating material [1].

A second source of energy deposition inside the wire, also present in hadron machines, and even when the wire material is insulating, results from collision and ionisation of the wire material atoms by the incident beam particles. Calculations are presented to evaluate the efficiency of this process and a possible solution is suggested which may reduce this limitation. An example is given for the case of the LHC.

1. INTRODUCTION

In wire scanner monitors, excessive heating may result in wire breakage. The main heating mechanism in proton accelerators results from energy deposition inside the wire due to ionisation of the wire material atoms by the incident beam. Calculations will first be developed in a view to evaluate the efficiency of this process. The two cases of 55 GeV leptons and 450 GeV protons are considered. The resulting limitations in the use of wire scanner monitors in LEP and in the future for the LHC [2] are discussed. A solution is suggested which, by using a special mechanical design of the monitor, permits to increase the beam current limit. An application is then made in the case of the LHC beam parameters.

2. HEATING FROM COLLISION LOSSES

2.1 Collision losses

For a high energy particle, ionisation losses are [3]:

$$\frac{1}{\rho} \frac{dE}{dx} = \frac{0.1535}{\beta^2} \frac{Z}{A} (F(\beta) - 2 \ln I - \delta(X)) [\text{MeV cm}^2 \text{g}^{-1}] \quad (1)$$

Z and A are the atomic and the mass numbers of the material atoms and ρ is the material density. The expression of $F(\beta)$ depends on the incident particle rest mass and energy [3], [4]. $F(\beta) = 19.032$ and 10.920 respectively for 55 GeV electrons and 450 GeV protons. The binding atomic electron energy into Carbon is $I = 78$ eV and $\delta(X)$, describing the density effect of the medium, is given by:

$$\delta(X) = 4.605 X + C, \text{ with } X = \log(\beta\gamma).$$

For high energy particles, $C = 2.868$. Hence, density effects decrease the ionisation losses by respectively 39 % and 22 % for either type of particle mentioned above such that $1/\rho \cdot dE/dx$ is equal to $2.41 \text{ MeV cm}^2 \text{g}^{-1}$ for an electron at 55 GeV and $2.56 \text{ MeV cm}^2 \text{g}^{-1}$ for a proton at 450 GeV.

2.2. Energy transferred to knock-on electrons

By collision with an incident particle of charge z , some atomic electrons are ejected from the wire material lattice. The number of these knock-on electrons with energy E is [4]:

$$\frac{d^2N}{dEdx} = 0.153 \frac{Z}{A} \frac{z^2}{\beta^2} \rho \frac{F}{E^2}$$

for $I \ll E \leq T_{\max}$, with T_{\max} , the maximum energy transfer. For leptons, T_{\max} is one half of the incident particle energy, and for 450 GeV protons T_{\max} is given by [4]:

$$T_{\max} \cong 2m_0 c^2 \beta^2 \gamma^2 / (1 + 2\gamma m_0/M) \\ = 154.4 \text{ GeV}$$

with m_0 and M the electron and proton rest mass. F is a spin dependent factor nearly equal to 1 in our case and $\rho = 2.2 \text{ g/cm}^3$ for Carbon. The energy transferred between E and $E + dE$ at a depth x by a particle is:

$$dW = \frac{d^2N}{dEdx} ExdE \\ = 0.153 (Z/A) \rho x dE/E$$

and between I , the binding electron energy, and T_{\max} , each particle will deposit:

$$W = \int_I^{T_{\max}} dW$$

$$W = 0.153 x \ln(T_{\max}/I), \text{ with } x \text{ in cm.} \quad (2)$$

For a complete scan, x is the average wire thickness seen by each particle of the beam, and is given by:

$$\langle x \rangle = \frac{\pi D^2}{4D} \frac{D}{vT} \\ = \frac{\pi D^2}{4vT}$$

where D is the wire diameter, v the wire speed and T the beam revolution period, $88.9 \mu\text{s}$ for LEP or the LHC and $22 \mu\text{s}$ in the SPS.

The energy transmitted to knock-on electrons by a beam of N particles during a scan is:

$$\Delta W_{\text{scan}} = N \langle x \rangle W$$

IONISATION PROFILE MONITOR TESTS IN THE SPS

C. Fischer, J. Koopman

European Organisation for Nuclear Research (CERN)
CH-1211 Geneva 23, Switzerland

Abstract

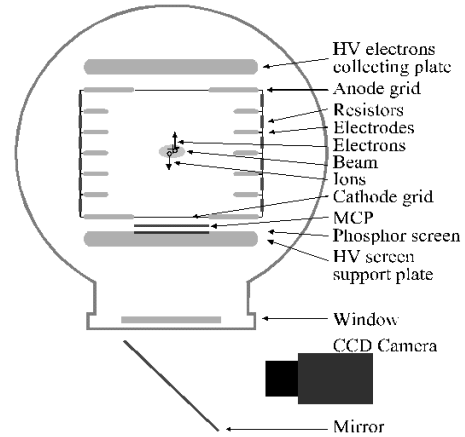
A beam profile monitor, from DESY, based on the ionisation of the rest gas, was installed in the SPS in 1997. Horizontal beam profiles obtained from the extracted positive ions are presented. It is known that in this case some broadening affects the signal, which limits the monitor resolution. This broadening results from the transverse momentum that the ions gain within the space charge field of the circulating beam.

In order to improve the resolution for LHC applications, the monitor was modified during the 1998/99 winter stop. A magnetic focusing was incorporated. The aim is to analyse the signal provided by collecting the electrons, rather than the ions, of the ionised rest gas. The details of this new set-up and the expectations for the resolution limit will be compared to the measurement results.

1. INTRODUCTION

Rest gas monitors are used in many high energy accelerators in order to reconstruct transverse beam distributions [1], [2], [3]. The signal which is used results from the collection of either the ions or the electrons produced by the ionisation of the rest gas due to the circulating beam passage. This type of device is used so far to analyse beam RMS dimensions larger than one millimetre. Ions or electrons are produced with a given transverse velocity. During part of their drift to the analysing device, they also experience space charge effects from the circulating beam, and their transverse momentum is enhanced. With their much larger rigidity, ions are less sensitive to these counteracting phenomena although their drift time through the beam space charge forces is longer. But a resolution better than 1 mm is difficult to achieve.

Such a device, obtained from DESY [1], was installed in the SPS in 1997. Tests were performed on proton beams. Figure 1 recapitulates the fundamentals of this monitor suited to work in the horizontal transverse plane. Two grids symmetrically positioned at 50 mm above and underneath the beam orbit, are set at inverse voltages, with a possible amplitude up to 5 kV. Ions and electrons are extracted in opposite directions, depending on the grid voltage polarity. In the basic configuration, positive ions are extracted towards the detection chain. They are then accelerated to a Multi-Channel Plate, which acts as a signal amplifier. The MCP gain can be adjusted by varying the voltage difference between input and output up to 1 kV. Electrons extracted from the MCP are accelerated, by potential differences up to 12 kV, to a high voltage plate supporting a phosphorescent screen. The transmitted light is reflected on a mirror to a CCD camera.



2. RESULTS WITH IONS

Profiles of 10^{13} proton beams were recorded during entire SPS super-cycles, from 26 GeV to 450 GeV, by looking at the signal provided by ions. Results are in Figures 2 and 3.

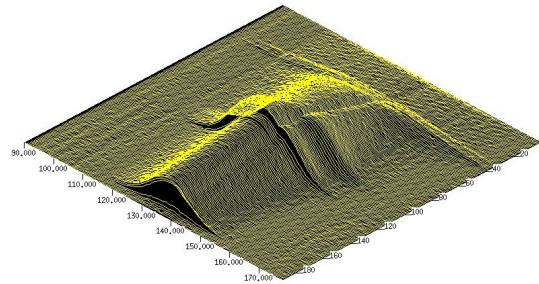


Figure 2: Proton beam horizontal profiles, measured from 26 GeV to 450 GeV using the signal from ions.

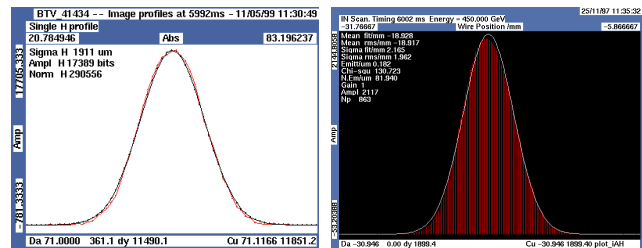


Figure 3: Horizontal proton beam profiles, with gaussian fit, at 450 GeV, taken with the IPM (left) and the wire scanner (right).

Figure 3 shows that both the IPM and the wire scanner monitor, which is our reference, provide a similar proton beam RMS value, respectively 1.9 mm and 2.1 mm. However, considering the ratio of the amplitude function values at the two monitor locations, the IPM should measure a narrower beam by a factor of 1.9, i.e. around 1mm. In this case, an enlarge-

PERFORMANCE OF THE NEW SPS BEAM POSITION ORBIT SYSTEM (MOPOS)

C. Boccard, T. Bogey, J. Brazier Ltd, J. de Vries, S. Jackson, R. Jones,
J.P. Papis, W. Rawnsley (TRIUMF), K. Rybaltchenko, H. Schmickler.

SL Division- European Laboratory for Particle Physics (CERN) - Geneva - Switzerland

Abstract

The orbit and trajectory measurement system COPOS of the CERN SPS accelerator has been in operation since the construction of the machine in 1976. Over the years the system has been slightly modified in order to follow the evolving demands of the machine, in particular for its operation as a p-pbar collider and, since 1991, for the acceleration of heavy ions.

In 1995 the performance of the system was reviewed and the following shortcomings were identified:

- lack of turn-by-turn position measurements due to the 1ms integration time of the voltage to frequency converters used for the analogue to digital conversion (to be compared with a revolution time of 23 μ s),
- ageing effects on the 200 MHz resonating input filters, which had over the years drifted out of tolerance. As a consequence the signal to noise ratio, the linearity and the absolute precision were affected,
- the calibration system based on electromechanical relays had become very unreliable, such that frequent calibrations were no longer possible,
- a remote diagnostic for the observation of timing signals relative to the beam signals was missing.

For the above reasons a large-scale upgrade program was launched, the results of which are described in the following sections.

1. DESCRIPTION OF THE NEW SYSTEM

1.1 Analogue processing chain

The new Multi Orbit Position System (MOPOS) is based on 200 MHz homodyne receivers, which follow a pair of matched 4.4 MHz bandpass filters. In order to enable the system to measure both high intensity proton beams and low intensity heavy ion beams, the dynamic range has been increased to 90 dB with the help of front-end low noise amplifiers. The resulting signal is then sampled or peak-detected, depending on the type of beam, and sent to the acquisition boards as a serial stream after conversion in 14 bit ADCS (see Figure 1).

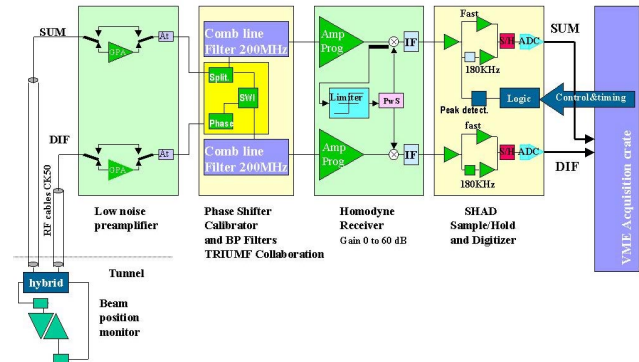


Figure 1: Synoptic of a MOPOS chain.

1.2 Acquisition architecture

The acquisition system is based around the CERN-SL standardised PowerPC (RIO2 8062) and makes full use of its memory, interfaces and processing power.

Using 3 VME slots, the CPU and 2 PCI extension boards can accept up to 6 PCI mezzanine cards (PMC). Each PMC can process data from 20 ADC channels (10 pickups). After treatment in a dedicated FPGA, a FIFO collects the acquired data in synchronism with the SPS revolution frequency. Sampling every 23 μ s gives a data stream of 8Mbytes/s.

The local PCI DMA controller transfers the data from each FIFO to the main memory at a rate of 70Mbytes/s. A total of 224 Mbytes of memory enables turn by turn data for up to 40 BPMs of a complete SPS super-cycle of up to 28s to be stored.

1.3 Software architecture

The 240 channel SPS Orbit acquisition system is implemented on 6 PowerPCs. These run under the LynxOS operating system, making use of its multi threaded real-time capabilities. Orbit acquisitions process the raw data on request. Calibration and initialisation data tables are stored externally in an Oracle database and locally in a non-volatile RAM board to enable a fast restart.

Analysis of the Proton Beam in the DESY Transport Lines by Video Readout

F. Solodovnik, IHEP and T. Limberg, K. Wittenburg; DESY

Abstract

Injection efficiency, beam optic matching and emittance preservation are very important parameters in achieving a high luminosity in large proton accelerators. We improved the analysing system of the phosphor screen readout of the proton transport lines in the accelerator chain of HERA with respect to the parameters above. The screens are read out by simple CCD video cameras. The signals are stored in local frame grabbers. An analogue output of the stored image is multiplexed and read-out by a fast PCI frame grabber card in a PC. The beam orbit and the beam emittance can be measured from each screen. A Visual Basic program is used to displays the trajectory and the envelope of the beam from a single transfer. The same program helps to drive bumps to achieve a proper steering through the line. The beam width can be measured from selected screens to calculate the emittance and other beam parameters including their errors. The read out and analysing system will be described and measurements will be shown.

1 INTRODUCTION

The Position and shape of the proton beam is observed in all transfer lines by thin luminescence screens read-out by TV video cameras (12 screens in the transport line from DESY III to PETRA (P-line) and 20 screens in the line between PETRA and HERA (PR-line)). Some cameras of the PR line were connected to a in-house developed local frame grabber, triggered by the transfer of protons to display a visible spot of a selected screen on a TV screen in the control room. The centre of gravity was determined in this system using all the light detected by the camera, including reflections. This led to large errors in the position measurement due to background problems. A measurement of the beam size was not foreseen. This old system has been upgraded with new hardware and software (see Fig. 1): 12 new local frame grabbers (Model MBS, Compulog) were installed in the P-line, observing the adjacent 12 screens. They store the two TV-frames following a transfer-trigger. Both grabber types provides an analogue TV output of the stored frames. The analogue signals are connected to two video multiplexers, one for each transport line. A dedicated PC containing a fast PCI frame grabber card (Type: DT3155, Data Translation) is used to control the multiplexers and to collect and analyse all frames from

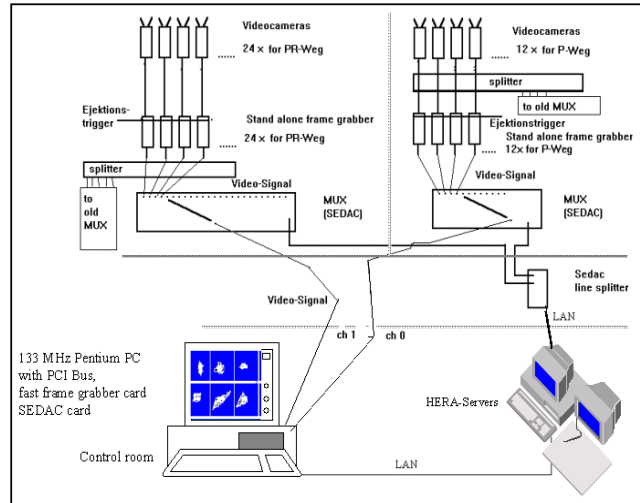


Figure 1: Layout of the readout scheme

one transfer. This provides a fast analysis of the TV signals without the traffic on the local area network (LAN) of the control system which would otherwise be needed to transfer all the frames though the LAN.

2 POSITION MEASUREMENT AND ORBIT CORRECTION

Fig. 2 shows a typical TV image of a screen stored after a beam transfer. The measured positions of the beam are displayed graphically in a Visual Basic program which provides full control of the screens, camera readout and correction magnets. Fig. 3 shows a

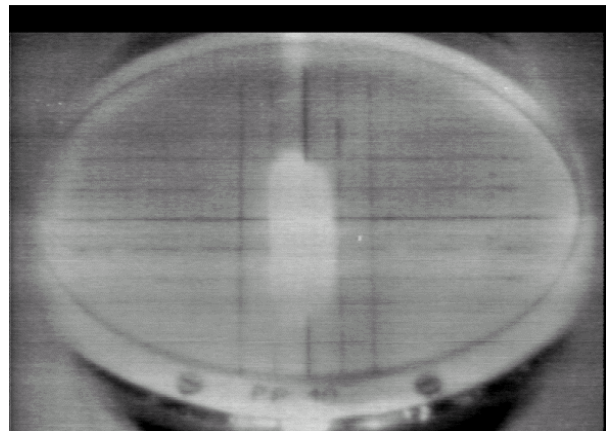


Fig. 2: Beam spot on a screen. The screen is illuminated by an external light source

COMPARATIVE TEST RESULTS OF VARIOUS BEAM LOSS MONITORS IN PREPARATION FOR LHC

J. Bosser, G. Ferioli
CERN, Geneva, Switzerland

Abstract

Beam loss detectors will play an important role in the protection of the superconducting LHC magnets.

Different types of detectors have been tested in the SPS ring and secondary beam lines with a view to their possible use for this application.

This paper describes the measurements made with: microcalorimeters at cryogenic temperatures, PIN diodes, ionisation chambers, scintillators, and ACEMs.

Measurements made using proton beams showing their relative sensitivities, linearities in counting or analog mode and minimum detection level will be presented.

1. INTRODUCTION

Beam loss monitors, BLM's, are commonly used on most of the CERN accelerators and transfer lines. They usually provide a relative diagnostic aimed to help the operators in their optimisation but also to protect the machine components against loss damages. For cryogening machines where excessive losses will induce magnet quenches their use is becoming mandatory.

For the LHC the "natural" losses level is such that the storage ring cannot be operated without transverse and longitudinal cleaning using collimators.

In the overall LHC project framework we have tested a few candidates [1] having in mind:

1.1 Criteria: First of all it is essential to have an estimate of the loss level, rate and distribution at the detector level. Then it is essential to question the requested time response and on the remnant dose at the monitor location.

1.2 Signal treatment: Two types are considered, the analog and the counting mode. In analog mode the BLM's signal is generally integrated or passed through filters. In counting mode the BLM's signal consists of pulses feeding a counter. Of course both the detector and its electronic must not saturate.

The LHC will be operated with 2835 bunches of 10^{11} protons each, separated by 25ns and distributed in 12 batches, with a revolution frequency of about 11KHz (10KHz for numerical applications).

With energies from 0.45 to 7 TeV, a magnet quench would occur for the following proton loss rates [2]:

Fast losses: $6 \cdot 10^9$ p/(m.10ms), and $6 \cdot 10^7$ p/(m.10ms) at 0.45 TeV and 7 TeV respectively.

Slow (or continuous) losses: 10^9 p/(m.s) and $8 \cdot 10^6$ p/(m.s) at 0.45 TeV and 7 TeV respectively.

Our comparative measurements were partially performed on the SPS machine but mostly on a SPS transfer line where a beam (with about 3cm diameter) of 10^4 - 10^7 protons at 120GeV/c, was extracted during 2.4s. This well monitored extraction line allows us to calibrate our measurements in view of LHC.

After a short description of the tested monitors we will give some guidelines for a preliminary choice of the monitors which could be retained. Data treatment or monitor controls as such will not be tackled in this paper.

2. DETECTORS

Our tests concerned: Scintillators with their PMT's, PIN Diodes, Ionisation monitors, ACEM's and Cryogenic microcalorimeters.

2.1 Scintillators

As is known, these devices emit light in which intensity is proportional to the energy lost by the particle passing through. The scintillator can be shaped in the most appropriate way (plates, cubes, rods,...). In the present case we make use of rectangular and rod shaped one's. Coupled to a Photo-Multiplier Tube (PMT), and associated with an appropriate electronics system, they allow large dynamic ranges in analog mode and in counting mode (up to 10^6 - 10^7). This BLM is very fast and bunch to bunch measurements can be achieved in both cases. Nowadays PMT sockets integrate high voltage power supply thus avoiding high voltage cables and the overall detector can be housed in a small volume (for our set-up l: 270mm, diam: 35 mm). The main drawback comes from the scintillator darkening when used in a high dose level environment. The gain of PMTs varies within a factor 10, a careful intercalibration of their sensitivities is necessary. Lastly this detector is expensive.

2.2 PIN-Diodes

Our experience is based on PIN Diode Beam Loss Monitor developed at DESY [3]. The system consists of two $10 \cdot 10 = 100\text{mm}^2$ area PIN diodes mounted face to face. The coincidence read out can measure a maximum count of 10 MHz with an intrinsic noise rate of less 1 Hz, which gives a dynamic range of more than 10^7 .

This BLM is sensitive to MIPs with an efficiency >30%, is very fast, not very expensive, and the radiation resistance is rather modest. Experience made at PS, where relative high dose levels are of concern showed that the detector lifetime did exceed one year.

BEAM PROFILE MEASUREMENTS AT 40 MHz IN THE PS TO SPS TRANSFER CHANNEL

G. Ferioli, J.J. Gras, *H. Hiller, R. Jung
 CERN, Geneva, Switzerland - *Bruun & Sørensen (France)

Abstract

Bunch to bunch beam profile measurements provide a valuable tool to control the injection lines to the SPS.

A fast profile monitor based on a 2.5µm Mylar coated with Aluminium Optical Transition Radiation (OTR) radiator, has been developed, installed and tested in the transfer line between the PS and SPS.

The OTR beam image is focused onto a fast Linear Multianode Photo Multiplier Tube and the associated electronics sample and store profiles every 25ns.

The paper describes the detector design, the electronic processing, and presents the results of different measurements made with bunches of 10^9 - 10^{11} protons at 26 GeV, and bunches of 10^6 Pb⁸² ions at 5.11 GeV/u.

1. INTRODUCTION

In the transfer line between PS and SPS different types of beams have to be monitored for a good injection in the SPS. For the Fixed Target operation 2 injections of $2 \cdot 10^{13}$ p at 14 GeV and 10.5 µs long are extracted horizontally in 5 PS turns. With the ions, 4 injections of 16 bunches of $1.5 \cdot 10^6$ Pb⁸² ions each at 5.11 GeV/u and spaced by 140 ns are used.

In view of the use of the SPS as LHC injector one injection of 16 bunches of 10^9 protons each at 26 GeV and spaced by 140 ns, is presently used for preliminary tests and, from this year one injection of 83 bunches spaced by 25 ns will be tested. For all beams the rms vertical and horizontal sizes are measured by Secondary Emission Grids (SEG) and OTR Beam Television Profiles (BTP).

The SEG electronics integrates all the signals coming from the grids for each injection at intervals defined by the master timing and gives only a single H/V profile. The CCD camera, used in the BTP monitor, integrates the signals during a TV frame (20ms), and the associated processing system computes a single H/V projection and a 2-Dimensional representation [1]. In both cases the evolution of the position, relative intensity, and profiles of the different bunches or structures is lost.

A new fast system able to acquire H/V profiles of bunches spaced by 25ns has been developed, installed in the transfer line and tested with different beams.

2. THE EXPERIMENTAL SET UP

Many OTR radiators made of 12 µm Titanium or 25 µm Mylar coated with 2 µm of Aluminium are currently used in the transfer lines to the SPS. These screens generate light, which reproduces the time structure of the beam and bunches spaced by 25ns can be analyzed [2].

The intensity of the OTR radiation, generated by ion or proton bunches injected in the SPS, is high enough to provide good diagnostics with a CCD camera or a Photomultiplier.

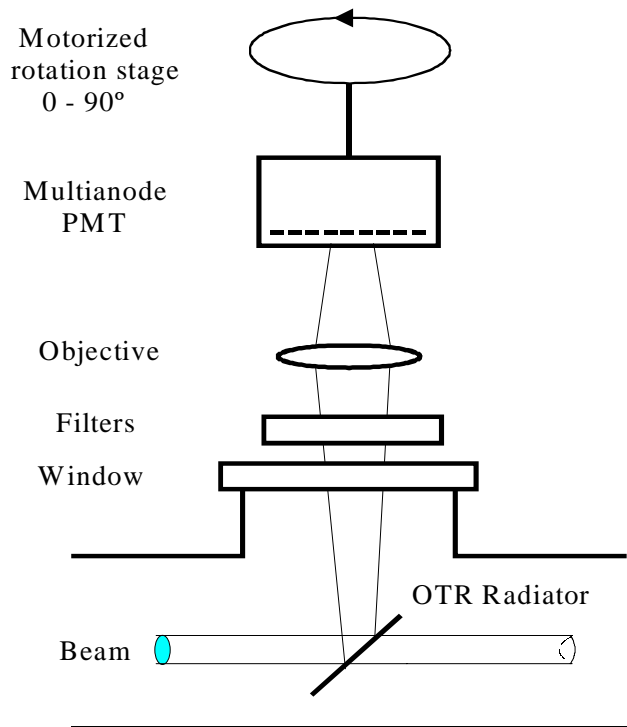


Figure 1: Schematic view of the monitor set-up

The measurement station (Fig. 1) uses a standard BTV SPS tank, where an OTR radiator is placed at 45° with respect to the beam. The radiation, through a window on the vacuum chamber and a set of neutral density filters, is focused by a 75 mm objective onto a Multianode Photo Multiplier Tube (MPMT).

This MPMT (type: Hamamatsu R5900U) with the proximity focusing dynode structure preserves the spatial distribution of intensity between photocathode and anode. This tube is a linear structured version with 16 anodes measuring 0.8*16 mm with a 1mm pitch, and an anode pulse rise time of about 0.6 ns.

A motorized rotation stage can rotate the MPMT from 0° to 90°, so with the same monitor, this allows to take alternatively horizontal or vertical profiles. The set of filters, the gain of MPMT and the rotation stage are remotely controlled.

THE FAST HEAD-TAIL INSTABILITY SUPPRESSION IN MULTIBUNCH MODE AT VEPP-4M

G.Karpov, V.Kiselev, V.Smaluk, N.Zinevich,
Budker Institute of Nuclear Physics, Novosibirsk, Russia

Abstract

In this paper the bunch-by-bunch transverse feedback system for suppression fast head-tail as well as coupled bunch instabilities is described. The experimental results of the feedback affecting on the current threshold are presented. The effects of reactive and resistive feedback on the current threshold are discussed. Two times as large the bunch current than the threshold current was obtained.

1 INTRODUCTION

The mode of operation of the VEPP-4M facility as a synchrotron light source intends 4 equally spaced along the ring bunches with each bunch average current of about 20 mA. The most fundamental limit for the bunch current at the VEPP-4M presently is vertical fast head-tail instability. The beam losses is usually observed in some tens of milliseconds after injection (this corresponds approximately to the time of radiation damping), Fig.1. The threshold current was 10÷11 mA.

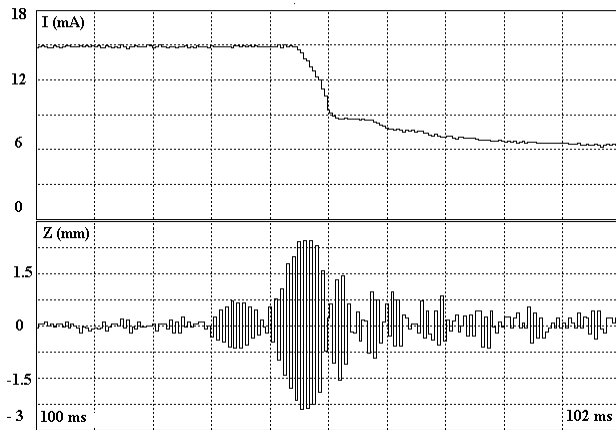


Figure 1: The bunch head-tail instability after injection.

The fast head-tail instability occurs when frequency of the head-tail mode “0” is shifted sufficiently to couple to the “-1” mode. In order to increase an instability threshold it is usually suggested to introduce the reactive feedback to compensate frequency shift of the mode “0”. However, as it follows from experiments [1] it is turned out that the introducing of the pure resistive feedback increases the threshold current up to substantially higher values.

This effect can be explained within the framework of the simple two particle model. In the papers [2,3] it was

found the eigenmodes and eigenvalues of the particles oscillations in the bunch. It was shown that in the vicinity of instability threshold eigenmodes are approximately the same, they have close eigenvalues and each mode has the approximately equal amplitudes of the dipole and quadrupole components.

When the resistive feedback is turned on an energy extraction occurs from the eigenmodes of oscillations excited by the head-tail interaction in a bunch through the dipole degree of freedom, thereby preventing the instability growth. This interpretation is additionally supported by the experimental data obtained at VEPP-4M [4].

In this paper the new bunch-by-bunch feedback system for suppression of vertical fast head-tail as well as coupled bunch instabilities is described.

The VEPP-4M related parameters are listed below.

Table 1: The VEPP-4M parameters

Energy	1.8÷5.5 GeV
Rev. frequency, f_{rev}	0.819 MHz
RF frequency	181 MHz
Number of bunches	4
Radiation dumping time at injection (long.,trans.)	30÷60 ms
Bunch length (injection)	20 cm
Tune, vertical	7.59
Tune, longitudinal	0.018
Bunch current threshold	10÷11 mA

2 DESCRIPTION OF THE SYSTEM

The block diagram of the feedback system over the vertical dipole oscillations of a beam is given in Fig.2. The 50 Ohm striplines are used as the pickup of transverse oscillations. The signals from the opposite striplines are applied to the subtracting transformer having the input impedance equal to the wave impedance of striplines. The length of striplines was chosen in such a way that their sensitivity has maximum values in the frequency range 150÷250 MHz.

To provide both the maximum dynamic range and the maximum signal-to-noise ratio we have chosen an analog scheme to process signal from bunches because little bunches number. The signals from four electron bunches are switched to four corresponding channels by front end GaAs FET switches. The gate duration is chosen to be 50 ns to provide bunch to bunch signals isolation.

BEAM PROFILE DETECTORS AT THE NEW FERMILAB INJECTOR AND ASSOCIATED BEAMLINES

Gianni Tassotto, Jim Zagel*

Abstract

During the commissioning of the Main Injector some of the detectors used to optimize the tune of the proton beam were: Flying Wires, Ionization Profile Monitors, and Multiwires.

1 INTRODUCTION

An 8 GeV proton beam is extracted from the Booster and channeled toward the Main Injector (MI) via the MI-8 beamline. From the MI the proton beam can be injected into the Tevatron (TeV) ring for collider and/or fixed target operation via P1 beamline or, to the Antiproton Source, via P1 and P2 beamlines.

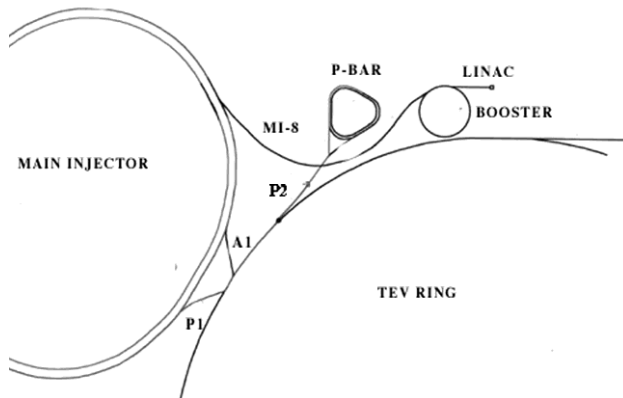


Figure 1: MI and Associated Beamlines Layout

A total of 27 Multiwires are distributed between MI-8, MI, P1, and P2 in order to optimize the beam tune. Just downstream of MI-8 injection is a horizontal (at Quad 102), and vertical (at quad 103), instrumentation section each comprising a multiwire (left) a flying wire (center) and an IPM (right).



Fig. 2: MI Beam Instrumentation Station

2 MULTIWIRES

These particle detectors are typically used to tune the proton beam and are then removed since they are intercepting devices and degrade the beam. They operate in beamline vacuum, which is of the order of 10^{-8} Torr.

2.1 Types of assemblies

In the 8 GeV transfer line the grids are assembled to display a single profile at the time. In the MI ring, P1, and P2 beamlines the grids are made by first winding a 0.003 inch diameter wire at 80 g of tension on a transfer frame, then transferring the wind over the wire planes and then soldering the wires on the pads. Each paddle contains both a horizontal and a vertical set of wires. No clearing field plane has been included in the design of this detector. The charge on the wires is measured with a scanner designed by the Controls Group [1].



Fig. 3: New MI Multiwire paddle

* Work supported by the U.S. Department of Energy under Contract No. DEAC02-76CH303000

PHOTON COUNTING DETECTORS FOR FILL STRUCTURE MEASUREMENTS AT VISIBLE WAVELENGTHS

H. L. Owen, CLRC Daresbury Laboratory, Warrington WA4 4AD, United Kingdom

Abstract

When making accurate measurements of the relative populations of electron bunches in a storage ring, notably in light sources operating with only a single bunch filled, the method of time-correlated single photon counting gives the greatest dynamic range. The timing resolution and background noise level of the photon detector employed is critically important in determining the overall performance of the system; hitherto the best performance has been obtained detecting X-ray photons using avalanche photodiodes. On the SRS at Daresbury a visible light diagnostic station offers greater ease of access to instrumentation and operational advantages. A review is given of the detector types which have been employed, and the performances which can be obtained using visible light.

1 MEASURING ELECTRON POPULATIONS

A measurement is often needed of the relative populations of the different bunches in a storage ring electron beam. For instance, when a light source storage ring is operated in a user mode which requires only a single bunch to be filled, it is important to be able to distinguish the (unwanted) small populations in the other bunches. The total dynamic range for detection of a small bunch relative to a larger bunch is determined by 2 factors - the time resolution of the detection system and the background noise. The accepted technique which provides the best trade-off between these two requirements for electron storage ring measurements is Time-Correlated Single Photon Counting (TCSPC).

In the TCSPC method individual photons emitted from a source are timed against a reference signal synchronous with the source repetition rate [1]. A histogram of the number of events versus time will give a statistical picture of the time-structure of the source over many events. The reference signal can conveniently be taken from the storage ring RF timing signal, but may also be derived directly from a single bunch beam by using a stripline pickup.

Photon detection, which provides the other channel of the TCSPC system, may be accomplished using a variety of detectors sensitive to different photon wavelengths; generally X-ray or visible photons are detected directly, or X-rays indirectly using scintillators. Photomultipliers (PMTs), microchannel plates (MCPs) or avalanche

photodiodes (APDs) have been used. The best dynamic range yet obtained is around 10^8 , using an APD directly detecting X-ray photons around 10 keV [3].

2 VISIBLE LIGHT DETECTION

One factor determining the choice of photon counting system is the effort and equipment required to implement it – the ideal is a cheap, turnkey system which can be installed onto an existing beamline. Visible light diagnostic beamlines are an attractive option as most light sources possess one for other diagnostic purposes. With the correct design of beamline - such as at the Synchrotron Radiation Source (SRS) at Daresbury - continuous access to and operation of the diagnostic equipment can be maintained even during storage ring injection – this can greatly increase the flexibility and efficiency of making measurements.

To provide the photon channel for the system, three options for visible photon detection are presented here: these are systems based on PMTs, MCPs or APDs.

2.1 PMT-Based System

This is the type of system presently in use on the SRS at Daresbury Laboratory. A timing base must clearly be used, together with a tube with exceptional timing and noise characteristics. At present, one of the fastest low-noise tubes commercially available is the Photonis (Philips) XP2020 tube [4] which has a transit-time spread of 250ps (similar tubes have been manufactured in the past with slightly better characteristics but are no longer available). Coupled with the appropriate base [5] a dynamic range of greater than 10^5 for most neighbouring bunches can be obtained; this is partly dependent upon the tube temperature (which determines the noise rate of the photocathode), so tubes are generally cooled thermoelectrically [5]. However, artefact peaks arising from the first few dynodes are generally present, and are well correlated in time and magnitude with each real peak; artefacts associated with the largest bunches overlap certain time regions in the beam fill structure, reducing the dynamic range there, although this can be partly overcome using software analysis [5]. The transit-time spread, together with the resolution of the timing electronics (see Figure 1) means that the overall response time is such that very close bunches (within a few ns from the main bunch) have a reduced dynamic range. Whilst this is a restriction for storage rings with bunch spacings of 2 ns it is less so for lower RF frequencies than

CLOSED-ORBIT CORRECTION USING THE NEW BEAM POSITION MONITOR ELECTRONICS OF ELSA BONN

J. Dietrich and I. Mohos, Forschungszentrum Jülich GmbH, Germany

J. Keil, Physikalisches Institut, Universität Bonn, Germany

Abstract

RF and digital electronics, developed at the Forschungszentrum Jülich/IKP were integrated to form the new beam position monitor (BPM) system at the Electron Stretcher Accelerator (ELSA) of the University of Bonn. With this system the preservation of the polarization level during acceleration was currently improved by a good correction of the closed-orbit. All BPM offsets relative to the magnetic quadrupole centers were determined by the method of beam-based alignment. The optics functions measured by the BPM system are in good agreement with theoretical predictions.

1 INTRODUCTION

The 3.5 GeV Electron Stretcher Accelerator at Bonn University was recently upgraded for the acceleration of polarized electrons [1]. During the beam acceleration several strong depolarizing resonances have to be crossed. Steering the beam through the magnetic quadrupole centers of ELSA can reduce the strengths of one type of resonances connected with the vertical closed orbit distortions. A common technique to determine the magnetic axis of a quadrupole relative to the axis of the beam position monitor is the method of beam-based alignment [2]. To make use of this method a BPM system with a good resolution and long term stability is required which can also be used at low currents of some mA typically for the operation of ELSA with polarized electrons. The new BPM electronics forming a 28 BPM orbit measurement equipment are integrated in the control system of ELSA.

2 FRONT-END ELECTRONICS

The BPM front-end electronics [3] were developed at the Forschungszentrum Jülich/IKP and produced by KFKI in Hungary. Each station consists of an RF narrowband signal processing unit and a data acquisition and control unit with capabilities for data preprocessing. Both units are enclosed in an RF-shielded crate with power supply and placed close to the four-button monitor chambers in order to reduce RF interference on the button signals. Altogether 28 monitor stations are connected via four optically coupled serial fieldbuses to the VME host computer.

2.1 RF Signal Processing Unit

A narrowband superhet RF electronics (Fig.1) detects the amplitudes of the four button signals at the fundamental frequency of $f_{RF} = 500$ MHz. At the input adjustable attenuators equalize the attenuation of the four channels and lowpass filters remove the higher harmonics of f_{RF} from the signal spectrum. An RF multiplexer with programmable button sequence scans the four buttons. The succeeding low noise narrowband preamplifier ($B = 5$ MHz, $G = 20$ dB) rejects the image range. For high signal levels a switchable 30 dB attenuator can be inserted. A balanced mixer transposes the desired frequency range to the intermediate frequency, where narrowband filters reduce the bandwidth to ≈ 200 kHz and an amplifier with controlled gain enhances the signal level appropriate for demodulation.

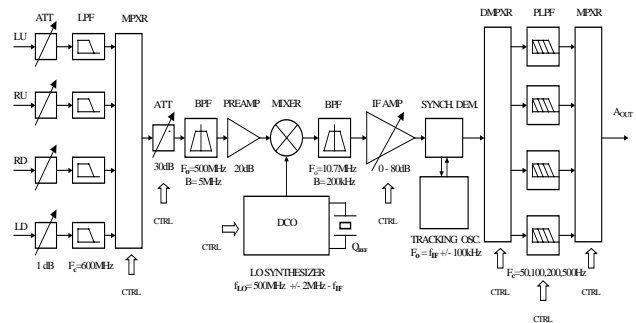


Figure 1: Block diagram of the RF signal processing module

On-board remote-controlled synthesizer generates the LO signal applied to the mixer, determining the band-center frequency of the signal processing.

The band-center frequency is adjustable in the range of $500 \text{ MHz} \pm 2 \text{ MHz}$ with steps of 50 kHz. Frequency changes within the IF bandwidth will be automatically tracked in real time. The output signal of the synchronous demodulator with a linearity of $\approx 0.5\%$ is proportional to the rms value and carries level changes with frequencies up to 500 Hz. The gain control range of the processing chain is about 100 dB.

Signal level dynamic range of the electronics is between -80 dBm and $+10 \text{ dBm}$. The typical equivalent beam position noise is $x_{rms} < 0.5 \mu\text{m}$ at $P_{in} = -46 \text{ dBm}$ and $B = 10 \text{ Hz}$ assuming that the BPM sensitivity is $K_{BPM} = 14.5 \text{ mm}$ (Fig. 2).

Figure 2: Equivalent rms position noise

REAL -TIME BETATRON TUNE MEASUREMENT IN THE ACCELERATION RAMP AT COSY – JÜLICH

J. Dietrich and I. Mohos, Forschungszentrum Jülich GmbH, Germany

Abstract

A new real-time method for betatron tune measurements at COSY was developed and tested from the early 1997. A bandlimited broadband noise source was used for beam excitation, the transversal beam position oscillation was bunch-synchronous sampled and digitized with a high resolution ADC. The Fourier transform of the acquired data represents immediately the betatron tune. After the first promising experiments an automatic tunemeter was constructed. The tunemeter is used as routine diagnostic tool since end of 1998.

1 INTRODUCTION

The cooler synchrotron and storage ring COSY, with a circumference of 184 m and single bunch, delivers medium energy protons. The corresponding revolution frequencies in the acceleration ramp are between 0.45 MHz (flat bottom) and 1.6 MHz (flat top). For beam diagnostic measurements magnetic impulse kicker [1] and broadband stripline exciter [2] can be used. The mode of excitation and the strength can be automatically set. A basic task for beam diagnostic is the measurement of the tune in the acceleration ramp.

The betatron tune (Q) is the quotient of the frequency of the betatron oscillation and the particle revolution frequency. The betatron frequency ($f_\beta = Q * f_0$) is usually higher than the revolution frequency, but only the fractional part (q) of the betatron tune can be measured:

$$f_\beta^n = n * f_0 \pm Q * f_0 = (n \pm q) * f_0.$$

For tune measurements the betatron oscillation of the particles is resonantly enhanced by RF-excitation via the stripline unit. Beam position monitors (BPM) [3] with low noise broadband amplifiers deliver signals proportional to the beam response on the excitation. The sampled and digitized difference signal is processed for monitoring the betatron tune. A bunch-synchronous pulse train, necessary for the sampling, is derived from the sumsignal of the same BPM.

2 SYNCHRONOUS SAMPLING AND FFT

Performing the discrete Fourier transformation of N subsequently acquired samples follows:

$$S\left(\frac{m}{NT}\right) = \sum_{n=0}^{N-1} s(nT) * e^{-j(2\pi m n)/N}$$

with T time interval of the samples,

$s(nT)$ the n -th sample of an array of N samples

$S\left(\frac{m}{NT}\right)$ the m -th Fourier component at $f_m = \frac{m}{NT}$

The frequency of a Fourier component relates to the sampling frequency ($f_s = 1/T$). Due to the bunch-synchronous sampling the frequencies in the FFT array are normalized to the revolution frequency.

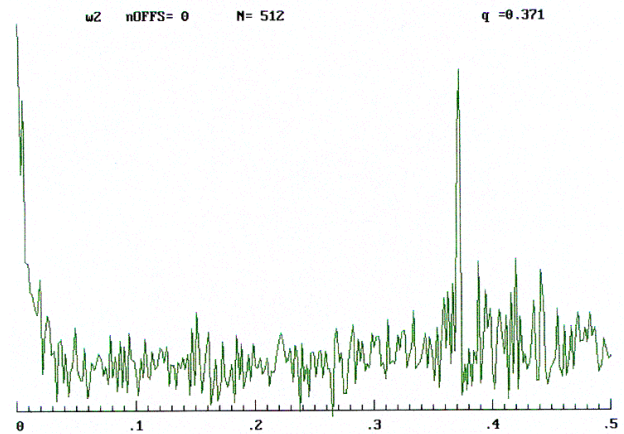


Figure 1: Betatron line in the normalized frequency domain

A sideband caused by the betatron oscillation appears as a peak in the normalized frequency domain. Fig. 1. shows a sideband line in the spectrum [4]. Because of using the revolution frequency as sampling frequency, it follows:

Measuring Beam Intensity and Lifetime in BESSY II ¹

R. Bakker, R. Goergen, P. Kuske, J. Kuszynski²

Berliner Speicherring-Gesellschaft fuer Synchrotronstrahlung mbH
(BESSY) Rudower Chaussee 5 D-12489 Berlin Germany

Abstract

The measurement of the intensity of the beam in the transfer lines and the storage ring are based on current transformers. The pulsed current in the transfer lines is measured with passive Integrating Beam Current Transformers (ICT). The bunch charge is transferred to a DC-voltage and sampled with a multifunction I/O-board of a PC. The beam current of the storage ring is measured with a high precision Parametric Current Transformer (PCT) and sampled by a high quality digital volt meter (DVM). A stand alone PC is used for synchronisation, real-time data acquisition and signal processing. Current and lifetime data are updated every second and send via CAN- bus to the BESSY II control system. All PC programs are written in LabVIEW.

1 INTRODUCTION

BESSY II started operation as a third generation synchrotron radiation light source at the beginning of this year. The facility consists of the 1.7 GeV electron storage ring and the full energy injection system comprised of the synchrotron cycled at 10 Hz and a 50 MeV microtron as a pre-injector [1]. Along the chain of accelerators and transfer-lines different types of current monitoring devices are employed and have to fulfil the following requirements: measurement of the intensity of the pulsed beams in the two transfer lines, the accurate determination of the intensity of the accelerated beam in the synchrotron, and the high precision current measurement of the stored beam in the ring. All measurements had to be performed in real-time and have to be updated every second in order to allow for the fast and accurate extraction of the injection efficiency and the lifetime of the beam. In addition to these measurements and the determination of related parameters, the system had to supply trigger and timing signals for the beam position monitor (BPM) system running in the single turn mode [2]. In this system 4 shots and the corresponding injected beam intensities are required to determine the position of the beam as accurately as possible. This is achieved by current normalising the 4 data sets. As a solution a stand-alone hardware triggered solution based on a PC running under LabVIEW was chosen and the

system has been realised with commercially available components.

2 HARDWARE

The current transformers were manufactured by BERGOZ [3, 4]. In the transfer lines the sensors are mounted over a short insulated piece of vacuum pipe and shielded by an aluminium cover. In the storage ring and in the synchrotron the installation of the DC current transformer (DCCT) has been realised with more care in order to prevent RF fields of the electron beam leaking to the sensor's head and heating it up. In addition onion-like thin soft iron sheets shield the sensor from magnetic stray fields created by nearby magnets. The vacuum chamber for the DCCT is based on the SLAC B-Factory design[5].

The layout of the beam current monitor system is shown in Fig. 1. The stand alone industry PC has been equipped with three additional boards. The first is a multifunction input/output-board AT MIO-16X from National Instruments. This board in combination with additional external trigger electronics creates all the required timing signals for the DVM, the synchronisation of the pulsed beam intensity measurements, and synchronises the single turn beam position measurements with the intensity measurements. The multiplexed 16 bit ADC on the multifunction board is used for the acquisition of the signals delivered by the ICTs. The digital outputs of the board are used to switch the external electronics to the desired modes of operation. The second board is the GPIB interface required for the communication to the high precision DVM HP3458A from Hewlett Packard which measures the current of the stored beam.

Signal processing is performed in the following way: The microtron delivers pulses of approximately 1 μ s duration and the bunch train extracted from the synchrotron has a length of 360 ns. Every 100 ms the charge passing through the transfer lines is detected by the ICT. Over a certain amount of time the beam charge monitor integrates the signal and produces a constant output voltage which is finally sampled by the multifunction I/O-board. With the sampling rate of 100kS/s of the ADC a 15 time over-sampling of each channel is obtained.

The beam current of the storage ring is measured with a high precision (PCT) and sampled by the DVM. The intensity of the beam accelerated in the synchrotron can

¹ This work is funded by the Bundesministerium für Bildung, Wissenschaft, Forschung und Technologie and by the Land Berlin.

² Email: kuszynski@bii.bessy.de

Radiation Protection System installation for the Accelerator Production of Tritium / Low Energy Demonstration Accelerator Project (APT/LEDA).

J. E. Wilmarth, M. T. Smith, T. L. Tomei
 Los Alamos National Laboratory, Los Alamos, NM

Abstract

The APT/LEDA personnel radiation protection system installation was accomplished using a flexible, modular proven system which satisfied regulatory orders, project design criteria, operational modes, and facility requirements. The goal of providing exclusion and safe access of personnel to areas where prompt radiation in the LEDA facility is produced was achieved with the installation of a DOE-approved Personnel Access Control System (PACS). To satisfy the facility configuration design, the PACS, a major component of the overall radiation safety system, conveniently provided five independent areas of personnel access control. Because of its flexibility and adaptability the Los-Alamos Neutron-Science-Center-(LANSCE)-designed Radiation Security System (RSS) was efficiently configured to provide the desired operational modes and satisfy the APT/LEDA project design criteria. The Backbone Beam Enable (BBE) system based on the LANSCE RSS provided the accelerator beam control functions with redundant, hardwired, tamper-resistant hardware. The installation was accomplished using modular components.

RADIATION PROTECTION SYSTEM

Los Alamos National Laboratory's MPF-365 at TA-53 is a four-story building attached to a 470-foot-long underground tunnel. See Figure 1. In 1997 the Accelerator Production Of Tritium (APT) Low Energy Demonstration Accelerator (LEDA) project started installation work in MPF-365. The LEDA project accelerator consists of five major components:

1. The Injector Support Platform, which is movable with a detachable Ion Source Injector (LEBT).
2. The Radio Frequency Quadrupole (RFQ) section.
3. High Energy Beam transport (HEBT).
4. Water Shielded Beam Stop Vessel.
5. Detachable/Movable pump cart which supplies high pressure water to the beam stop.

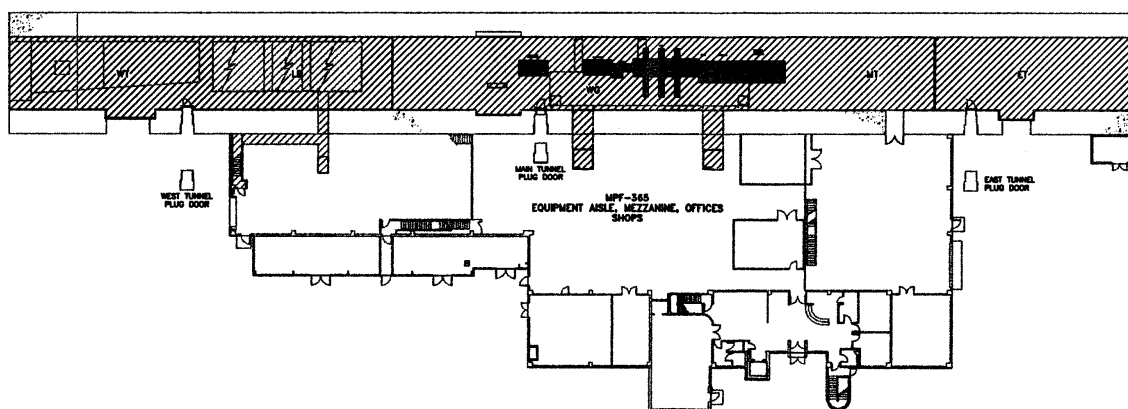


Figure 1 Layout of MPF-365 building

The LEDA accelerator is located over RF tunnels through which the waveguides travel to the RFQ. The foot print of the LEDA accelerator uses only about one-fourth of the accelerator tunnel's available floor area. The accelerator tunnel was divided into three major areas for Personnel Access Control Systems (PACS) protection. The East Tunnel (ET) is separated from the main tunnel (MT) section, where the accelerator is located by a sliding gate

and chain link fence. The West Tunnel (WT) is separated from the Main Tunnel (MT) section by a second gate and chain link fence. The Wave Guide Basement (W/G), the fourth PACS area, has two shafts and tunnels from the equipment aisle to a room below the main tunnel. There are two hatches located between the main tunnel and waveguide lower room. The fifth PACS area is an old laser

FIRST RESULTS ON CLOSED-LOOP TUNE CONTROL IN THE CERN-SPS

L. Jensen, O. R. Jones, H. Schmickler

CERN SL/BI, Geneva, Switzerland

Abstract

This paper presents the first measurements performed with the SPS Qloop. The emphasis will be laid on the model used for designing the regulation loop and how well it fits reality.

1. MOTIVATION

The SPS Qloop project was started as a follow-up to the ‘LHC Dynamic Effects Working Group’ workshop [1]. One of the results from this workshop was the expressed need for real-time feedback on the betatron tunes in the LHC, since the extensive use of super-conducting magnets mean that feed-forward tables will not suffice.

2. FEEDBACK PRINCIPLE

The use of feedback is well known in everyday life. An example is the use in air-conditioners. Designing a regulation loop involves knowledge of the time-constants and delays in the system one is trying to control. In the following paragraph we explain how a model was derived for the SPS Qloop.

3. MEASUREMENT OF QD TRANSFER FUNCTION

In the SPS Qloop, we use the main SPS quadrupole strings QD and QF for the correction of the betatron tunes. Measurements done by A. Beuret et al in 1995 showed that the transfer function of the power converter to the magnet has a -3 [dB] cut-off frequency of approx. 40 [Hz]. The measurement did not however take into account the possible time delay between the powering the magnets and their action on the beam. This delay is caused by the time it takes for the magnet flux to pass through the vacuum chamber and plays an important role for the limited bandwidth of the LEP Qloop. The measurement of the transfer function $H(s) = Qv(s)/Iqd(s)$ was done during two SPS MD’s, where sine-wave signals of varying amplitude and frequency were super-imposed on the quadrupole DC reference current. By doing harmonic analysis, the transfer function could be calculated [2]. In figures 1A and 1B, the resulting transfer function of the main SPS QD magnet string can be seen. A 2nd order Butterworth low-pass filter has been fitted to the results and a good agreement can be found up to the -3 [dB] frequency of around 28 [Hz].

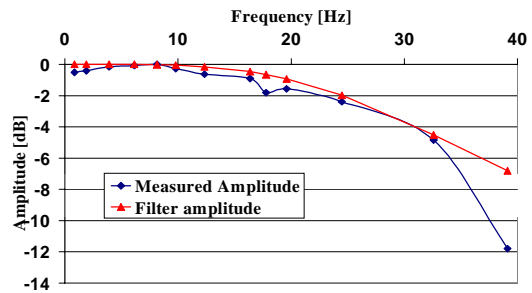


Figure 1A: Amplitude response for transfer function

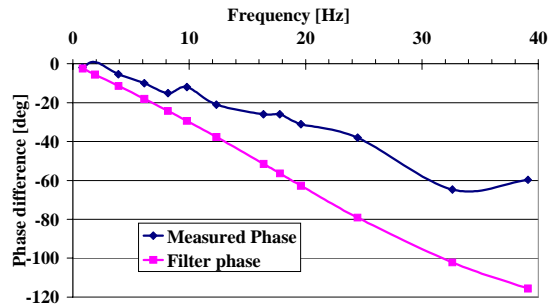


Figure 1B: Phase response for transfer function

4. MATLAB SIMULATIONS

From the above measurements, we learnt that we could approximate the transfer function by a 2nd order low-pass filter with a cut-off frequency of around 28 [Hz]. A widely used computer program called ‘Matlab’, with the ‘Controls’ toolbox and the ‘Simulink’ package, was used to design the regulation loop for the SPS Qloop. One of the most important parameters is the time between corrections, which in our specific case is given by the interval between individual tune measurements. Computation and transmission latencies for the corrections can be neglected in our case. For the tune measurements we are using 10 ms long chirp excitations and FFT transforms of the beam motion with automatic peak finding in the amplitude spectrum. In order to avoid possible problems due to coupling, only one plane is excited at a time. The tunes can therefore not be measured at an interval shorter than 20 ms.

The regulation loop should reduce the error as fast as possible without creating an excessive overshoot (thus requiring a certain phase and gain margin). Several books describe the design criteria for regulation loops (see e.g. [3]).

New Digital BPM System for the Swiss Light Source

M. Dehler, A. Jaggi, P. Pollet, T. Schilcher, V. Schlott, R. Ursic, PSI, Villigen, Switzerland
 R. DeMonte, ELETTRA, Trieste, Italy

Abstract

This paper presents a new digital beam position monitor (DBPM) system which is currently under development for the Swiss Light Source (SLS). It is designed to provide sub-micron position data in normal closed orbit, and feedback mode as well as turn by turn information for machine studies and real time tune measurements. The self calibrating four channel system consists of a RF front end, a digital receiver and a DSP module. The same electronics will be used in all sections of the SLS accelerator complex. The system can be reconfigured in real time to perform different kind of measurements like: pulsed for linac and transfer lines, first turn, turn-by-turn, closed orbit, feedback and even tune mode for booster and storage ring. These reconfigurations only involve downloading of new signal processing software and will be performed via EPICS control system. An independent system for monitoring mechanical drifts of the BPM stations will be installed as well. The measured data will be permanently updated in a database and taken into account, when processing the final electron beam positions.

1 INTRODUCTION

The SLS is a high brilliance synchrotron radiation source presently under construction at the Paul Scherrer Institut (PSI) in Villigen / Switzerland. It is designed to supply highest brightness in the photon energy range from vacuum ultraviolet to soft X-rays and to provide flexibility to accommodate a variety of operation modes. Therefore, the SLS beam position monitor system has to ensure the adequate beam quality throughout the accelerator complex, consisting of a 100 MeV linac, two transfer lines, a full energy booster synchrotron and a 2.4 GeV storage ring.

In order to guarantee simplicity and uniformity of the system it was aspired to implement only one kind of BPM electronics for all SLS machine sections and operation modes. The most challenging requirements in terms of resolution and stability result from the necessity to reduce beam jitter to less than $\sigma/10$ of the vertical beam size in the ID sections of the storage ring. This corresponds to sub-micron beam position measurements, which have to be provided at a few kHz bandwidth, in order to successfully operate a fast (global) orbit feedback [1]. Concurrently, machine studies request snap shots of the beam orbit in turn-by-turn mode (TBT). Therefore, the BPM electronics has to deliver position data with more than

0.5 MHz bandwidth. A summary and description of the supported operation modes is given below. The technical specifications are listed in table 1.

- Pulsed Mode
Intended for injector and transfer line BPM measurements. Assuming 3 Hz injection, one sample will be taken every 333 ms.
- Booster Mode
Each BPM will provide position measurements throughout the acceleration cycle. Two orthogonal modes are envisioned. First, a single BPM measurement or a group of them is displayed in time domain. This allows tracking of positions as the beam is accelerated. Second, booster closed orbit is displayed at selectable time intervals.
- Turn-by-Turn
User can select N (1024,...,8192) successive measurements to be taken per each sync. cycle. Time as well as frequency domain data formats are selectable.
- Closed Orbit
Position measurements are taken continuously. Data is used for closed orbit (CO) display in control room.
- Feedback Mode
Measurements are taken in the same way as in closed orbit mode and processed continuously to provide position information to global feedback.
- Tune Mode
Data are taken in the same way as in turn-by-turn mode. However, software algorithm on DSP will calculate FFT and extract tunes.

Table 1: DBPM Specifications

Parameter	CO and Feedback	Pulsed and TBT
Dynamic Range	1-500 mA	1-20 mA
Beam Current Dependence		
full range	< 100 μ m	-
relative 1 to 5 range	< 5 μ m	-
Position Measuring Radius	5 mm	10 mm
Resolution	< 1 μ m	20 μ m
Bandwidth	> 2 kHz	0.5 MHz
RF and IF Frequencies		
Carrier RF	500 MHz	500 MHz
Carrier IF	36 MHz	36 MHz
Pilot RF	498.5 MHz	498.5 MHz
Pilot IF	34.5 MHz	34.5 MHz

EMITTANCE MEASUREMENTS AT THE NEW UNILAC PRE-STRIPPER USING A PEPPER-POT WITH A PC-CONTROLLED CCD-CAMERA

M. Dolinska¹, M. Domke, P. Forck, T. Hoffmann, D. Liakin², A. Peters, P. Strehl
 GSI, Darmstadt, Germany.

Abstract:

The complex mathematical algorithms and procedures to extract emittance data from intensity distributions measured with a single shot pepper-pot device are described. First results of mathematical evaluation from the commissioning of the new GSI pre-stripper linac structures are presented.

1 INTRODUCTION

At present commissioning of the new UNILAC pre-stripper is performed. To assess the performance of new types of ion sources, fluctuations of beam emittances from pulse to pulse and, even within one pulse, a single shot pepper-pot system has been developed. The design criteria have been already reported in [1].

2 STRUCTURE OF SOFTWARE

The software was designed to provide the interconnection between all parts of the installed measuring hardware, a user friendly interface for hardware control and a detailed graphical output for the obtained results. Figure 1 shows the general structure of the software. To control the CCD camera the manufacturer developed system drivers and DLL's have been used. This offers the operator the possibility to change the operation mode of the camera, the exposure time, the resolution and some other parameters related to the actual parameters of the ion beam or the calibration signal. Furthermore, in case of low intensity of the observed light spots it is possible to integrate a series of single shots to improve the quality of the images.

The objective of the CCD-camera is controlled by means of the Tiger-BASIC based microprocessor system, which has been connected to the PC through a conventional RS485 interface. Therefore, no additional system driver had to be installed.

The collected data may be processed immediately via the "Calculation routines DLL" for evaluation of emittances or may be stored on the hard disk in binary or ASCII format for later calculations. Additionally, data may be saved and reloaded in Windows bitmap format.

Information about a current measurement, including commentary and preview pictures, are stored in the local database to provide easiest and systematic access to all

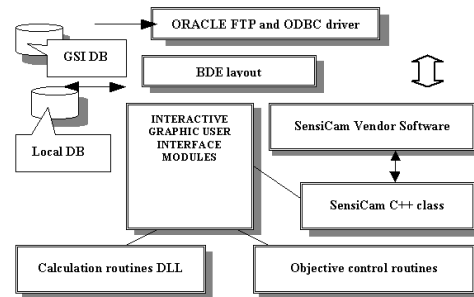


Figure 1: General structure of the pepper-pot system software

results. Information about the kind of accelerated ions, their charges, energy etc., is obtained from the global GSI database.

3 DATA PROCESSING

3.1 Calibration procedure

In the calibration process a parallel light beam from a laser (see [1] for details) is used to determine the correspondence between the pixels of the camera image and the real physical dimensions. It is assumed that the coordinates on the image, correlated to the locations of the holes in the pepper-pot plate can be obtained from the center of intensity of each light spot. Since all spots of the pepper-pot holes are arranged in the nodes of a regular rectangle grid it is sufficient to apply the implemented searching algorithm only for a whole row or column. The results are stored as reference information for future calculations in the project database.



Figure 2: Light spots from the calibration with the laser beam (left) and real beam data, obtained with the CCD – camera.

¹ INR-Kiev, work done at GSI

² ITEP-Moscow, work done at GSI

A FAST PROTECTION SYSTEM FOR NARROW-GAP INSERTION DEVICE VESSELS

M J Dufau, R J Smith, CCLRC Daresbury Laboratory, Warrington, UK.

Abstract

Presented in this paper are details of an electronic, beam position based interlock system, which has been designed to protect narrow - gap insertion device vessels from the thermal damage that would result from mis steered beam. Details of system design and operational experience are presented, and the paper concludes with an outline proposal for a system enhancement, that would offer diagnostic information immediately prior to an excessive beam displacement trip.

1 INTRODUCTION

In 1998 a major programme of upgrade work was completed on the Synchrotron Radiation Source (SRS), Daresbury Laboratory UK. The upgrade involved the installation of two insertion devices, multipole wigglers, with the intention of enhancing the versatility of the SRS as a synchrotron light source.

When an analysis in to the effect of beam impinging the walls or flanges of either of the associated narrow-gap vessels, as a result of mis-steer, was conducted, a probability of permanent thermal damage, occurring within several seconds of time was indicated. Water-cooling as an engineering solution could be applied to the upstream flanges, but the walls of the vessels would still be extremely vulnerable. Thus the requirement for a protection system to prevent potential thermal destruction of either vessel was founded.

Two systems have been built to the design that subsequently evolved, and have since January of this year provided vessel protection with unfaltering reliability.

2 SYSTEM DESCRIPTION

Protection of a vessel is accomplished by tripping off the Radio Frequency (RF) source when conditions that are potentially thermally damaging to a vessel prevail. The primary interlock signals to achieve this are generated by excessive vertical beam displacement through a vessel, or excessive rise in temperature of the walls of a vessel. Vertical beam displacement signals are provided by Electron Beam Position Monitors (EBPMs) installed within a vessel (two off, upstream and downstream). An array of thermocouples supervised by a Programmable Logic Controller (PLC) provides the excessive temperature signal.

Since all combinations of stored beam and injection energy are deemed to be a safe operating area, an Energy Sensitive Bypass renders beam displacement interlocks inactive during injection. This facilitates steering through

the narrow gap of a vessel at injection, by permitting a wider tolerance on beam displacement.

The organisation of primary interlocks is illustrated in Figure 1.

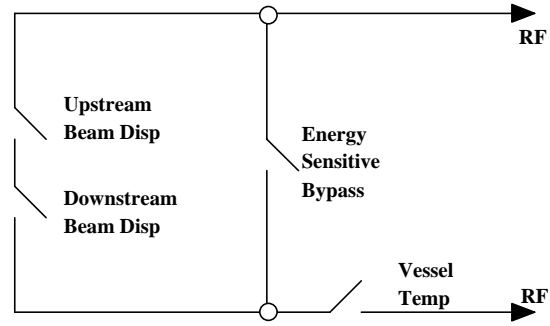


Figure 1: Organisation of primary interlocks

Because confidence in the reliability of primary interlocks is paramount, secondary interlock signals are required to become active, when the integrity of electronic hardware or support signals is suspect. These secondary interlock signals monitor the performance of the electronics for the EBPMs, Total Current Monitor (TCM), power supplies, PLC and also a Direct Current Transformer (DCCT) which provides an energy level proportional signal from the dipole magnet current.

The organisation of all system interlocks both primary and secondary is illustrated in Figure 2, which also includes a keyswitch-controlled bypass of the beam displacement interlocks.

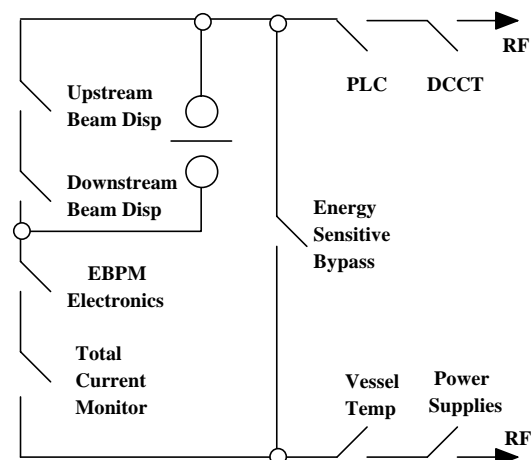


Figure 2: Organisation of primary and secondary interlocks

The Closed-Orbit Measurement System for the CERN Antiproton Decelerator

M. Le Gras, L. Sjøby, D. J. Williams
 CERN, Geneva, Switzerland

Abstract

The closed-orbit measurement system for the new Antiproton Decelerator (AD) employs 59 electrostatic pick-ups (PU). The intensity range from 2×10^{10} down to 10^7 particles poses challenging demands on the dynamic range and noise of the head amplifier. A low noise-amplifier has been developed, having an equivalent input noise of $0.6 \text{ nV} / \sqrt{\text{Hz}}$, allowing beam positions to be measured to $\pm 0.5 \text{ mm}$ with 5×10^6 particles. Two different gains take care of the large dynamic range. After amplification and multiplexing, the PU signals are fed to a network analyser, where each measurement point corresponds to one PU. The network analyser is phase locked to the RF of the AD, thus acting as a “tracking filter” instrument. An orbit measurement takes from 0.2 to 12 s depending on the IF-bandwidth of the network analyser, selected according to the beam intensity, and the precision required. At the end of the network analyser sweep the data are read via a GPIB interface and treated by a real-time task running in a VME based Power PC.

1 INTRODUCTION

The AD is a new machine, replacing the previous low-energy antiproton facility, which consisted of AC, AA and LEAR. In the AD, antiprotons of 3.5 GeV/c are injected and decelerated down to 100 MeV/c, to be ejected to the experimental area in the centre of the machine. During deceleration, on intermediate plateaus, stochastic cooling and electron cooling is performed. On each intermediate energy level the orbit must be measured, and if necessary, corrected.

2 BEAM AND SIGNAL PARAMETERS

The PUs in the AD are made of metal sheets, accurately cut and mounted in metal tubes fitted inside the vacuum chamber. One annular electrode provides the intensity signal (Σ). The difference signal (Δ) is derived from 2 semi-sinusoidal electrodes. The Δ/Σ -ratio together with the PU sensitivity gives an intensity independent beam position. The signal levels on the electrostatic PU electrodes are calculated using Eq. 1 below:

$$\hat{V} = \frac{Ne}{C} \frac{l}{S} \frac{\pi}{2} B_f \quad [V] \quad (1)$$

Where N is the number of particles, C the electrode capacitance, e the elementary charge, l the electrical

length of the PUs, S the AD circumference, $\pi B_f / 2$ the ratio of peak to average line density. $B_f = 1$ yields a signal level of $4.2 \mu\text{Vp}$ per electrode at 1×10^7 particles and a differential PU sensitivity of $0.1 \mu\text{Vp} / \text{mm}$. In a 20 MHz system with an equivalent amplifier input noise of $2 \text{ nV} / \sqrt{\text{Hz}}$, the signal-to-noise (S/N) ratio is approximately 0.01 for 1 mm of beam position, or in other words a resolution of $\sim 100 \text{ mm}$!. It is clear that a reduction of bandwidth and input noise is necessary. On the other hand, one wants to observe the bunches of high intensity beams of 10^{10} particles on an oscilloscope, which demands a large bandwidth. In the AD the revolution frequency varies from 1.6 to 0.17 MHz and the minimum bunch length is in the order of 100 ns. For good bunch observation a system bandwidth of 10 kHz-20 MHz is thus necessary.

3 THE HEAD AMPLIFIER

It was therefore decided to build a head amplifier of the following specification:

	Intensity range: $1 \times 10^7 - 5 \times 10^8 P$	Intensity range: $5 \times 10^8 - 10^{10} P$
Input imp.	$5 \text{ M}\Omega // 49 \text{ pF}$	$5 \text{ M}\Omega // 18 \text{ pF}$
Gain	47 dB	20 dB
Bandwidth	10 kHz-20 MHz	10 kHz-50 MHz
Input noise	$0.6 \text{ nV} / \sqrt{\text{Hz}}$	$6 \text{ nV} / \sqrt{\text{Hz}}$
CMRR	>66 dB	>66 dB
Max. Output	1.5 Vp in 50Ω	1.5 Vp in 50Ω

Table 1: Head amplifier specification

To achieve the very low noise performance required of the head amplifier in the high gain mode, a technique using paralleled Junction Field Effect Transistors (JFETs) [1] was used. A simplified diagram of an input stage is shown in Fig. 1.

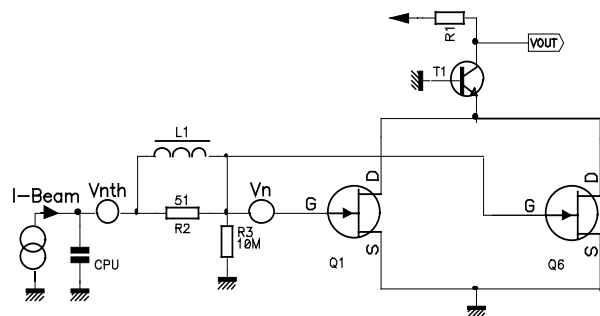


Figure 1: Simplified diagram of head amplifier

EMITTANCE AND DISPERSION MEASUREMENTS AT TTF

M. Castellano, A. Cianchi, V. A. Verzilov, INFN-LNF, CP 13, 00044 Frascati, Italy
L. Catani, G. Orlandi INFN- Roma 2, Italy

Abstract

It is well known that beam dispersion, along with the Twiss parameters and emittance, contributes to the beam spot size. So that, in general, anomalous dispersion is an undesirable event and must be minimized by careful tuning the machine. If not, when the spot size is used to infer beam emittances, as it is the case of the "quadrupole scan" method, basically employed at TTF, the unknown dispersion can lead to overestimated values for the emittance. This paper presents the first attempt to determine the dispersion function at several points of the TTF Linac and to separate its contribution to the local emittance measurement, performed by means of the OTR imaging technique.

1 INTRODUCTION

Since the beginning of this year, TESLA Test Facility (TTF) is operated with Injector II equipped with a laser driven rf gun. Injector II is designed to generate electron beams with an emittance of 20 mm mrad (normalized) at a bunch charge of 8 nC, an option needed for a TESLA Linear Collider, and with an emittance of 2 mm mrad at 1 nC in a FEL mode [1]. In both cases it is important to preserve emittances as small as possible up to the end of the linac. For this purpose the beam emittance is monitored at several points along the accelerator.

The results of the TTF commissioning with Injector I have shown that, while at the injector level the measured values for the emittance were in agreement with designed specifications, in the high energy region of the linac a certain emittance growth was observed. Measurements were performed by means of the "quadrupole scan" method in which the rms beam size is measured as a function of the strength of one or several quadrupoles situated upstream a beam profile monitor. Since in this method the beam size is used to infer beam emittances, there are suspicions that an unknown dispersion could contribute to the beam spot size, thus leading to overestimated values for the emittance.

In practice, the beam dispersion arises due to misalignment of beam line elements or off-axis beam transporting. Once generated at some place, it will propagate through the machine. In general, an anomalous dispersion is an undesirable event, since it can significantly increase the beam size at places where that is expected to be particularly small: at interaction points of colliders or undulator sections of FELs. Careful tuning the machine is sometimes needed to minimize the beam dispersion.

This paper presents the first attempt to determine the dispersion function of the TTF Linac. Measurements were performed by means of the OTR imaging technique widely employed at TTF [2]. Two different kind of dispersion

measurements were done at two positions of the linac.

2 DISPERSION AND EMITTANCE MEASUREMENT BY MULTIPLE "QUADRUPOLE SCAN".

At the position between first and second acceleration modules, after the so-called "bunch compressor II", we attempted to determine simultaneously the beam emittance and both the spatial and angular dispersions by means of a multiple scan. A schematic diagram of a layout is shown

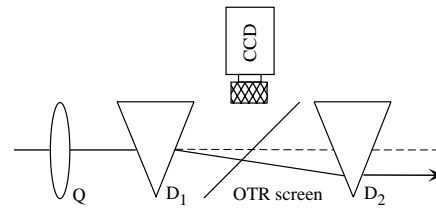


Figure 1: Schematic layout for multiple scan dispersion and emittance measurements.

in Fig. 1. A quadrupole Q followed by a bending dipole D_1 allowed to change the beam spot on a OTR screen, images of which were registered by a CCD camera. A second dipole D_2 behind the screen was employed to drive the beam through the second acceleration module and, thereby, prevent quenches in superconducting cavities due to the beam dumping inside the cryomodule.

As known, in the presence of the dispersion the first-order squared beam size on the screen is given by

$$x_{rms}^2 = \sigma_{11}(s) + \left(\eta(s) \frac{\Delta p}{p} \right)^2, \quad (1)$$

where $\sigma_{ij}(s)$ stands for elements of the σ -matrix defined at the position s (OTR screen), $\eta(s)$ is the dispersion function at this position and $\Delta p/p$ is the momentum spread. In the linear optics, an evolution of the σ -matrix from point to point of the beam line is controlled by the transfer matrix. In particular, the transformation of the element σ_{11} from the entrance face of the quadrupole Q (position 0) to the position s is described as follows

$$\sigma_{11}(s) = m_{11}^2 \sigma_{11}(0) + 2m_{11}m_{12} \sigma_{12}(0) + m_{12}^2 \sigma_{22}(0), \quad (2)$$

where m_{ij} denotes elements of the 3×3 transfer matrix. In the same manner, the dispersion function on the screen is determined by its value and derivative at the entrance of the quadrupole

$$\eta(s) = m_{11}\eta(0) + m_{12}\eta'(0) + m_{13}. \quad (3)$$

DIPOLE MODES STUDY BY MEANS OF HOM COUPLERS AT SBTF

N. Baboi*, M. Dohlus, A. Jöstingmeier, N. Holtkamp, M. Wendt, M. Nagl,
J. Boster and H. Hartwig, DESY, Notkestr. 85, 22603 Hamburg, Germany

Abstract

High order modes (HOM) are generated by the interaction of a bunched beam with an accelerator environment. They may act destructively on following particle bunches, leading to an increase of the transverse oscillation amplitude and finally to the deterioration of the emittance. Dipole modes have been studied at the S-Band Test Facility at DESY. One accelerating structure, specially designed for this test linac, is equipped with waveguide pick-ups for measuring the HOMs. For one part of the experiments, a modulation of the transverse offset of the bunches at the structure entrance has been induced using a fast broadband kicker and the effect was measured with a precise stripline BPM. No high impedance modes were clearly found in the structure, which has been detuned and damped by both the tapered geometry of the structure and an absorbing stainless steel coating applied on the iris tips.

1 THE S-BAND TEST FACILITY

The very high luminosity, $10^{33} \text{ cm}^{-2} \text{ s}^{-1}$, required for future linear colliders presume high charge, small cross section bunches. The main problem is that these bunches strongly interact with the accelerator environment, leading to the excitation of electromagnetic fields, the so-called high order modes (HOM). Off-axis bunches excite transverse HOMs, generating the transverse wake field:

$$W_{\perp}^{\lambda}(s) = \sum_l 2k_{\perp l}^{\lambda} \sin(\omega_l \frac{s}{c}) \exp(-\frac{\omega_l}{2Q_l} \frac{s}{c}), \quad (1)$$

where $s > 0$ is the distance behind the bunch and ω_l , $k_{\perp l}^{\lambda}$ and Q_l are the angular frequency, the transverse loss factor per unit length and the quality factor of mode l .

This wake field acts on the following bunches entering the structure, which leads to the deterioration of the beam properties, mainly to an increase in the emittance and a large energy spread. The modes with a low Q may be damped before the next bunches arrive, so that the main contribution to the wake fields will be given only by the modes with a high k_{\perp}^{λ} and a high Q .

The S-Band Test Facility (SBTF) was built at DESY in the framework of a study of a 500 GeV linear collider based on the S-Band technology [1]. Based on the experience in this frequency range (e.g. SLC), an accelerating structure was specially designed for SBTF, paying attention to reducing the HOMs quality factors. The main purpose of the here described experiments is to find most dangerous HOMs that are excited by using the beam.

* Home address: NILPRP, Bucharest

Layout The electron beam is accelerated to a maximum of about 100 MeV by the injector section and a first accelerating structure [2]. The two next accelerating structures, specially designed for this test facility, could give the beam 300 MeV maximum. The first and the second structures are fed through a power splitter by the same klystron [3], while a second klystron feeds a third one.

In Fig. 1 the second accelerating structure, is represented together with a stripline BPM ([4]) which allowed the monitoring of single bunches, distanced by a minimum of 8 ns. A kicker and a steering magnet are placed between the first and the SBTF structures. The current monitors and some elements that were not used during the experiments are not shown. The very fast counter travelling wave kicker [5] can

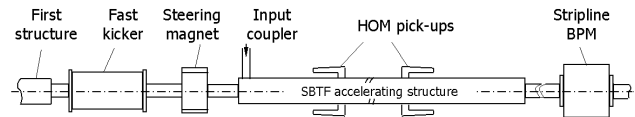


Figure 1: Experimental setup of the kicker experiment

impart on bunches with 35 MeV energy a maximum kick of $400 \mu\text{rad}$, which, in case no HOMs act on the bunches, would be seen at the location of the BPM as an offset of 2.4 mm (the autofocusing was taken into account).

The SBTF accelerating structure and HOMs The 6 m long accelerating structure is a constant gradient one, working in the $2\pi/3$ mode at a frequency of 3 GHz. The iris radii are tapered along the 180 cells. In order to avoid phase and amplitude dependent transverse kicks, the input coupler is symmetric and has a power splitter on top.

Special attention has been given to the HOM attenuation. It has been found in simulations that the main contribution to the transverse wake field is given by the modes in the first, third and sixth dipole passbands. While the level of $k_{\perp l}^{\lambda}$ in the first passband is of the order of $7.5 \cdot 10^{12} \text{ V/Cm}^2$, in the sixth passband a few modes with loss parameters up to $6.8 \cdot 10^{13} \text{ V/Cm}^2$ have been found [6].

The frequency detuning induced by the iris tapering leads to the decoherence of the long range wake field. Due to the recoherence effects of the HOMs, damping of the dipole modes is also necessary. On the other hand, modes in the first passband are trapped inside the structure, which makes the use of a few HOM dampers along the structure not efficient. Instead, damping is achieved by covering the iris tips of the cells with a thin stainless steel layer [7, 1]. For the SBTF structures, only the iris tips of cells 1 to 20 and 111 to 121 were covered with such a layer. The calculations made for the first dipole band for a SBTF structure

Aspects of Bunch Shape Measurements for Slow, Intense Ion Beams

P Forck, F Heymach, U. Meyer, P Moritz, P Strehl

Gesellschaft für Schwerionenforschung GSI, Planck Strasse 1, 64291 Darmstadt, Germany.

Abstract

For the characterisation of the ion beam delivered by the new High Current LINAC at GSI, the time structure of bunches and the knowledge concerning their intensity distribution in longitudinal phase space is of great importance. At least 100ps time resolution and the capability of measuring long tails in the distribution were design parameters. Taking advantage of Rutherford-scattering to reduce the count rate, a direct time of flight measurement technique using diamond detectors can be applied. First results are reported. Plans for determine the energy of individual ions by detecting secondary electrons emitted from a thin C foil using 1m drift are discussed.

1 DESIGN OF BUNCH SHAPE MEASURING DEVICES

Knowledge of the distribution of ions within a bunch and longitudinal emittance is needed for the matching between different LINAC acceleration components as well as for the comparison to calculations, in particular in the case where space charge effects play a role. For the new high current heavy ion LINAC developed at the GSI, which consist of a 36 MHz RFQ (energy 120 keV/u) and two IH-structures (final energy 1.4 MeV/u) [1] space charge effects have to be considered. The commissioning just started in spring 1999 and will be continued until the end of '99 and a maximum pulse current of 15 emA for heavy ions like U^{+} , corresponding to 10^9 ions per bunch is expected. Having a typical phase spread of $\pm 15^\circ$ corresponding to 2ns in time, a resolution of at least 100ps is needed to visualise mismatch or space charge effects. Due to the low velocities, capacitive pick-ups cannot be used.

During the commissioning a movable test bench is installed behind each section [2, 3]. To measure the time structure and the longitudinal emittance of the bunches a new designed device is mounted there, which is based on a time-of-flight method using diamond particle detectors [5], where the arrival time of the ions is measured relative to the acceleration rf, see Fig. 1. The excellent time resolution of a diamond detector is used, but one has to make sure, that less than 1 ion per bunch hits the detector. For this purpose Rutherford-scattering by a thin gold foil is used as an attenuator. The technical outline and preliminary results are discussed.

In addition a second method is under development,

which is suitable for the bunch time structure measurement within one macro pulse. This is an adaption of the well known method by Ostroumov et al. [6], but instead using secondary electrons from an intersecting wire, the electrons of the residual gas atoms will be used. The time information carried by the electrons is converted to spatial differences by an rf-deflector and detected with a spatial resolving MCP. The reader is referred to [3] for further details.

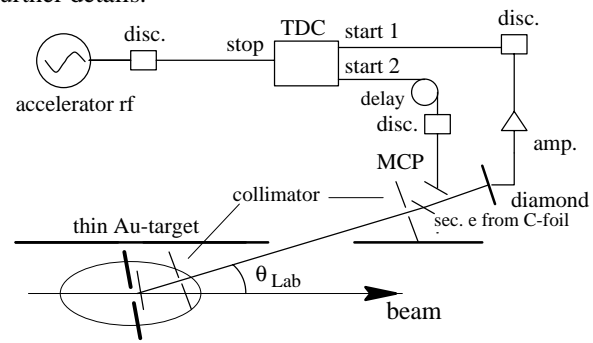


Figure 1: Schematic sketch of the designed TOF method with particle detectors for the bunch shape measurement (see Sec. 2) and phase space distribution (see Sec. 5).

2 RUTHERFORD-SCATTERING CONSIDERATIONS

The precise timing signal from particle detectors is used since several decades for the determination of the bunch structure and the energy spread of slow ion beams. But the direct bombardment of the detector can only be used for very low ion currents to prevent multiple ion hits within one bunch. We like to study space charge effects and therefore the count rate on the detector is reduced by Rutherford-scattering, see Fig. 1. A $120 \mu\text{g}/\text{cm}^2$ (equals to a thickness of $\approx 60 \text{ nm}$) gold foil is used as the target. We choose a laboratory angle $\Theta_{\text{Lab}} = 7.5^\circ$ together with a collimator having $\varnothing 0.5 \text{ mm}$ holes and 16 cm distance on pneumatic feed-throughs. The attenuation of this system is shown in Fig. 2 as a function of the laboratory angle for the RFQ output energy for different ions. The chosen angle prevents from multiple hits for moderate ion currents, while for the highest possible ion currents the count rate can be varied by de-focusing the ion beam. For these considerations, the centre-of-mass energy as well as the broadening of the centre-of-mass solid angle due to the target recoil has been taken into account [4], which depend on the scattering angle, the projectile energy and the ratio between the projectile and target masses. As shown in the figure, the attenuation for the gold target

EXPERIENCE WITH STRIPLINE BEAM POSITION MONITORS ON THE TESLA TEST FACILITY LINAC

P. Castro, DESY, Hamburg, Germany
 P. Patteri, F. Tazzioli, INFN, Frascati, Italy

Abstract

Measurement and correction of beam position are very important for the optimization of beam characteristics and alignment in the Tesla Test Facility (TTF) linac. We describe and present measurements with beam of the performance of the stripline beam position monitors (BPMs) in operation and in order to determine the beam response.

1 INTRODUCTION

Beam position measurement and correction are essential in the TTF linac for collider applications and for the VUV FEL experiment [1]. Beam orbit correction algorithms use the knowledge of the machine lattice in the form of response matrix (element R_{12} in Transport [2] notation) in order to find a combination of corrector strengths which reduces the rms beam position offsets at the BPMs. These correction procedures involve several BPMs and corrector magnets, and require precise measurements of beam position and a good knowledge of the transport matrix.

A series of experiments has therefore been performed to determine the linearity region and range of the BPM response and its offset with respect to the magnetic centres of adjacent quadrupoles. Measurements of the response matrix are compared to the one calculated from known quadrupole gradients and measured beam energy. Results on BPM gains fitted to the measurements will be presented. Correlated beam position jitters, which affect trajectory and emittance measurements, have been measured. Here we will present only a choice of characteristic measurements. For a more exhaustive treatment see [3].

Several measurements have been performed both on TTF phase one and phase two layouts. Phase one had an injector with low charge per bunch (40 pC), high bunch repetition rate (216 MHz) and only one accelerating module (beam energy up to 120 MeV). Phase two has an injector with high bunch charge (1-8 nC), low rep. rate (1 MHz) and two accelerating modules (energy up to 250 MeV).

In Fig. 4 is shown a sketch of the lattice layout of the TTF phase one in the high energy area after the accelerating module, with the location of the stripline BPMs. The focusing is provided by quadrupole doublets.

There are also other types of BPMs on the TTF linac, both outside and inside the cryostats, which contain the accelerating modules. These additional BPMs are based on cavities and have a higher resolution than the stripline BPMs. Here we will limit our discussion to the stripline monitors, which were specified for a resolution of 0.1mm, considered sufficient for beam alignment in the low frequency TTF accelerating modules, having a large bore.

2 STRIPLINE BPMs

We will summarize briefly the characteristics of the stripline BPMs, which have been extensively described elsewhere [4, 5]. The stripline BPMs are 17 cm long and have a 3 cm bore radius. The readout electronics are based on the AM/PM circuit, which gives directly a normalized output proportional to beam displacement and independent of current. The response is linear within ± 5 mm and then deviates from linearity and saturates at about 1 cm. An output curve measured by scanning with a correcting magnet without any magnetic lenses between it and the BPM, is shown in Fig. 1.

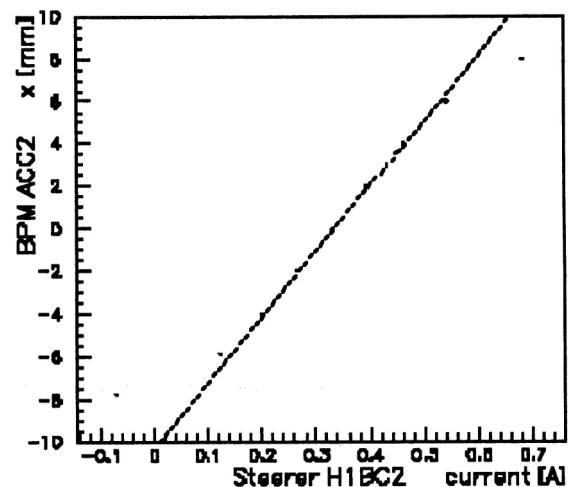


Figure 1: BPM reading versus corrector current.

The front end electronics had to be redesigned for the phase two, where the period between bunches is larger. The new design provides for single bunch response [6]. A typical output pulse is shown in Fig. 2. The acquisition system tracks the waveform until the middle of the flat top and then holds the corresponding value.

High Current Precision Long Pulse Electron Beam Position Monitor

Scott D. Nelson¹, Yu Ju (Judy) Chen, Thomas Fessenden, Clifford Holmes,
Lawrence Livermore National Laboratory, Livermore, California, USA

Abstract

Precision high current long pulse electron beam position monitoring has typically experienced problems with high Q sensors, sensors damped to the point of lack of precision, or sensors that interact substantially with any beam halo thus obscuring the desired signal. As part of the effort to develop a multi-axis electron beam transport system using transverse electromagnetic stripline kicker technology [1,2], it is necessary to precisely determine the position and extent of long high energy beams for accurate beam position control (6 - 40 MeV, 1 - 4 kA, 2 microsecond beam pulse, sub millimeter beam position accuracy.) The kicker positioning system utilizes shot-to-shot adjustments for reduction of relatively slow (< 20 MHz) motion of the beam centroid. The electron beams passing through the diagnostic systems have the potential for large halo effects that tend to corrupt position measurements.

1 INTRODUCTION

The constraints dictated by these beam diagnostic requirements indicate a system that has the advantage of only measuring high energy beams (such that sensitivity to intensity can be small). On the other hand, positional accuracy needs to be sub millimeter in order to define the outer bounds of the beam for determination of the correct transport parameters. As a result, a low Q structure allows for a faster response time and different parts of the beam will not effect the measurement of the beam position during later times. The completed diagnostic system involves a high accuracy beam position detection system, a data acquisition system, a computer controlled feedback system (to control the stripline kicker pulser waveforms) and the kicker pulsers themselves.

The precision beam position monitors are utilized as part of the kicker beam deflection system [3] which requires precise beam control to successfully position the beam through the subsequent output divergent septum beampipe. Accuracies of 0.5 mm are desirable for use with the kicker system and accuracies of 0.1 mm are needed for the proposed target system [3].

2 BASELINE BUG TESTING

As part of the development effort, the existing beam position monitors (a.k.a. BPM's or beam bugs) were tested to evaluate their long pulse performance. Since evolution

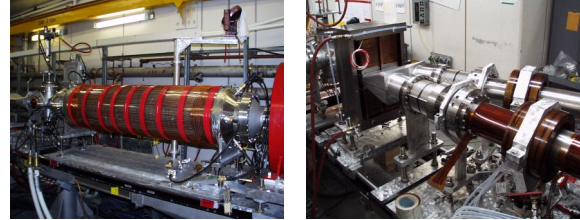


Figure 1. The quad stripline kicker (left) in the Experimental Test Accelerator (ETA-II) beamline as part of the verification experiments [3]. Downstream of the kicker, the deflected beam passes through the septum magnet (right) and into the divergent beam lines.

of the existing BPM's has been an on-going process for many years, they were used as part of the baseline experiments to determine the feasibility of using this type of design for long pulse efforts. Other designs used in beam position measurements were examined but these designs have compatibility problems with long pulse beams, with beams with high degrees of halo, or suffer from charge build up problems over the course of the beam pulse.

To simulate the long pulse beam, a pulser capable of several microseconds and kilovolts was used to drive the test stand. The stand consists of a tapered coaxial section



Figure 2. The beam position monitor test stand (left) used for measuring the accuracy and response of the various BPM's. The stand was driven by a variety of pulsers including a fast rise time pulser and a long pulse VelonexTM pulser with capabilities above one kilovolt and beyond six microseconds (left).

on each end of the test stand. This provides an impedance match to 50 Ω and exhibited excellent spectral uniformity agreeing to within 0.15 dB. These sections drive the straight section of beampipe which is offset to allow for displacing the current conductor with respect to the BPM. Displacements of up to one centimeter were examined. Displacements significantly beyond one centimeter cause

¹Email: nelson18@llnl.gov

Status of the DELTA Synchrotron Light-Monitoring-System

U. Berges, K. Wille

University of Dortmund, Institute for Accelerator Physics and
Synchrotron Radiation, 44221 Dortmund, Germany

Abstract

A synchrotron radiation source like DELTA needs an optical monitoring system to measure the beam size at different points of the ring with high resolution and accuracy.

The measurements with the present synchrotron light monitors show that beam sizes larger than $250\ \mu\text{m}$ can be measured. The measured emittance is of the order of the theoretical values of the optics and goes down to $8\ \text{nm rad}$. The magnification of the system can simply be increased by adding another lens to measure smaller emittances and beamsizes down to $100\ \mu\text{m}$. In this case you still have an optical image of the beam available, but sometimes the position of the camera has to be adapted due to the great magnification of the optical system. The image processing system which is based on a VME Framegrabber makes a two dimensional gaussian fit to the images from different synchrotron light-monitors.

First tests with monochromatic components of the synchrotron radiation ($500\ \text{nm}$ and $550\ \text{nm}$) and with short time cameras (shutter time down to $1/10000\ \text{s}$) have been performed. A two-dimensional PSD has been installed to measure slow beam motion. To measure small beam sizes, especially in the vertical plane, diffraction elements will be used.

This paper gives an overview over the present installation and the results.

1 INTRODUCTION

The **D**ormund **E**lectron **T**est **A**ccelerator facility DELTA consists of a $35 - 100\ \text{MeV}$ LINAC, a $35 - 1500\ \text{MeV}$ ramped storage ring called **B**ooster **D**ortmund (BoDo) and the electron storage ring called Delta ($300 - 1500\ \text{MeV}$).

Both transverse beam sizes of the Booster and the electron storage ring Delta are measured by optical monitoring using synchrotron radiation from bending magnets and commercial CCD-cameras. Therefore, we installed several optical synchrotron radiation monitors at different points of the two rings (see figure 1). By using nearly dispersion free points of the storage ring, we are able to measure the transverse horizontal emittance down to $8\ \text{nm rad}$. Because of the not optimal orbit due to not optimal alignment of the magnets at the moment the beam size and emittance seems to be larger than the theoretical values.

In addition to the imaging system a photodiode is sometimes used at the synchrotron light monitor 1 to measure beam current. The results are in good agreement with the

data of a BERGOZ PCT current monitor at Delta.

We also use a two-dimensional PSD at the synchrotron light monitors 2 (Delta) and 4 (BoDo) to measure slow beam motion.

2 DESIGN OF THE SYNCHROTRON LIGHT MONITORING SYSTEM

Two types of synchrotron radiation monitors both using the visible components of the synchrotron radiation are installed in the ring. One synchrotron light monitor of Delta reflects the optical part of the synchrotron radiation outside the shielding, so that parts of the optical system are accessible during runtime of the machine. The other synchrotron light monitors are completely inside the shielding.

2.1 Synchrotron light monitor inside shielding

This type of synchrotron light monitor is installed at the booster [1] and at the storage ring. Only the optical magnification of the systems is different because of the higher emittance of the booster and the corresponding beamsizes. The synchrotron radiation coming from a bending magnet hits a copper mirror inside the vacuum. The optical part is reflected 90° in the vertical plane, the X-rays are absorbed. The mirror made of OFHC-Copper is mounted on a watercooled mirror holder and has optical quality for the visible region of the synchrotron radiation. Up to now no surface damage due to radiation or heat loading could be observed ($315\ \text{mA}$ average beam current @ $1.3\ \text{GeV}$ and $170\ \text{mA}$ @ $1.5\ \text{GeV}$). After passing a vacuum quartz window the intensity of the synchrotron light can be varied by several neutral density filters (up to optical density 12.8 at the moment). The source point of the synchrotron radiation is focused on the CCD-camera. We achieve a magnification of 1.43 (Delta) respectively 0.14 (BoDo). Due to the magnification the alignment of the CCD-camera is critical. A computer driven mirror is installed so that the image of the beam on the CCD-Chip can be moved in both transverse directions as there is no access to the optical components during runtime of the machine because of the radiation protection. The longitudinal position of the camera is important to choose the correct focus point. It is adjustable during runtime of the machine. Because of the big depth of focus of the optical systems it is less critical.

The sensitivity of this synchrotron light monitor at Delta is high enough to detect the first turn. At BoDo this synchrotron light monitor works reliable at energies higher

ROLE OF PRE-WAVE ZONE EFFECTS IN TR-BASED BEAM DIAGNOSTICS

V.A.Verzilov, INFN-LNF, CP 13, 00044 Frascati, Italy

Abstract

Transition radiation (TR) is nowadays intensively exploited by a number of techniques to characterize different beam parameters. These methods are based, sometimes implicitly, on standard formulae, and used often without paying due attention to their applicability. In particular, standard expressions are only first-order asymptotic, i.e., strictly speaking, valid at infinity. In this paper TR is examined in a spatial domain where conventional results are no more exact and variations in radiation properties are observed. Under certain conditions, for example, at long wavelengths or very high energies the effect is so considerable that should be taken into account in accurate beam measurements.

1 INTRODUCTION

Transition radiation is nowadays intensively exploited by a number of techniques to characterize different beam parameters. These methods are based, sometimes implicitly, on the standard theory of TR, whereas, often it is not fully applicable under conditions of measurements. Therefore, refinements of the theory become essential for both the design of experiments and interpretation of results.

There is a class of phenomena appearing because the electromagnetic field of a relativistic particle has quite macroscopic dimensions. In fact, while the particle itself can certainly be considered a point, its electromagnetic field occupies a finite space, outer border of which scales in the transverse (to the particle trajectory) plane roughly as $\lambda\gamma$, where λ is the radiation wavelength and γ is the relativistic factor. Since, eventually, the source of TR is the particle field interacting with the interface between two media, its size is that of the field. Strong variations in radiation properties are expected when $\lambda\gamma$ exceeds the dimension of a screen used to produce the radiation. Another relevant effect is that, the transverse extension of the TR source appears to be responsible for that the radiation needs to propagate over a substantial distance before acquiring all the well-known properties. Both effects may occur at the same time interfering with each other. In this paper an outline of the second problem is given along with the results of calculations related to applications in beam diagnostics.

2 THEORETICAL BACKGROUND

It is widely accepted that forward TR is formed over the so-called *formation length*, whereas, backward TR can be collected very close to the source. Meanwhile, as shown below, it is not always the case. Even backward TR evolves over a distance of the same order as the formation length of forward TR. This fact has to be taken into account in

beam diagnostics, since backward TR is typically used in measurements and a space available for the experimental instrumentation is often limited by practical reasons.

Only in the *wave zone* the standard formulae can be used. The wave zone is treated in this paper as a spatial domain where the radiation field at any arbitrary point can be considered a plane wave. In other words, in the wave zone the source is seen as a quasi-point one. Therefore, the "border" of the wave zone is determined by the dimension of the source.

To make clear physical arguments we consider an extended coherent source of a radiation. Let O and S be

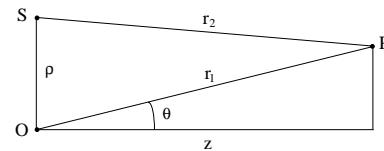


Figure 1: Waves emitted by two different points O and S of the source reach an arbitrary point P with a phase difference $\Delta\varphi = k(r_2 - r_1)$, where k is the wave vector.

two points on the source surface separated by a distance ρ (Fig. 1). Generally, waves emitted by these points at the same phase will arrive at an arbitrary observation point P with a phase difference $\Delta\varphi$. For all the source points between O and S to contribute at P fully constructively, the phase difference must be $|\Delta\varphi| \ll \pi$. Assuming the observation point to be far from the source, so that $z \gg \rho$, the above condition becomes

$$\left| \frac{\rho^2}{z} - 2\rho\theta \right| \ll \lambda. \quad (1)$$

Thus, for the given distance z only a source region of the size ρ satisfying Eq. (1) forms mainly the field at P . On the other hand, to obtain a constructive interference from all the points of the source, the radiation must be collected far enough. It should be noted that in our definition, with ρ being the size of the source, Eq. (1) specifies the border of the wave zone. The obvious conclusion is the larger the dimension of the source the farther the wave zone from it.

For TR the size of the source is of the order of $\lambda\gamma$ and the characteristic angle of emission is $\theta \sim 1/\gamma$. This gives for the wave zone

$$z \gg \lambda\gamma^2. \quad (2)$$

Now we will touch upon the mathematical aspect of the problem. Let's consider backward TR emerging when a normally incident particle with a charge q and a velocity $v \rightarrow c$ hits a perfectly conducting infinite screen. In this case only transverse components of the field are essential

A METHOD FOR MEASUREMENT OF TRANSVERSE IMPEDANCE DISTRIBUTION ALONG STORAGE RING

V. Kiselev, V. Smaluk, BINP, Novosibirsk, Russia

Abstract

A new method for measurement of transverse couple impedance distribution along storage ring is described. The method is based on measuring of a closed orbit deviation caused by local impedance. Transverse impedance acts on the beam as a defocusing quadrupole, strength of which depends on the beam current. If a local bump of closed orbit has been created at the impedance location, then the orbit deviation occurs while varying the beam current. The local impedance can be evaluated using the orbit deviation measured. Measurement technique is described, the method accuracy is evaluated. The method described was successfully used for measurement of the impedance distribution along the VEPP-4M storage ring.

1 INTRODUCTION

The impedance approach is widely used to describe interaction of bunch particles with induced wake fields. In this case, vacuum chamber is considered as set of sections with frequency dependent impedance.

Knowledge of impedance allows qualitative estimates and predictions of the beam stability, and evaluation of the instability thresholds and increments. Calculation of impedance for complex vacuum chamber is quite a cumbersome problem, which should be solved at the initial stage of accelerator design. Since the accelerator was already built, measurement of the impedance and its distribution along the ring makes possible an explanation of various collective effects observed.

There are precise methods to measure some integral characteristics of the impedance.

So, by measuring energy loss factor and current dependence of bunch length one can evaluate integral values for both resistive and reactive components of longitudinal impedance. The resistive component of transverse impedance can be found from measurements of decrement of fast damping of coherent betatron oscillations. The reactive component of transverse impedance can be found by measuring current dependence of coherent betatron frequency shift [1,2].

Methods for measurement of local impedance using beam orbit measurement system are developed and successfully used in CERN [1]. So, distribution along the ring of the resistive component of longitudinal impedance one can obtain by calculation of the difference of two radial orbits measured with different current values. Measurement of betatron phase advance

on pickups gives distribution of the reactive component of impedance. These methods yield impressive results if the total effects measured are rather big and much greater than pickup coordinate resolution and accuracy of betatron phase measurement. There are 300 μm of the orbit deviation and 30° of the phase advance for LEP. Terminal number of sections having impedance simplifies matters. For LEP, as for the most of modern accelerators, major part of total impedance is determined by high order modes (HOM) of RF cavities, placed in one or two straight sections.

Our attempts to use these methods at the VEPP-4M had failed, firstly because of the effect predicted is an order less than at LEP, secondly because the impedance structure differs essentially from the LEP one.

The main contribution into the total impedance of the VEPP-4M [2] is made by about 50 places of violation of vacuum chamber homogeneity like sharp change of cross section or ceramic insert, and 16 vertical electrostatic separators and 3 radial ones. All of them are mainly placed in the technical and experimental straight sections and in the half-ring inserts, and results in TMC-instability of vertical motion. The radial aperture is more than twice larger than the vertical one, and collective effects are 5 times weaker.

To solve the problem a new method for impedance measurement was developed.

2 BASIS OF THE METHOD

A possibility to measure impedance of an individual section is based on the following assumptions.

By comparing the expression for coherent shift of betatron frequency [2]:

$$\Delta Q = -\frac{1}{8\pi} \cdot \frac{I_a \cdot \langle Z_{\perp} \beta \rangle}{E/e}$$

with the formula for small detuning of betatron frequency by an additional defocusing force:

$$\Delta Q = -\frac{1}{4\pi} \cdot \frac{\Delta G l}{H\rho} \cdot \beta$$

one can conclude that the product of an amplitude value of bunch current I_a by the transverse impedance Z_{\perp} is the defocusing lens strength $\Delta G l$. Current dependence of this strength indicates a possibility of its switching on/off. If at the lens location we induce the local distortion of closed orbit (bump) and then compare two orbits measured with the lens switched on (large current) and switched off (small current), we obtain the orbit